

LANDFILL SITE SELECTION AND LANDFILL LINER DESIGN FOR
POLATLI, ANKARA

A THESIS SUBMITTED TO
THE GRADUATE SCHOOL OF NATURAL AND APPLIED SCIENCES
OF
MIDDLE EAST TECHNICAL UNIVERSITY

BY

GÖKALP ÖNER

IN PARTIAL FULFILLMENT OF THE REQUIREMENTS
FOR
THE DEGREE OF MASTER OF SCIENCE
IN
GEOLOGICAL ENGINEERING

NOVEMBER 2019

Approval of the thesis:

**LANDFILL SITE SELECTION AND LANDFILL LINER DESIGN FOR
POLATLI, ANKARA**

submitted by **GÖKALP ÖNER** in partial fulfillment of the requirements for the degree of **Master of Science in Geological Engineering Department, Middle East Technical University** by,

Prof. Dr. Halil Kalıpçılar
Dean, Graduate School of **Natural and Applied Sciences**

Prof. Dr. Erdin Bozkurt
Head of Department, **Geological Engineering**

Prof. Dr. Haluk Akgün
Supervisor, **Geological Engineering, METU**

Examining Committee Members:

Prof. Dr. Erdal Çokça
Civil Engineering, Middle East Technical University

Prof. Dr. Haluk Akgün
Geological Engineering, METU

Prof. Dr. Candan Gökçeoğlu
Geological Engineering, Hacettepe University

Assoc. Prof. Dr. Hakan Nefeslioğlu
Geological Engineering, Hacettepe University

Assoc. Prof. Dr. Mustafa Kerem Koçkar
Civil Engineering, Hacettepe University

Date: 13.11.2019

I hereby declare that all information in this document has been obtained and presented in accordance with academic rules and ethical conduct. I also declare that, as required by these rules and conduct, I have fully cited and referenced all material and results that are not original to this work.

Name, Surname: Gökalp Öner

Signature:

ABSTRACT

LANDFILL SITE SELECTION AND LANDFILL LINER DESIGN FOR POLATLI, ANKARA

Öner, Gökalp
Master of Science, Geological Engineering
Supervisor: Prof. Dr. Haluk Akgün

November 2019, 118 pages

The purpose of this study is to select the best alternative for a landfill site for the Polatlı County. There currently is no proper landfill site in the county. Renewable materials are sent to the Ankara-Mamak Landfill site and the remaining waste material is deposited in an improper open dump site that is situated to the south of the county. Because of all these problems, the county urgently needs a proper landfill site with a landfill liner system. In the context of this thesis, site selection has been performed by considering criteria including, air traffic safety, geology, land use, distance to settlements, distance to roads, hydrogeology (drainage), slope, erosion, distance to faults and distance to earthquake epicenters. These criteria have been modeled and evaluated in a GIS environment and eventually the best site has been chosen. In addition, disturbed fine grained silty samples have been collected from the alternative sites and geotechnical (i.e., sieve analysis, Atterberg limit tests, hydrometer, compaction, falling head permeability) and mineralogical (i.e., SEM, XRD, methylene blue absorption) tests have been conducted on these samples. Three samples representative of alternative sites were mixed with 5% bentonite to decrease their permeability values. Falling head permeability tests were additionally conducted on those samples. By using the data obtained from these tests, the design of the liner and

the hydrologic evaluation of the landfill has been performed through utilizing the HELP (Hydrologic Evaluation of Landfill Performance) software.

Keywords: Landfill, Polatlı, Site Selection

ÖZ

ANKARA İLİ POLATLI İLÇESİ İÇİN KATI ATIK SAHASI YER SEÇİMİ VE TASARIMI

Öner, Gökalp
Yüksek Lisans, Jeoloji Mühendisliği
Tez Danışmanı: Prof. Dr. Haluk Akgün

Kasım 2019, 118 sayfa

Bu çalışmanın amacı Ankara ili Polatlı ilçesi için uygun bir katı atık sahası yer seçimi ve tasarımının yapılmasıdır. İlçede modern anlamda bir katı atık sahası bulunmamaktadır. Yenilenebilir malzemeler Ankara-Mamak katı atık sahasına gönderilmekte, kalan artık malzemeler ilçenin güneyindeki uygunsuz bir sahada depolanmaktadır. Bu saha geçirimsiz örtü tabakasından yoksun olup, baskın rüzgar yönlerinden dolayı lokasyonu çeşitli sorunlara yol açmaktadır. Bütün bu sorunlardan dolayı ilçenin uygun bir katı atık sahası ve geçirimsiz örtü tabakasına acil bir şekilde ihtiyacı vardır. Bu çalışma kapsamında, yer seçimi, hava ulaşım güvenliği, jeoloji, arazi kullanımı, yerleşim yerlerine uzaklık, yollara uzaklık, hidrojeoloji (drenaj), şev, erozyon, faylara uzaklık ve deprem merkez üslerine uzaklık faktörleri göz önüne alınarak yapılmıştır. Bütün bu faktörler CBS ortamında oluşturulmuş ve en uygun saha seçilmiştir. Ayrıca belirlenen alternatif sahalardan örselenmiş numuneler alınmış ve jeoteknik (elek analizi, Atterberg kıvam limitleri, hidrometre, kompaksiyon, düşen seviyeli permeabilite) ve mineralojik (SEM, XRD, Metilen mavisi) deneyleri yapılmıştır. Alternatif sahaları temsil eden 3 numune permeabilite değerlerini düşürmek için 5% bentonit ile karıştırılmış, düşen seviyeli permeabilite deneyleri bu numunelere ayrıca uygulanmıştır. Bu deneyler sonucunda elde edilen veriler

kullanılarak HELP yazılımı yardımıyla katı atık sahasının geçirimsiz taban tasarımı yapılmış ve sahanın hidrolojik süreci değerlendirilmiştir.

Anahtar Kelimeler: Katı Atık Sahası, Polatlı, Yer Seçimi

To my Family

ACKNOWLEDGEMENTS

It is a pleasure for me to thank those who made this thesis possible. First of all, I would like to express my deep gratitude to Prof. Dr. Haluk Akgün for his guidance, support and patience. It was a unique experience for me to work with him.

There are many valuable professors and colleagues who helped me through this long and complicated process. First of all, I would like to thank Prof. Dr. Asuman Günal Türkmenoğlu for her aid in writing the entire geology section of this thesis. Assoc. Prof. Dr. Mustafa Kerem Koçkar guided me with his technical and moral support. Mrs. Arzu Arslan Kelam helped me in all stages of this thesis and Mr. Selim Cambazoğlu supported me in the TOPSIS analysis. Karim Yousefi-Bavil and Ecem Cansu Asan accompanied me along the field trips and shared their experience. I am grateful to them. I also would like to thank Caner Öz and Aytül Tasak for helping me through the laboratory experiments. Gözde Yal helped me on ArcGIS software. Dr. Arif Mert Eker and Dr. Mohammad Azarafza guided me on many technical subjects. It was a pleasure for me to work with them.

I would like to thank my family. Nevzat, Mürüvvet and Kağan Berkay Öner for their continuous support and endless questions about when to finish my thesis. I couldn't achieve this without them. I also would like to thank Hacer Marie Özkan for her efforts and inspiration. I am really grateful.

TABLE OF CONTENTS

ABSTRACT	v
ÖZ	vii
ACKNOWLEDGEMENTS	x
TABLE OF CONTENTS	xi
LIST OF TABLES	xv
LIST OF FIGURES	xvii
CHAPTERS	
1. INTRODUCTION	1
1.1. Purpose and Scope.....	1
1.2. Study Area	3
1.2.1. Population	5
1.2.2. Hydrogeology	5
1.2.3. Climate.....	6
1.2.4. Vegetation cover	7
1.3. Previous Studies	7
1.4. Method of Study	8
2. REGIONAL GEOLOGY	11
2.1. Geology and Stratigraphy of the Area.....	11
2.1.1. Tpk (Kartal formation).....	13
2.1.2. Tpek (Kırkkavak Formation)	14
2.1.3. Tpei (İlgınlıkdere formation).....	14
2.1.4. Tee (Eskipolatlı formation).....	14

2.1.5. Teb (Beldede Formation)	15
2.1.6. Tmh (Hançili Formation)	15
2.1.7. Tmpla (Alagöz formation).....	16
2.1.8. Tmplay (Fan-fluvial member)	16
2.1.9. Tmplag (Lacustrine member)	16
2.1.10. Tmplav (Volcanite member)	17
2.1.11. Qeal (Old alluvion).....	17
2.1.12. Qym (Slope debris)	17
2.1.13. Qal (Alluvium)	17
3. INTEGRATION OF GEOGRAPHIC INFORMATION SYSTEM AND MULTI- CRITERIA DECISION ANALYSIS	19
3.1. GIS and MCDA Methodology	19
3.2. Standardization.....	20
3.3. Linear Scale Transformation.....	21
3.4. Criterion Weighing	22
3.5. Multi-criteria Decision Making Methods	27
4. DECISION CRITERION AND LANDFILL SITE SELECTION.....	29
4.1. Geographic Information System (GIS) Layers	29
4.1.1. Distance to Settlement.....	30
4.1.2. Distance to Roads	32
4.1.3. Digital Elevation Model (DEM).....	34
4.1.4. Slope.....	35
4.1.5. Geology	37
4.1.6. Distance to Faults	39

4.1.7. Hydrogeology (Drainage)	41
4.1.8. Land Use	43
4.1.9. Erosion	47
4.1.10. Distance to Earthquake Epicenters	49
4.2. Other Criteria	51
4.2.1. Air Traffic Safety	51
4.2.2. Political and Social Criteria	51
4.3. TOPSIS Analysis	52
4.4. Sensitivity Analysis and Discussion	55
5. LANDFILL LINER DESIGN	59
5.1. Introduction	59
5.2. Standards and requirements	60
5.2.1. US Environmental Protection Agency-Criteria for Municipal Solid Waste Landfills	60
5.2.2. Turkish Republic, Ministry of Environment - Criteria for Municipal Solid Waste Landfills	61
5.3. Data Description for Visual HELP	62
5.3.1. Weather data	62
5.3.1.1. Evaporative zone depth	63
5.3.1.2. Maximum leaf area index (LAI)	63
5.3.1.3. Growing season start and end days	63
5.3.2. Soil and design data	66
5.3.2.1. Geotechnical Tests	67
5.3.2.2. Mineralogical Tests	76

5.4. Analysis of the Results.....	86
6. SUMMARY AND CONCLUSIONS.....	95
REFERENCES	97
A. Test Results	105

LIST OF TABLES

TABLES

Table 3.1. Pairwise comparison matrix developed for the selection criteria	23
Table 3.2. Normalized pairwise comparison matrix developed for the selection criteria	24
Table 3.3. Weights of the evaluation criteria	24
Table 3.4. Random consistency index (RI) values according to Saaty, 1991	26
Table 3.5. Consistency ratio calculation matrix	26
Table 4.1. Suitability rankings based on the distance to settlements	30
Table 4.2. Suitability rankings based on distance to roads	32
Table 4.3. Suitability rankings based on slope values	35
Table 4.4. Suitability rankings based on geological formations	37
Table 4.5. Suitability rankings based on the distance to fault (Sharifi, 2009)	39
Table 4.6. Suitability rankings based on the distance to the flow line (modified from Sharifi et al., 2009)	41
Table 4.7. Land use suitability rankings (Yal and Akgün, 2013)	45
Table 4.8. Erosion suitability rankings (modified from Yal and Akgün, 2013)	47
Table 4.9. Suitability rankings based on distance to earthquake epicenters	49
Table 5.1. Weather input data for the HELP model	64
Table 5.2. Specific gravity of the samples	68
Table 5.3. Atterberg limits of the samples	68
Table 5.4. Particle size distribution of the samples	69
Table 5.5. Summary of the maximum dry unit weight (kN/m^3) and optimum water content (w_{opt}) values for the soil samples	70
Table 5.6. Hydraulic conductivity values determined from falling head permeability testing	72

Table 5.7. Standard proctor compaction test results for soil samples mixed with 5% bentonite.	73
Table 5.8. Mineralogical and index properties of the karakaya bentonite used in this study (From Karakaya, 2019 as quoted by Ören et al., 2014).....	74
Table 5.9. Hydraulic conductivity of soil samples mixed with 5% bentonite.....	75
Table 5.10. Mineralogical characteristics of main clay minerals (Velasco, 2013)....	82
Table 5.11. Methylene blue test results	82
Table 5.12. Some of the input parameters utilized in the analysis (from Schroeder, 1994).....	91

LIST OF FIGURES

FIGURES

Figure 1.1. View of illegal waste dumping in Polatlı	2
Figure 1.2. Location map of the study area and the three alternative landfill sites, namely, Site A, Site B and Site C	4
Figure 1.3. A view from alternative Site B	5
Figure 1.4. Precipitation data for the Polatlı County between the years 1998-2018 ...	6
Figure 1.5. Monthly average temperature values for the years 1998-2018	7
Figure 2.1. Generalized stratigraphic column of the Çanakçı-Yıldızlı succession (from Bilgin et al., 2009).....	12
Figure 2.2. 1/100000 Scale geological map of the Polatlı County (from Bilgin et al., 2009)	13
Figure 4.1. Distance to settlement suitability map.....	31
Figure 4.2. Distance to roads suitability map.....	33
Figure 4.3. Digital elevation model (DEM) of the study area	34
Figure 4.4. Slope suitability map of the study area.....	36
Figure 4.5. Geological suitability map of the study area	38
Figure 4.6. Distance to faults suitability map	40
Figure 4.7. Hydrogeology (Drainage) suitability map of the study area	42
Figure 4.8. Land use map of the study area (EEA, 2018).....	44
Figure 4.9. Land use suitability map of the study area	46
Figure 4.10. Erosion suitability map of the study area	48
Figure 4.11. Distance to earthquake epicenters suitability map of the study area.....	50
Figure 4.12. Map showing the closest airport to the alternative sites	51
Figure 4.13. Modal builder data tree sample for geology and drainage layers.....	53
Figure 4.14. Final landfill site suitability map	54

Figure 4.15. The number of cells corresponding to suitability class 4 (most suitable)	56
Figure 4.16. The number of cells corresponding to suitability class 1 (least suitable)	57
Figure 5.1. Annual precipitation totals for Ankara between 1998 and 2018	65
Figure 5.2. Mean monthly temperatures for Ankara between 1998 and 2018	65
Figure 5.3. Soil sampling locations	66
Figure 5.4. Borehole locations around the study area	67
Figure 5.5. Schematic sketch of falling head permeability test apparatus (from Met, 1999; not to scale)	71
Figure 5.6. Hydraulic conductivity (m/s) vs bentonite content (%)	76
Figure 5.7. XRD graph of B1	78
Figure 5.8. XRD graph of C3	79
Figure 5.9. XRD graph of A3	79
Figure 5.10. Methylene blue stain test (from Chiappone, 1999)	81
Figure 5.11. SEM images of sample C3	83
Figure 5.12. EDAX analysis of the sample C3	84
Figure 5.13. SEM images of sample A3	84
Figure 5.14. EDAX analysis of the sample A3	85
Figure 5.15. SEM images of sample B1	85
Figure 5.16. EDAX analysis of the sample B1	86
Figure 5.17. Visual HELP profile 1 (modified from Schroeder, 1994)	87
Figure 5.18. Visual HELP profile 2 (modified from Schroeder, 1994)	88
Figure 5.19. Visual HELP profile 3 (modified from Schroeder, 1994)	89
Figure 5.20. Visual HELP profile 4 (modified from Schroeder, 1994)	90
Figure 5.21. Cumulative unitized expected leakage rate (m ³ /year/10,000 m ²) for 20 years of simulation	92
Figure 5.22. Cumulative average leakage head (m) for 20 Years of simulation	93
Figure 0.1. Particle size distribution plot of sample B1	105
Figure 0.2. Particle size distribution plot of sample B2	105

Figure 0.3. Particle size distribution plot of sample B3	106
Figure 0.4. Particle size distribution plot of sample C1	106
Figure 0.5. Particle size distribution plot of sample C2	107
Figure 0.6. Particle size distribution plot of sample C3	107
Figure 0.7. Particle size distribution plot of sample A1	108
Figure 0.8. Particle size distribution plot of sample A2	108
Figure 0.9. Particle size distribution plot of sample A3	109
Figure 0.10. Dry unit weight vs moisture content graph of C1	109
Figure 0.11. Dry unit weight vs moisture content graph of C2	110
Figure 0.12. Dry unit weight vs moisture content graph of C3	110
Figure 0.13. Dry unit weight vs moisture content graph of A1	111
Figure 0.14. Dry unit weight vs moisture content graph of A2	111
Figure 0.15. Dry unit weight vs moisture content graph of A3	112
Figure 0.16. Dry unit weight vs moisture content graph of B1	112
Figure 0.17. Dry unit weight vs moisture content graph of B2	113
Figure 0.18. Dry unit weight vs moisture content graph of B3	113
Figure 0.19. Dry unit weight vs moisture content graph of C3 (%5 Bentonite).....	114
Figure 0.20. Dry unit weight vs moisture content graph of A3 (%5 Bentonite).....	114
Figure 0.21. Dry unit weight vs moisture content graph of B1 (%5 Bentonite).....	115
Figure 0.22. Hydraulic conductivity vs pore volume of flow graph of C3 (%5 Bentonite).....	115
Figure 0.23. Hydraulic conductivity vs pore volume of flow graph of A3 (%5 Bentonite).....	116
Figure 0.24. Hydraulic conductivity vs pore volume of flow graph of B1 (%5 Bentonite).....	116
Figure 0.25. Hydraulic Conductivity vs time graph of sample B1	117
Figure 0.26. Hydraulic Conductivity vs time graph of sample A3	117
Figure 0.27. Hydraulic Conductivity vs time graph of sample C3	118

CHAPTER 1

INTRODUCTION

1.1. Purpose and Scope

A municipal solid waste landfill (MSWLF) is a discrete area of land or excavation that receives household waste. A MSWLF may also receive other types of nonhazardous wastes, such as commercial solid waste, nonhazardous sludge, conditionally exempt small quantity generator waste, and industrial nonhazardous solid waste. In 2009, there were approximately 1,908 MSWLFs in the continental United States all managed by the states where they are located. Modern landfills are well-engineered and managed facilities for the disposal of solid waste. Landfills are located, designed, operated and monitored to ensure compliance with federal regulations. They are also designed to protect the environment from contaminants, which may be present in the waste stream. Landfills cannot be built in environmentally-sensitive areas, and they are placed using on-site environmental monitoring systems. These monitoring systems check for any sign of groundwater contamination and for landfill gas, as well as provide additional safeguards. Today's landfills must meet stringent design, operation and closure requirements in the United States established under the Resource Conservation and Recovery Act (RCRA).

According to the US Environmental Protection Agency (EPA) there are four basic management strategies for integrated solid waste management (ISWM) (EPA, 2010): (1) source reduction, (2) recycling and composting, (3) combustion (waste-to-energy facilities) and (4) landfills.

Even though it is the last step of the solid waste management, landfills are inevitable and very common around the world. This is mainly due to the fact that even after every step of the solid waste management strategy was performed, there will be considerable

amount of garbage left since it is not possible to completely eliminate every substance. Landfills have to be constructed in a manner that they shouldn't harm the environment, meet the regulatory requirements and conform to the local community's needs.

Although it has a high and growing population, there is no proper municipal solid waste landfill in the Polatlı County. The renewable materials are sent to the Ankara-Mamak Landfill site and the remaining garbage is collected at an improper site (Figure 1. 1.). This site lacks a proper lining system and is located improperly due to the adverse dominant wind direction. There have been fire incidents reported at the site in the past, and waste materials are scattered throughout the neighborhood of the waste site and throughout the city because of the lack of fencing at the site. Because of all these problems a proper landfill site with a landfill lining system is urgently needed.



Figure 1.1. View of illegal waste dumping in Polatlı

Within the context of this study, site selection has been performed by considering criteria including, air traffic safety, geology, land use, distance to settlements, distance to roads, hydrogeology (drainage), slope, erosion, distance to faults and distance to earthquake epicenters. These criteria were modeled and evaluated in a GIS environment and eventually the best site was selected. In addition, disturbed samples have been collected from the alternative sites and geotechnical (sieve analysis, Atterberg limit tests, hydrometer, compaction, falling head permeability) and mineralogical (SEM, XRD, methylene blue absorption) tests were conducted in order to assess the suitability of the natural soil material of the Polatlı to be used as an impermeable fine soil liner material. After determination of these parameters, 5% bentonite was added to the selected representative samples to decrease the permeability of materials to the acceptable level of 1×10^{-9} m/s (EPA 2010, TSCWR, 2010). Standard proctor and falling head permeability tests were additionally conducted on these samples. Also, by using the data obtained from these tests, the design of the liner and the hydrologic evaluation of the landfill was performed through utilizing the HELP (Hydrologic Evaluation of Landfill Performance) model. The HELP model was employed in order to determine the leachate head and leakage amounts through assuming a 20-year lifespan for the landfill. Four different profiles from least conservative to most conservative were created and analyzed.

1.2. Study Area

Polatlı is one of the most populated counties of Ankara. It is also the largest in terms of the surface area. Polatlı is a municipality and a district in the Ankara Province that is situated in the Central Anatolia region of Turkey, 80 km west of the Turkish capital Ankara, on the road to Eskişehir. The district covers an area of 3,789 km², and the average elevation is 850 m. The location map of the Polatlı County is given in Figure 1.2. Three locations, namely Site A, Site B and Site C were selected to conduct the landfill site selection procedure, after taking wind direction, geology, transportation costs into consideration. Hançili Formation was selected due to its fine soil character and its wide distribution. In Figure 1.3., a view from alternative Site B is presented.

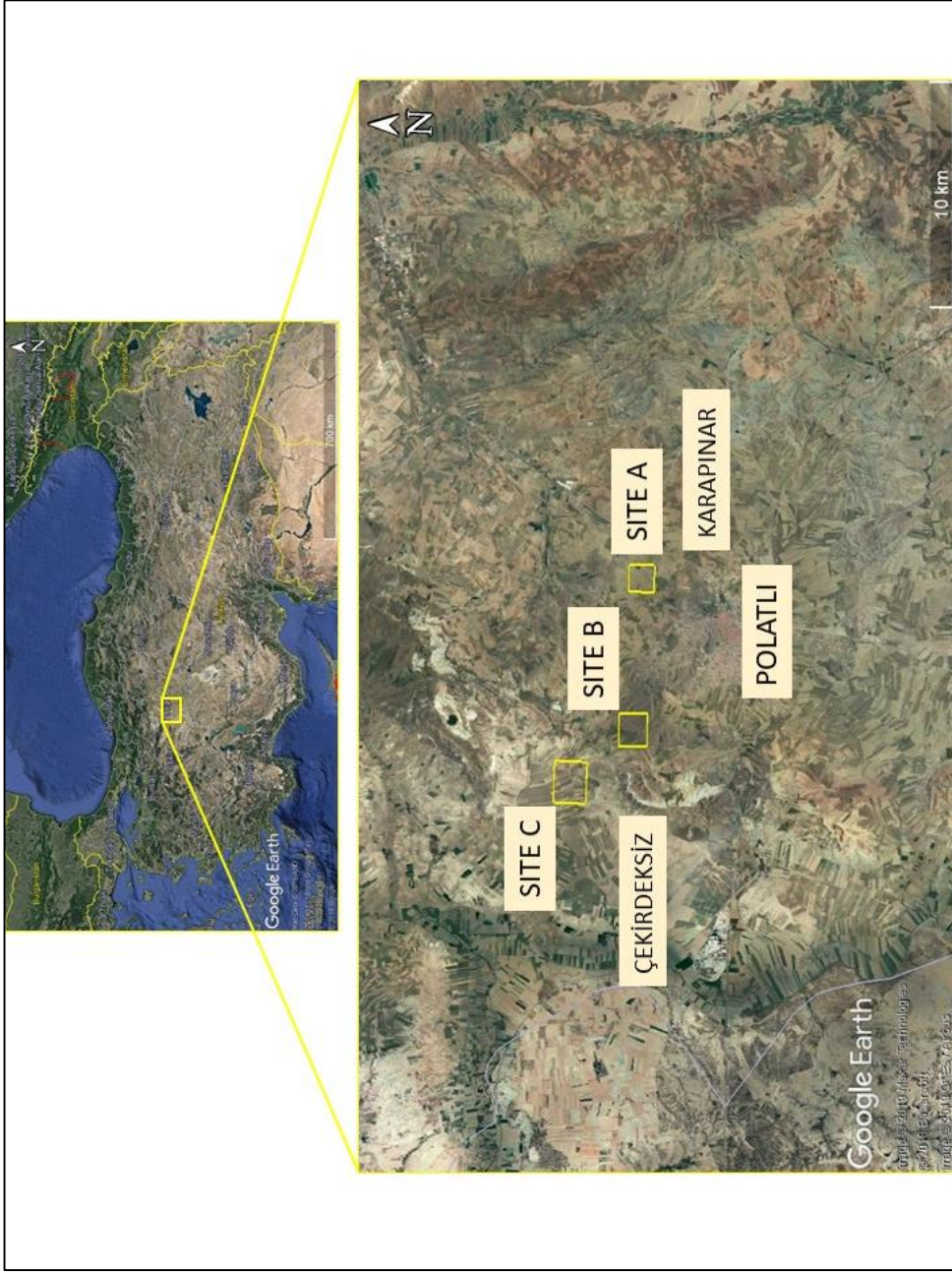


Figure 1.2. Location map of the study area and the three alternative landfill sites, namely, Site A, Site B and Site C



Figure 1.3. A view from alternative Site B

1.2.1. Population

According to the 2016 census, the county has a population of approximately 123,000. The birth rate of the county is determined as 1773 person per year. Death rate on the other hand is 569 people per year. So, it can be deduced that the growth rate is 1204 person per year which stands for 0.97% (Turksat, 2016).

1.2.2. Hydrogeology

The hydrogeology of the region has been studied by Pasvanoglu et al. (1998). According to this study, 28°C hot mineral water is found at a 700 m depth with 8.4 l/s flow rate in the Ilıcapınar region. Also, several drilling studies have been conducted with depths up to 15 meters for construction purposes. No groundwater was

encountered as a result of drilling. Based on this information, it can be assumed that groundwater level is very deep in the region and wasn't considered as a restricted criterion in this thesis.

1.2.3. Climate

Meteorological data for Polatlı was gathered from the State Meteorological Works of Turkey. Polatlı Weather Station which is located at a latitude of 39 15' and a longitude 32 12' was used. The lowest and highest average temperatures recorded at the Polatlı Weather Station are -0.07°C in January and 23.0°C in July, respectively. The minimum precipitation corresponds to the month of August with a value of 1.10 mm/month and the maximum precipitation is in May with a value of 114.20 mm/month. Figures 1. 4. and 1. 5. present the average monthly temperature and precipitation data for the period 1998-2018 at the Polatlı Weather Station. The dominant wind direction of the area is NNE according to the Polatlı Weather Station within the period of 1998- 2018.

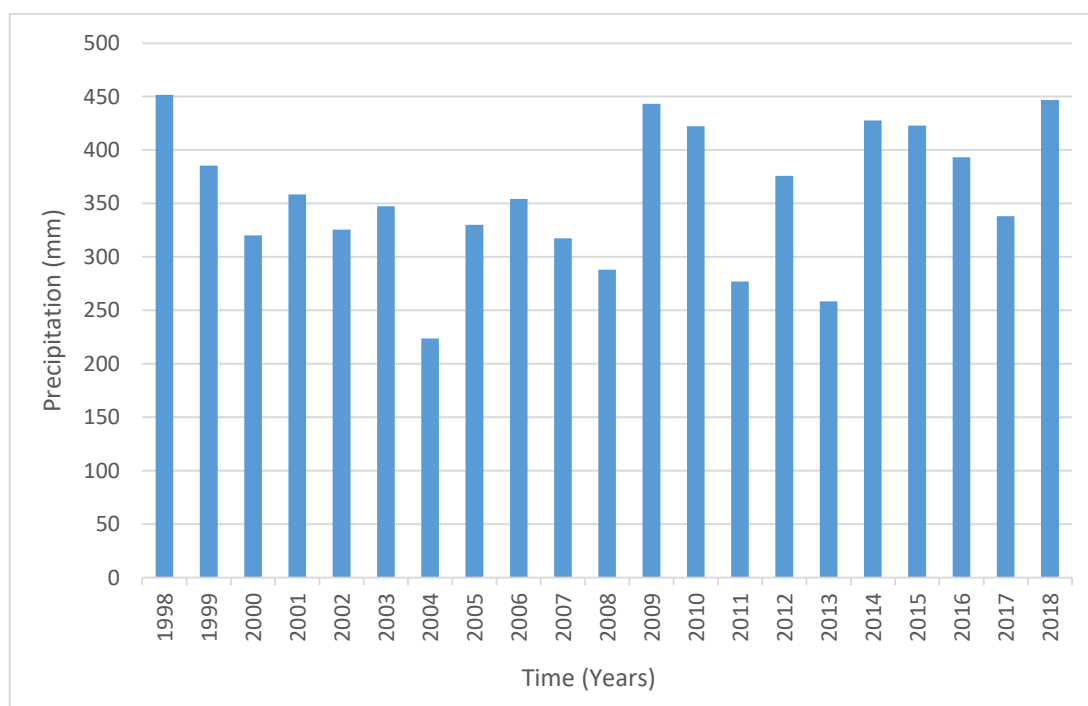


Figure 1.4. Precipitation data for the Polatlı County between the years 1998-2018

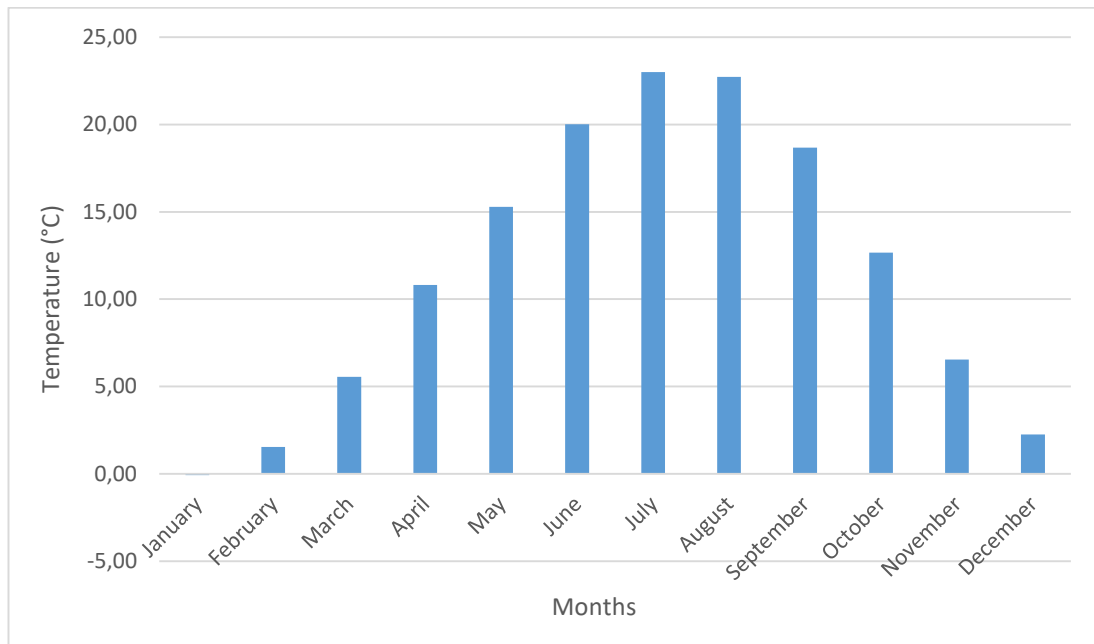


Figure 1.5. Monthly average temperature values for the years 1998-2018

1.2.4. Vegetation cover

Polatlı is located at the center of the high Anatolian plateau, a large steppe covered with grass. Far from the coast, it has a typical steppe climate. The winters are generally cold, the summers dry and dusty. The springs are the most humid times of the year. Polatlı is one of the most productive agricultural districts in Turkey and is best known for its barley and wheat production.

1.3. Previous Studies

There are many studies on landfill site selection in the literature. Yal and Akgün (2013; 2014), performed landfill site selection and landfill liner design for Ankara by utilizing the TOPSIS Methodology. Sener (2004), also performed landfill site selection for Ankara, using a total of 16 criteria, by employing the AHP (Analytical Hierarchy Process) and SAW (Simple Additive Weighting) methods. Yesilnacar et al. (2012), integrated MCDA with GIS to select possible sites for a MSW landfill in Şanlıurfa, Turkey. In addition to the site selection studies, there are some studies in the literature

about using fine-grained soils as a liner material. Akgün (2010) and Akgün and Koçkar (2017) studied the characterization and design of compacted bentonite/sand mixtures to be utilized in underground waste isolation. Met and Akgün (2015) and Akgün et al. (2017) investigated Ankara clay in order to be used as a landfill liner material. Sharifi et al. (2009), integrated GIS and multi-criteria decision analysis for hazardous landfill sitting in western Iran. Beskese et al., (2015), performed landfill site selection study using fuzzy AHP and fuzzy TOPSIS for İstanbul, Turkey. Kumar and Yong (2002), investigated effect of bentonite on compacted clay landfill barriers.

As mentioned above, there are studies in the literature which are about site selection and liner materials, but there is no specific landfill site selection study for the Polatlı County. From this point of view, this study is considered to be original.

1.4. Method of Study

In this study, the most appropriate landfill site for Polatlı County was selected by utilizing TOPSIS multi-criteria analysis. The steps of the site selection study are given below:

1. Identifying the selection criteria,
2. Gathering and standardizing the relevant data, and
3. TOPSIS analysis.

After completing the TOPSIS multi-criteria decision analysis, first, the optimum landfill site was selected from out of 3 candidate sites. The second step was to design a feasible landfill profile to be used for the next 20 years by using the Visual HELP software which is a quasi-two-dimensional, multi-layer hydrologic model that requires the following input data for each of the model profiles:

- Weather data (precipitation, solar radiation, temperature, evapotranspiration parameters),
- Soil properties (porosity, field capacity, wilting point, and hydraulic conductivity)
- Design information (liners, leachate and runoff collection systems, surface slope).

The weather data was acquired from the Turkish State of Meteorological Works as mentioned in the above sections. The soil properties were gathered from the laboratory tests and the software's own database. The design information was entered into the software in accordance with the EPA and Turkish regulatory requirements. four different profiles from least conservative to most conservative were modeled by HELP.

CHAPTER 2

REGIONAL GEOLOGY

2.1. Geology and Stratigraphy of the Area

Study area situated around Ayaş-Temelli-Polatlı region and comprises 1/100000 scaled Ankara İ28 Quadrangle area. Differences in regional geology contributed to the study of varied successions in the study area. Haymana-Polatlı, Çanakçı-Yıldızlı and Ayaş successions occurred in the basins, each of which is different from one another, following the morphological change resulted from regional tectonism in a range of age from Turonian to Maastrichtian. Within the context of this study Çanakçı-Yıldızlı succession was studied due to its wide distribution in the area. It is comprised of deposits of a transition-continental environment, Danian-Selandian Kartal formation is the lowermost unit of this succession. This is overlain by Thanetian-Ilerdian Kırkkavak formation, facies of which passes from a shallow marine to mudflat environment, followed by shallow marine carbonates of Late Thanetian-Cuisian Iğnıkdere formation only observed in upper levels of this succession together with flysch deposits of Cuisian-Lutetian Eskipolatlı formation and Cuisian-Lutetian Beldede formation, represented by shallow marine deposits (Figure 2. 1.). Hançili formation lies over this succession as well as two other successions. It is built from lacustrine deposits and contemporaneous volcanism. In this study, field samples were collected from the Hançili formation. Hançili formation was selected due to its fine soil content since one of the main aim of this study is to find a suitable landfill liner material. Additionally, this formation has a wide distribution in and around the study area. Detailed geological map of the area is presented in Figure 2. 2.

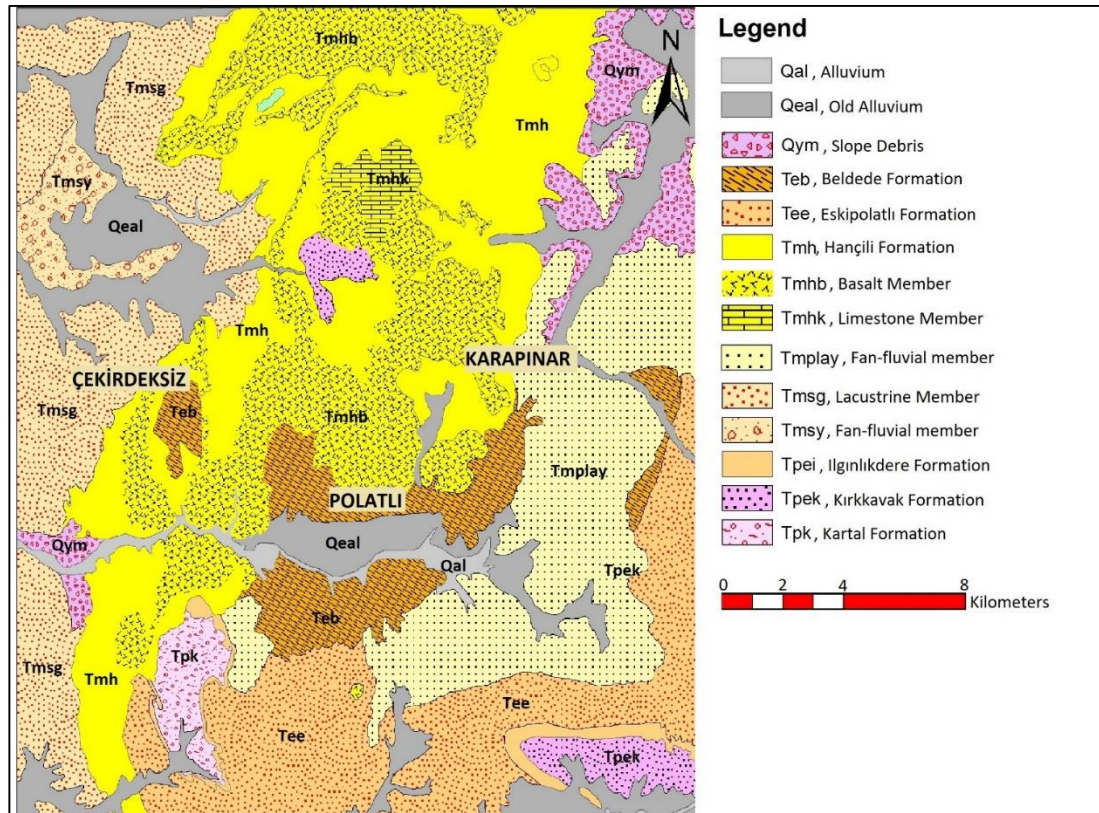


Figure 2.2. 1/100000 Scale geological map of the Polatlı County (from Bilgin et al., 2009)

2.1.1. Tpk (Kartal formation)

It is first named by Rigo de Righi and Cortesini (1959). It is mostly dark red in color and is composed of pebble, sandstone, marl and limestone. Pebbles are poorly graded and grain size varies from a few centimeters to 20-25 centimeters. There are 2-5 cm thick coal strips in the lower parts of the formation. It overlies the Upper Cretaceous Beyobasi formation and is overlain conformably by the Thanetian Kırkkavak formation. The formation is measured to be 1362 m thick in the type section. It is determined to be Danian-Selandian aged.

2.1.2. Tpek (Kırkkavak Formation)

It is first named by Rigo de Righi and Cortesini (1959). It is mainly composed of pebble, sandstone, marl, clayey limestone, sandy limestone, limestone with algae and limestone with coralline and varied alternations of these units. It is observed widely in the Kuşçu, Macunköy, Köseler, Kayabaşı towns and in the south of the Eskipolatlı town. This formation's rock unit vary both vertically and horizontally. Between the Macunköy and Kuşçu towns, there are sandy limestones at the bottom and limestone-sandstone alternations at the upper parts. Overlying them are gray colored shales and sandstone parts. At the top there are shales with gastropodes. Kırkkavak formation is underlain by Kartal formation with suspicious unconformity, and overlain unconformably by Eskipolatlı formation. It is determined to be 639 m thick. The formation has mostly shallow sea characteristics. According to the fossils found the area, Kırkkavak formation is determined to be Tanesian-Ilerdian aged.

2.1.3. Tpei (Ilgınlıkdere formation)

The formation was first defined by Unalan et al. (1976). It is mostly composed of limestones with Alveolina fossils. In addition, pebble, sandstone and shale are also common in this unit. Ilgınlıkdere formation outcrop in İğciler and south of Sakarya towns. Bilgin et al. (2010), suggests a thickness of 146 meters in Kale Tepe which is located at the south of the study area. According to field observations, formation is found to be consistent with the underlying Kırkkavak and overlying Eskipolatlı formations. Age of this unit is determined to be Ilerdian-Lutesian based on the paleontological information gathered from the field samples.

2.1.4. Tee (Eskipolatlı formation)

It is first named by Rigo de Righi and Cortesini (1959). It is widely observed around the Eskipolatlı, Sakarya and Kargalı towns. In the bottom of the formation there are mostly pebbles. Above that there is sandstone mixed with shale overlain by marl units. Then, turbiditic limestones and at the top gray-green colored marl units are located. Eskipolatlı formation conformably overlies Ilgınlıkdere formation and is

unconformably overlain by Beldede formation in the south of the İğciler town. It is measured 567-meter-thick in its type section. Eskipolatlı formation starts from shallow sea sediments at the bottom and continues with rock characterized for a deep sea environment. In the light of the paleontologic and stratigraphic data sets, it is found to be Kuvisian-Lutetian aged.

2.1.5. Teb (Beldede Formation)

Beldede formation was first defined by Unalan et al. (1976). It is mainly composed of pebble, sandstone and sandy marl. The units in the south and west of the Polatlı County are reddish-brown in color. West of the Kargalık Town around the Beldede Hill is the type locality of this formation. In the bottom, mostly pebble, gravelly sandstone and sandstone is observed. In the upper parts, carbonate sandstone, sandy limestone and marls commonly observed. It is consistent with the underlying Eskipolatlı formation and it lies below the Hançili formation's sediments and discontinuous basalts. Beldede Formation consists of fan, delta, lagoon and shallow shelf sediments. It is determined to be Kuvisian-Lutetian aged.

2.1.6. Tmh (Hançili Formation)

Hançili Formation was first named by Akyurek et al. (1980). It is mainly composed of clayey limestone and marl, and lesser amounts of siltstone, sandstone, pebble and rarely tuffite, gypsum and coal. This formation is observed widely in the south of the Polatlı-Ayaş road and in the north of the Polatlı-Temelli-Ankara creek. It is usually light green, white, greenish-yellowish white, light grey in color, thin to medium layered and composed of alternating clayey limestone, marl, siltstone, sandstone, pebble, chert and tuffs. There is less amount of coal and gypsum as well. Concurrent volcanic activity is ongoing. There are pebbles on top of the pile as a result of the regressive sedimentation. The Hançili formation laterally and vertically grades into the underlying Altıntaş formation. Full section of this unit cannot be observed precisely due to intense faulting and folding. Thickness of the formation is considered to be 300-400 meters. Hançili formation is not very rich with regard to fossil content.

In the northeast of the study area *Megacricetodon minor* (Lartet) fossils were found. After comprehensive examination of the paleontological and radiometric information from the study area, age of the Hançili formation is determined to be Early-Middle Miocene. Hançili formation is the result of a settling of a large lacustrine environment located at the north and southwest of the study area. In the last stage of the formation, regressive fluvial sedimentation was observed around Çile mountain.

2.1.7. Tmpla (Alagöz formation)

This formation was first named by Bilgin et al. (2009). Alagöz formation is composed of fan-fluvial and lacustrine materials at the bottom, continues with lacustrine limestones and volcanites at the top. This unit can be subdivided into three members namely, Fan-fluvial member, Lacustrine member and Volcanite member which are described in following sections.

2.1.8. Tmplay (Fan-fluvial member)

It is mainly composed of pebble, sandstone, marl and mudstone and can be considered within the Alagöz formation (Tmpla). These units are red, dark red, brown, yellow and yellowish green in color. It can be observed in Türkobası, Malıköy, Alagöz towns, Temelli County and the east of the Polatlı County. Pebbles are poorly graded, round shaped and have different sources. Layers can be observed easily and usually are horizontal to nearly horizontal. It overlies all of the older formations with angular unconformity. It is 70 meters in thickness and sedimented in a fan-stream environment. This member is Late Miocene-Pliocene aged.

2.1.9. Tmplag (Lacustrine member)

It is within the Alagöz formation. This member can be observed in the towns Malıköy, Yenihisar, Yenidoğan, Alikolan and Temelli County. It is mainly composed of white, yellowish white, beige colored, solid, thick layered clayey limestone and trace amounts of chert. This member usually conformably overlies the Fan-river member.

It has a thickness of 50 meters. According to its stratigraphic position, its age is accepted as Late Miocene-Pliocene.

2.1.10. Tmplav (Volcanite member)

Volcanite member was first named after Bilgin et al. (2009). Unit consist of competent basalt lavas which has a dark gray, dark brown and blackish outer surface and fresh surface with grayish colored. It can easily be observed around basalt mines in Yenidoğan town, south of Temelli and north of Sonkut town. Thickness of this member can reach up to 50 meters at some locations. Age of this unit is determined to be Late Miocene-Pliocene with other members of Alagöz formation.

2.1.11. Qeal (Old alluvion)

It is composed of uncemented gravel, sand and mud which are observed in the low angle portion of the hills. These are the sediments accumulated as a result of the gully erosion at the slopes. According to the stratigraphic position, it is estimated to be Late-Pleistocene aged.

2.1.12. Qym (Slope debris)

It is composed of uncemented gravel, sand and mud-sized geomaterials as a result of streaming of water at the slopes. It is in control of topography and is conformable with slope angle.

2.1.13. Qal (Alluvium)

It is composed of sand, gravel and sludge which is found throughout the current rivers and in the trenches these rivers create.

CHAPTER 3

INTEGRATION OF GEOGRAPHIC INFORMATION SYSTEM AND MULTI-CRITERIA DECISION ANALYSIS

3.1. GIS and MCDA Methodology

Geographic information systems and multi-criteria decision analysis has been used in making decisions for complex situations with many aspects and potentials over the years. Many researchers have combined GIS with MCDA to select landfill sites (Chang et al., 2008, Akbari et al., 2008, Nas et al., 2008). Landfill siting is a complicated and difficult process which requires variable criteria to be evaluated. The Decision Maker has to take into consideration the environmental, technical and financial aspects properly. Since the process requires many inputs, GIS is very suitable for the selection study due to its ability to manage large amounts of spatial data from different types of sources (Sener et al., 2006). Multi-criteria analysis on the other hand is used when handling large amounts of complex information. The main principle of this method is to split the decision problems into smaller and understandable parts, analyze each part separately, and then integrate the parts in a logical manner (Malczewski, 1997). The integration of GIS and MCDA is a powerful tool for the landfill site selection problem because while GIS provides efficient manipulation and presentation of the data, MCDA supplies consistent ranking of the potential landfill areas based on different criteria (Sener et al., 2006).

Several evaluation criteria are selected in order to build a GIS model. For the selection process to be consistent, the set of attributes are:

- Comprehensible,
- Measurable,
- Complete,
- Operational, and
- Decomposable.

Every attribute is represented by a criterion map. The criterion map displays the spatial distribution of an attribute which measures the degree to which its associated objective is achieved (Malcewski, 1999). These maps which contain advisory information will be used in landfill site selection.

3.2. Standardization

Given the variety of scales on which attributes can be measured, multi-criteria analysis requires that the values contained in the various criterion map layers be transformed to comparable units. More specifically, if one needs to combine the various criterion maps layers, the scales must be commensurate. A number of approaches can be used to make criterion map layers comparable. To this end, criterion maps can be classified on the basis of the types of information available for constructing the maps. This classification is related to the distinction between deterministic decisions and decisions under uncertainty (probabilistic and fuzzy decisions). Accordingly, criterion maps can be categorized as deterministic, probabilistic, or fuzzy. Deterministic maps assign a single value to each object (point, line, polygon, or pixel) in a map layer. It follows that for deterministic criteria there will be a deterministic relationship between an alternative and its consequences. Linear scale transformation is the most frequently used deterministic method for transforming input data into commensurate criterion maps. Another way of deriving commensurate criterion maps is to use value/utility function approaches. Although these approaches are based on common methodology,

there is an essential difference between the value function and the utility function approach. While the value function method is applicable in deterministic situations, the utility function method is appropriate for decision situations involving uncertainty (Malcewski, 1999).

Since the criterion maps used in this study are deterministic maps where a single value is assigned to each pixel, a linear scale transformation method was used in order to standardize the maps.

3.3. Linear Scale Transformation

The most common procedures in linear scale transformation are the maximum score and score range procedures. Detailed information about these procedures are given in the following paragraphs.

Maximum Score Procedure: Each raw score is divided by the maximum value for a criterion by employing Eqs. (3.1) and (3.2):

$$x'_{ij} = \frac{x_{ij}}{x_j^{\max}} \quad (3.1.)$$

$$x'_{ij} = 1 - \frac{x_{ij}}{x_j^{\max}} \quad (3.2.)$$

where x'_{ij} is the standardized score for the i^{th} object and the j^{th} attribute, x_{ij} is the raw score, and x_j^{\max} is the maximum score for the j^{th} alternative. Higher score values denote more attractive criterion values. Eq. (3.1.) is the benefit criterion where the criterion is to be maximized. Eq. (3.2.), on the other hand is the cost criterion where the criterion is to be minimized meaning the lower the score, the better the performance. This method that allows linear transformation of the data has a shortcoming in the interpretation of the least attractive score due to the fact that the lowest standardized score does not necessarily equal zero.

In standardizing the attributes, the score range procedure is employed.

$$X'_{ij} = \frac{X_{ij} - X_j^{\min}}{X_j^{\max} - X_j^{\min}} \quad (3.3.)$$

$$X'_{ij} = \frac{X_j^{\max} - X_{ij}}{X_j^{\max} - X_j^{\min}} \quad (3.4.)$$

Where x_j^{\min} is the minimum score for the j^{th} attribute, $x_j^{\max} - x_j^{\min}$ is the range of a given criterion, and the remaining terms are as defined previously. Here Eqs. (3.3.) and (3.4.) are benefit and cost criterion, respectively. Score measures ranges from 0 to 1, 1 being the most attractive and 0 being the least attractive score (Malczewski, 1999).

3.4. Criterion Weighing

A weight can be defined as a value assigned to an evaluation criterion which indicates its importance relative to other criteria under consideration (Sener, 2004). Assigning weight values to the evaluation criteria is important for many reasons: changes in the range of variation for each evaluation criterion and different levels of importance being attached to these levels of variation. There are four different methods in the literature, namely, ranking, rating, pairwise comparison and trade analysis method. In this study the pairwise comparison method was employed due to its relatively high precision and trustworthiness (Yal and Akgün, 2014). The pairwise comparison method is developed by Saaty, 1980, within the context of analytic hierarchy process. This method determines the relative importance of an entity by comparing all entities in pairs.

The main steps of this method are development of the pairwise comparison matrix, generating the normalized pairwise comparison matrix and obtaining the criterion weights. When constructing the pairwise comparison matrix, evaluation criteria are written on the left hand side and on top of the matrix. If the criteria on the left are more important than the top, a numerical value greater than one has to be used. In the

opposite situation, reciprocal of that value should be used. Tables 3. 1. and 3. 2. show the pairwise comparison matrix and the normalized pairwise comparison matrix, respectively.

Table 3.1. *Pairwise comparison matrix developed for the selection criteria*

Evaluation Criteria	Geology	Land Use	Distance to Settlement	Distance to Roads	Hydrogeology (Drainage)	Slope	Erosion	Distance to Faults	Distance to Epicenters
Geology	1	2	3	4	5	6	7	8	9
Land Use	1/2	1	2	3	4	5	6	7	8
Distance to Settlement	1/3	1/2	1	2	3	4	5	6	7
Distance to Roads	1/4	1/3	1/2	1	2	3	4	5	6
Hydrogeology (Drainage)	1/5	1/4	1/3	1/2	1	2	3	4	5
Slope	1/6	1/5	1/4	1/3	1/2	1	2	3	4
Erosion	1/7	1/6	1/5	1/4	1/3	1/2	1	2	3
Distance to Faults	1/8	1/7	1/6	1/5	1/4	1/3	1/2	1	2
Distance to Epicenters	1/9	1/8	1/7	1/6	1/5	1/4	1/3	1/2	1
SUM	2,83	4,72	7,59	11,45	16,28	22,08	28,83	36,5	45

Table 3.2. Normalized pairwise comparison matrix developed for the selection criteria

Evaluation Criteria	Geology	Land Use	Distance to Settlement	Distance to Roads	Hydrogeology (Drainage)	Slope	Erosion	Distance to Faults	Distance to Epicenters	Average
Geology	0,3535	0,4239	0,3951	0,3493	0,3071	0,2717	0,2428	0,2192	0,2000	0,3070
Land Use	0,1767	0,2120	0,2634	0,2620	0,2457	0,2264	0,2081	0,1918	0,1778	0,2182
Distance to Settlement	0,1178	0,1060	0,1317	0,1747	0,1842	0,1811	0,1734	0,1644	0,1556	0,1543
Distance to Roads	0,0884	0,0707	0,0659	0,0873	0,1228	0,1358	0,1387	0,1370	0,1333	0,1089
Hydrogeology (Drainage)	0,0707	0,0530	0,0439	0,0437	0,0614	0,0906	0,1040	0,1096	0,1111	0,0764
Slope	0,0589	0,0424	0,0329	0,0291	0,0307	0,0453	0,0694	0,0822	0,0889	0,0533
Erosion	0,0505	0,0353	0,0263	0,0218	0,0205	0,0226	0,0347	0,0548	0,0667	0,0370
Distance to Faults	0,0442	0,0303	0,0220	0,0175	0,0154	0,0151	0,0173	0,0274	0,0444	0,0259
Distance to Epicenters	0,0393	0,0265	0,0188	0,0146	0,0123	0,0113	0,0116	0,0137	0,0222	0,0189

After generating the normalized pairwise matrix, weights of the selected criteria were determined and can be seen in the Table below.

Table 3.3. Weights of the evaluation criteria

Evaluation Criteria	Weight
Geology	0,31
Land Use	0,22
Distance to Settlement	0,15
Distance to Roads	0,11
Hydrogeology (Drainage)	0,07
Slope	0,05
Erosion	0,04
Distance to Faults	0,03
Distance to Earthquake Epicenters	0,02

After determining the weights of the selected criteria by using the pairwise comparison method, consistency of this calculation has to be checked in order to control its trustworthiness. To achieve this, the following equations were used:

$\lambda_{\max} = n$ whenever $A = \{a_{ij}\}$ is consistent, otherwise:

$$\lambda_{\max} > n \quad (3.5.)$$

T. Saaty defined consistency index CI of A as follows:

$$CI(A): x = \frac{\lambda_{\max} - n}{n - 1} \quad (3.6.)$$

and, consistency ratio as:

$$CR(A) = \frac{CI}{RI} \quad (3.7.)$$

Here, RI(n) is called random index which is defined as the mean value of CIs for positive reciprocal PC matrices of dimension n. The values of RI(n) for n =3, 4,...,15 are given in Table 3.4. (Saaty, 1991). According to Saaty (1991), the consistency ratio (CR) should be less than 0.1, otherwise the matrix would be inconsistent and the calculations have to be re-checked.

Table 3.4. *Random consistency index (RI) values according to Saaty, 1991*

Matrix size	Random consistency index (RI)
1	0
2	0
3	0,58
4	0,9
5	1,12
6	1,24
7	1,32
8	1,41
9	1,45
10	1,49

Consequently, consistency ratio (CR) was calculated by using the above mentioned equations. It was determined to be approximately 0.06 which is below 0.1 and hence, this result shows that the comparisons were consistent. The results of the calculation steps are presented in Table 3. 5.

Table 3.5. *Consistency ratio calculation matrix*

Consistency Ratio Calculation Matrix									SUM	λ	CI	CR
0,31	0,44	0,45	0,44	0,40	0,30	0,28	0,24	0,18	3,04	9,71	0,09	0,06
0,16	0,22	0,30	0,33	0,32	0,25	0,24	0,21	0,16	2,19			
0,10	0,11	0,15	0,22	0,24	0,20	0,20	0,18	0,14	1,54			
0,08	0,07	0,08	0,11	0,16	0,15	0,16	0,15	0,12	1,08			
0,06	0,06	0,05	0,06	0,08	0,10	0,12	0,12	0,10	0,74			
0,05	0,04	0,04	0,04	0,04	0,05	0,08	0,09	0,08	0,51			
0,04	0,04	0,03	0,03	0,03	0,03	0,04	0,06	0,06	0,35			
0,04	0,03	0,03	0,02	0,02	0,02	0,02	0,03	0,04	0,24			
0,03	0,03	0,02	0,02	0,02	0,01	0,01	0,02	0,02	0,18			

3.5. Multi-criteria Decision Making Methods

Multi-criteria decision making (MCDM) methods have a significant advantage over traditional methods where all criteria need to be converted to the same unit, since they can assess a variety of options against a variety of criteria that have different units. There are a variety of MCDM methods in the literature, namely, priority based, outranking, distance based, ideal point and mixed methods. In this thesis, “The technique for order preference by similarity to ideal solution (TOPSIS)” was used as the ideal point method.

TOPSIS views a MCDM problem with m alternatives as a geometric system with m points in the n -dimensional space, where n represents the number of criteria to be used in the evaluation. It was developed by Hwang and Yoon (1981). It defines an index called similarity (or relative closeness) to the positive-ideal solution and the remoteness from the negative-ideal solution. Then, the alternative with the maximum similarity to the positive-ideal solution and remoteness from the negative-ideal solution is chosen (Yoon and Hwang 1995). This method is found to be suitable for landfill site selection since it selects the alternative that is closest to the ideal solution and farthest from the negative ideal solution. This way a landfill site alternative closest to the best and farthest from the worst can be selected, with regards to the defined criteria (e.g., Yal and Akgün, 2014). Many researchers utilized TOPSIS method in their site selection and MCDM studies (e.g., Beskese et al., 2015; Cambazoglu et al., 2019; Nyimbili et al., 2018).

In the light of the given information in above mentioned sections, initially, criteria to be used in the analysis were defined. The importance of these criteria were determined by considering the characteristics of the study area and similar studies in the literature followed by performing TOPSIS analysis. The following paragraph presents a summary of the analysis steps which are in conjunction with Malczewski, (1999):

1. Determine the feasible alternatives and decision criteria (attributes).
2. Standardize each attribute map layer by transforming the various attribute dimensions (x_{ij}) to unidimensional attributes (v_{ij}); this transformation allows for comparison of the various layers.
3. Define the weights (W_j) assigned to each attribute; where the set of weights must be such that $0 \leq w_j \leq 1$ and $\sum_j w_j = 1$.
4. Construct the weighted standardized map layers by multiplying each value of the standardized attribute layer v_{ij} by the corresponding weight w_j , where each cell of the layers contains the weighted standardized value v_{ij} .
5. Determine the maximum value (v_{+j}) for each of the weighted standardized map layers (the values determine the ideal point).
6. Determine the minimum value (v_{-j}) for each weighted standardized map layer (the values determine the negative ideal point).
7. Using a separation measure, calculate “the distance” between the ideal point and each alternative; where a separation can be calculated by using the Euclidean (or straight-line) distance metric.

$$S_{i+} = [\sum_j (v_{ij} - v_{+j})^2]^{0.5} \quad (3. 8.)$$

8. Using the same separation measure, determine “the distance” between the negative ideal point and each alternative:

$$S_{i-} = [\sum_j (v_{ij} - v_{-j})^2]^{0.5} \quad (3. 9.)$$

9. Calculate the relative closeness to the ideal point (c_{i+}) by using the equation:

$$c_{i+} = \frac{S_{i-}}{S_{i+} + S_{i-}} \quad (3. 10)$$

$0 < c_{i+} < 1$; that is, an alternative is closer to the ideal point as c_{i+} approaches 1.

CHAPTER 4

DECISION CRITERION AND LANDFILL SITE SELECTION

4.1. Geographic Information System (GIS) Layers

The ultimate goal of the landfill site selection process is to make sure that the disposal facility is located at the best location possible with little or no impact to the environment and to the population (Sener et al., 2006).

In this study, criteria used in the analysis are air traffic safety, distance to roads, distance to settlement, geology, hydrogeology (drainage), distance to faults, distance to earthquake epicenters, slope, erosion and land use. Assignment of the criteria weights is based on previous knowledge of the criteria characteristics and local conditions of the study area, as well as on the experience of the scientists involved in the weight assignment process (Sener et al., 2006). For example, Sener et al., 2006 assign higher weight values to environmental criteria than the economic criteria, namely, land use and distance from surface water considering the distance to Lake Beyşehir and to the dense forest areas. In the study of Sener (2004), urban centers and villages are selected as criteria with highest weight value followed by surface water, flood, swamp and geology. Village road and railways are given the lowest suitability values. Similarly, Yesilnacar et al. (2012), assign the highest weight to the settlement followed by the land use, aquifer and geology. Nas et al. (2008), assign the highest weight to agricultural land class since there are many cultivated areas in Konya. Yal and Akgün (2014), on the other hand, choose the settlement as the highest weighted criterion.

In this study, the highest weight is assigned to geology followed by the land use. This is due to the potential utilization of the in situ material as a landfill liner material. Land use of the area is also important since landfills should not be placed in highly

populated areas, environmentally protected areas and irrigated lands. Detailed information on the GIS layers is presented in the following sections where the ultimate goal is to select one of the three alternative landfill sites, namely, Site A, Site B or Site C that are presented in Figure 1.2.

4.1.1. Distance to Settlement

Landfills should not be placed near a residential or an urban area to avoid any kind of negative effect on population. According to Baban and Flanagan (1998), landfills should be placed within 10 km of an urban area. Additionally, a landfill site should not be located within 250 m of a residential area according to the Turkish Solid Waste Control Regulations (TSWCR 2010). In this thesis, rankings suggested by Sharifi et al. (2009) were used (Table 4. 1.). The resulting map is presented in Figure 4. 1.

Table 4.1. *Suitability rankings based on the distance to settlements*

(Sharifi et al., 2009).

Distance to Settlement (m)	Rank
0 – 500	0
500 – 1000	0.25
1000 – 1500	0.5
1500 – 2000	0.75
> 2000	1

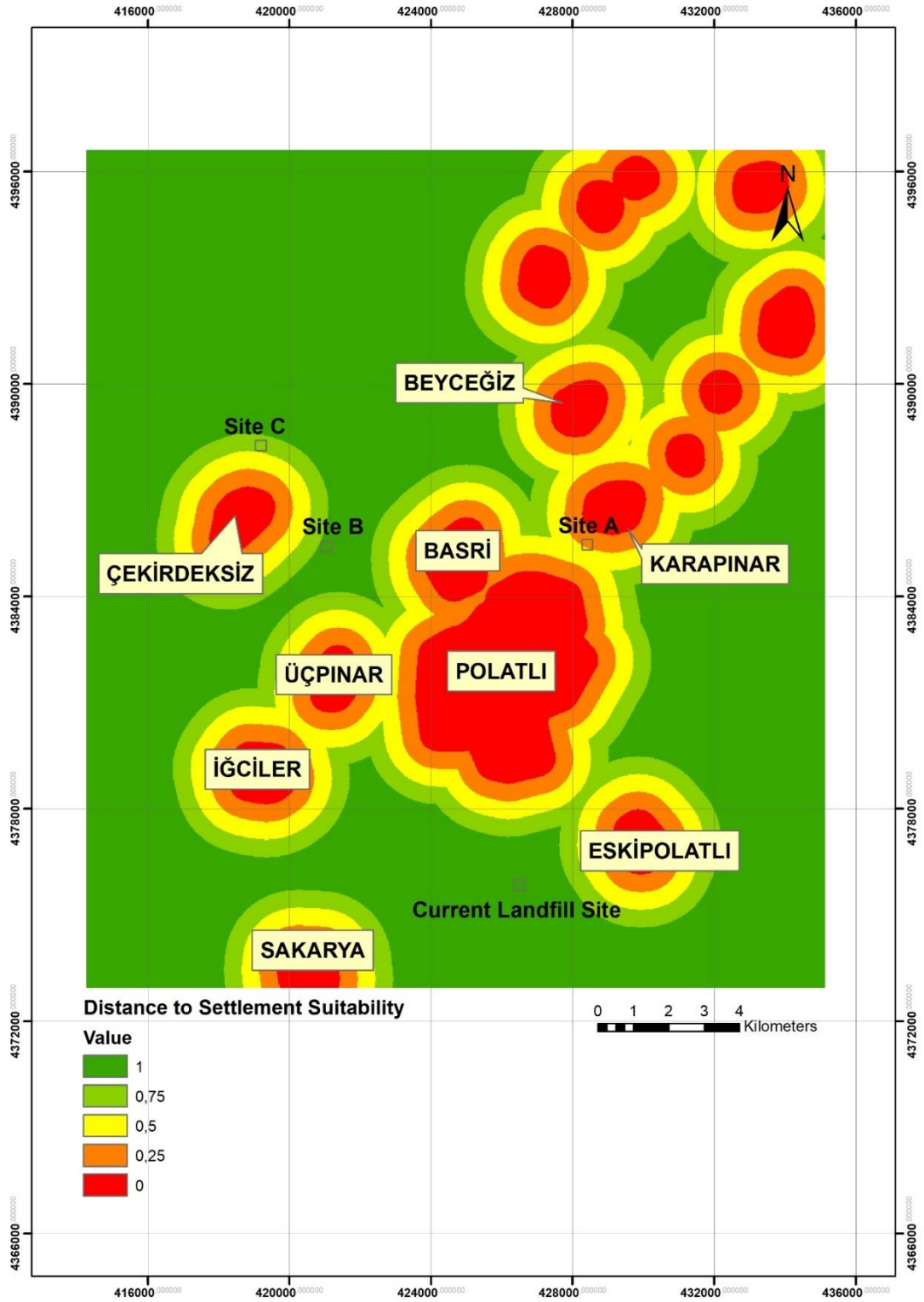


Figure 4.1. Distance to settlement suitability map

4.1.2. Distance to Roads

Information for the local roads were extracted from the topographic map produced by the General Command of Mapping (2002) and digitized in the ArcGIS software. Landfills should not be constructed very close to the roads in order not to interfere too much with the traffic (Guiqin, 2009). However, they should not be constructed too far away from the roads due to additional transportation costs. Consequently, various researchers have used different ranking values in their studies. Sener (2006) drew a 250 m buffer zone around roads and rankings were increased linearly away from these roads. Nas et al. (2008) stated that landfills should not be placed within 200 m of any existing highways or city streets. In this study, a buffer zone of 100 m was applied to all existing roads and the suitability ranking was increased linearly away from the alternative landfill sites. The related ranking values can be seen in Table 4.2.

Table 4.2. *Suitability rankings based on distance to roads*

Distance to Roads (Meters)	Suitability Rank
0-100	0,25
100-200	0,40
200-300	0,50
300-400	0,60
400-500	0,75
500+	1

Road suitability map is given in the Figure 4. 2. below:

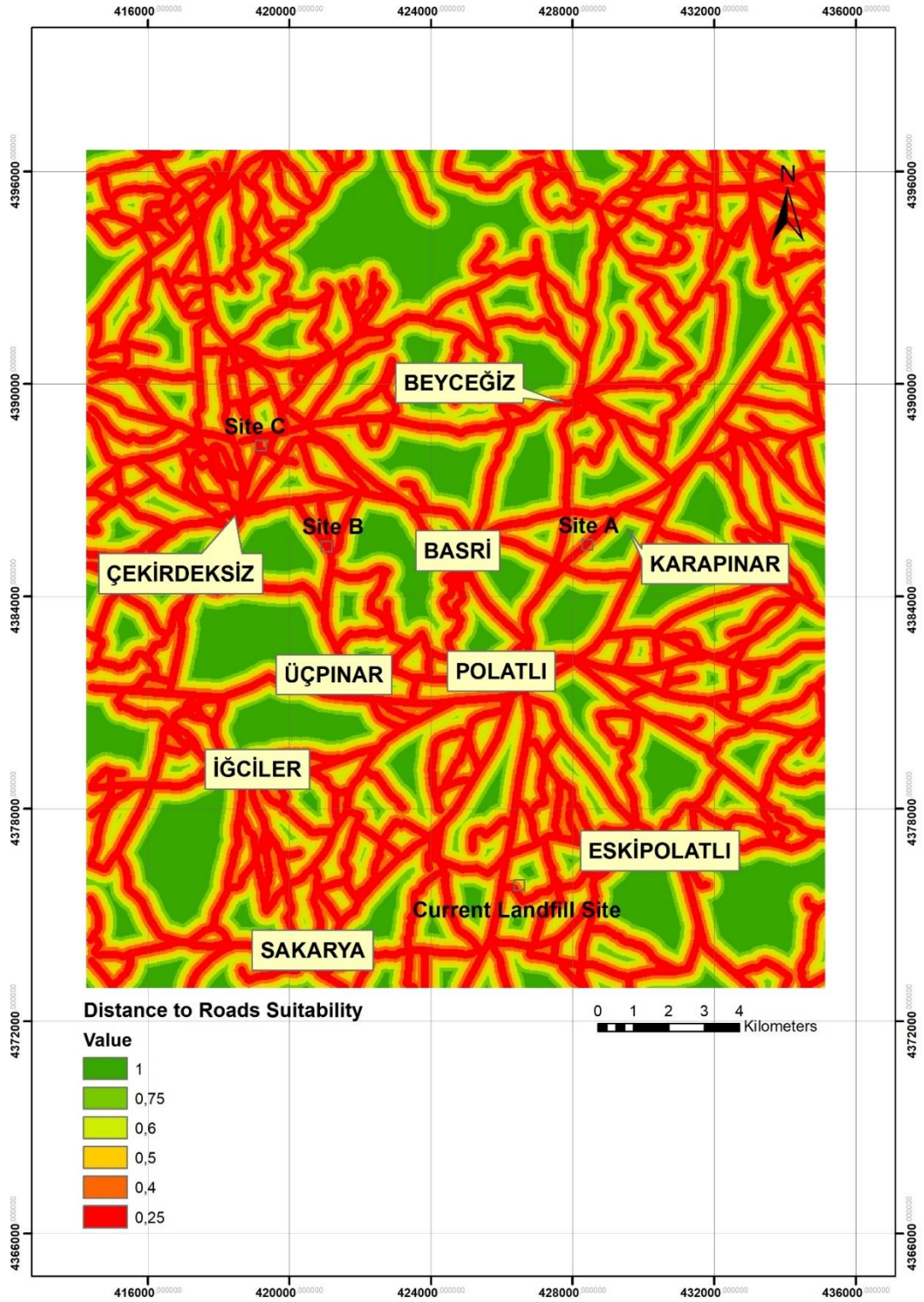


Figure 4.2. Distance to roads suitability map

4.1.3. Digital Elevation Model (DEM)

The digital elevation model (DEM) of the area was gathered from the publicly available “Advanced Spaceborne Thermal Emission and Reflection Radiometer Global Digital Elevation Model (ASTER GDEM)”. The ASTER GDEM covers land surfaces between 83°N and 83°S and is composed of 22,600 1°-by-1° tiles. The ASTER GDEM is in GeoTIFF with geographic lat/long coordinates and a 1 arc-second (30 m) grid of elevation postings. GDEM is referenced to the WGS84/EGM96 geoid. Estimated accuracies are 20 meters at 95% confidence for vertical data and 30 meters at 95 % confidence for horizontal data.

Digital Elevation Model of the region were created by utilizing the ArcGIS software. First, topographical maps were gathered from the General Command of Mapping. Then, topographical contours were digitized by using the ArcGIS software. The minimum curvature method was employed in creating the DEM. The created DEM can be observed in Figure 4.3.

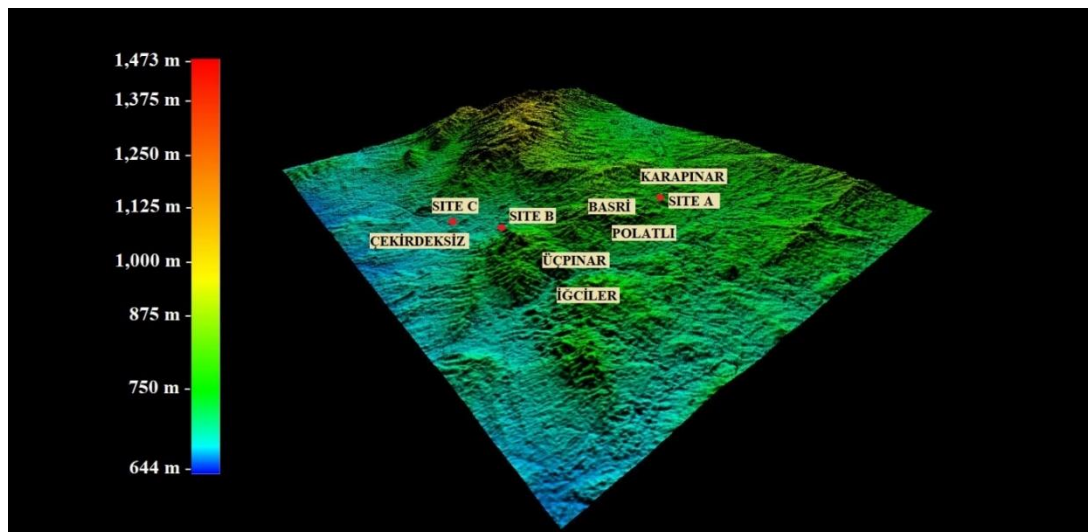


Figure 4.3. Digital elevation model (DEM) of the study area

4.1.4. Slope

Constructing a landfill in a steep slope would cause a lot of excavation costs. Also, too flat areas might be unsuitable due to flooding problems. Because of these reasons, it can be inferred that landfills should not be constructed in too steep or in too flat areas. Many researchers used different ranking for slope values in their site selection studies. According to Bagchi (1994), areas with slope values greater than 15% should be considered as unsuitable and below 15% suitable for siting a landfill. Akbari et al. (2008), on the other hand, stated that slopes steeper than 20% are not suitable for landfills. In this study slope values were categorized in 4 classes. Related classes can be observed in Table 4.3.

Table 4.3. *Suitability rankings based on slope values*

Slope (Degree)	Suitability Rank
0-5	0,25
5-10	1
10-15	0,75
15+	0

The slope map of the study area was generated from the digital elevation model (DEM). The slope tool was utilized in the ArcGIS software to transform DEM into a slope map layer. The resultant map presented by Figure 4.4. was separated into 4 suitability classes as mentioned above.

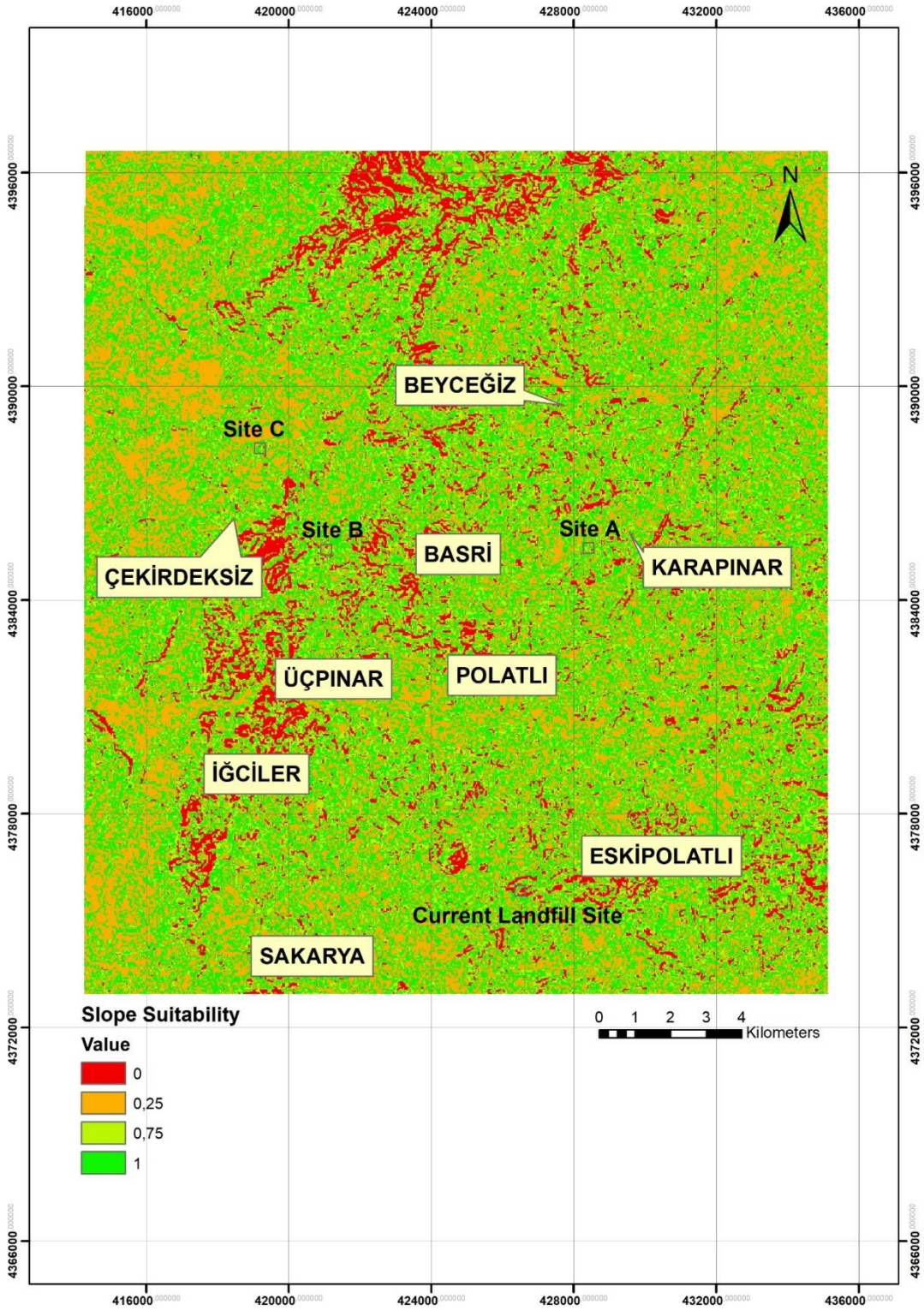


Figure 4.4. Slope suitability map of the study area

4.1.5. Geology

The 1/100000 geological map acquired from General Directorate of Mineral Research and Exploration was used for obtaining information on the geology of the area. The geological formations were digitized, and a vector map was generated utilizing the ArcGIS software.

The lowest suitability rank was assigned to alluvium, slope debris and old alluvium formations since they possess the possibility of a shallow groundwater level and possibility of flooding due to the presence of the uncemented gravel and sand units. The highest ranking, on the other hand was given to the Hañçili Formation (Tmh) due to its high fine-grained soil content which is considered as a suitable landfill liner material. The other geological formations were assigned values between 0 and 1 with respect to their suitability as a landfill site material which is presented by Table 4.4. Figure 4.5. presents the geological suitability map generated for the study area.

Table 4.4. *Suitability rankings based on geological formations*

Formation	Suitability Rank
Tmh	1
Teb, Tmsg, Tmplag, Tmhb, Tmsy	0.75
Tpek, Tpk, Tmplay, Tee, Tpei	0.25
Qal, Qeal, Qym	0

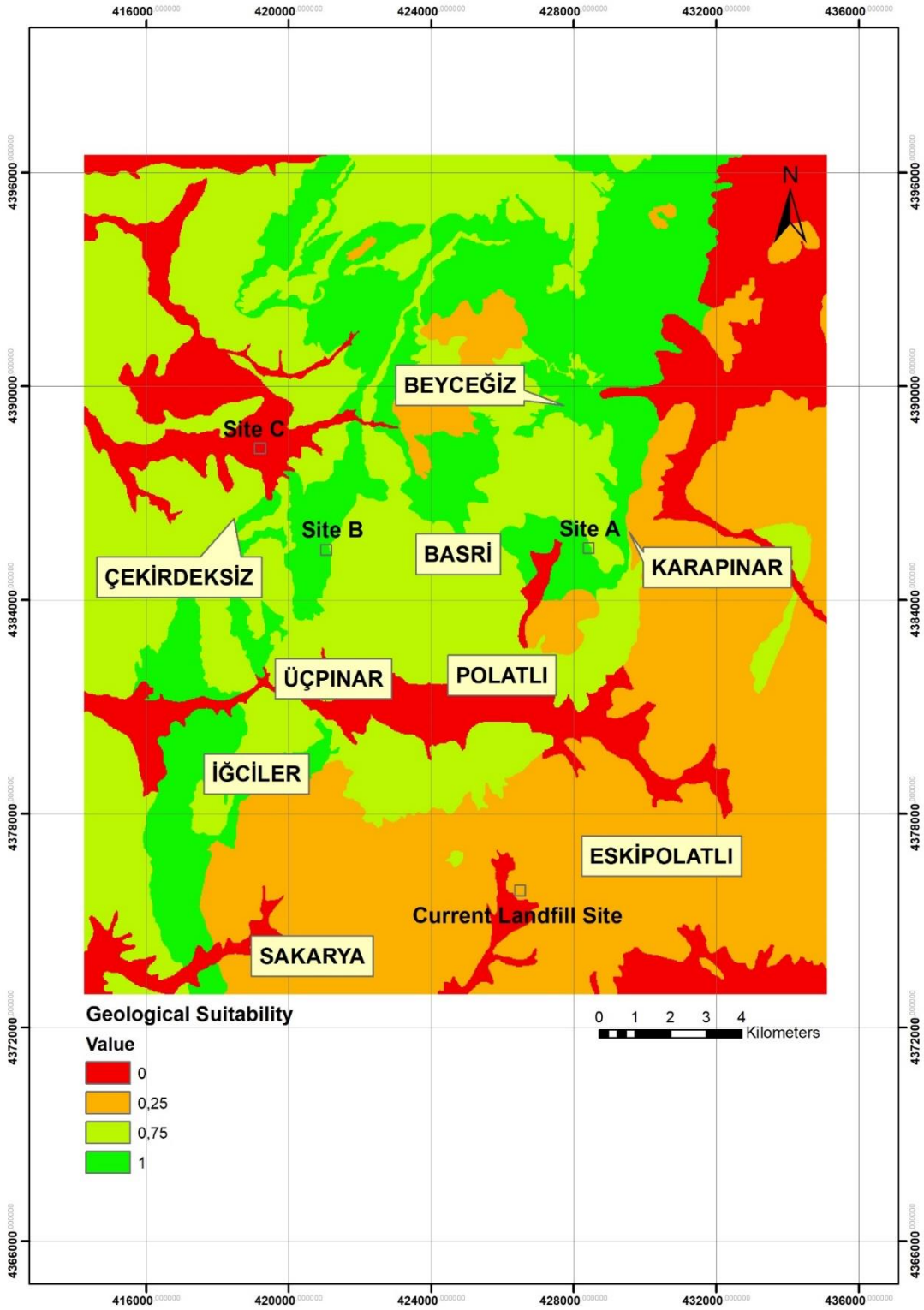


Figure 4.5. Geological suitability map of the study area

4.1.6. Distance to Faults

Different researchers used different distance values for lineaments in their site selection studies. For example, in the study of Sener et al. (2006), all lineaments were buffered and weighed between 0-200 meters. Sharifi (2009) applied a buffer zone of 100 meters. Akbari et al. (2008), used a buffer zone of 100 meters around the faults. By considering this information, a total of five distance classes were specified and the corresponding rankings were assigned (Table 4.5.). The faults in the study area were extracted from the 1/100000 scaled geological map of Ankara prepared by General Directorate of Mineral Research and Exploration. The faults were digitized by using the ArcGIS software so that the resultant suitability map presented by Figure 4.6. was obtained.

Table 4.5. *Suitability rankings based on the distance to fault (Sharifi, 2009)*

Distance to Faults (m)	Suitability Rank
0 – 100	0
100 – 400	0.25
400 – 1500	0.5
1500 - 5000	0.75
1500+	1

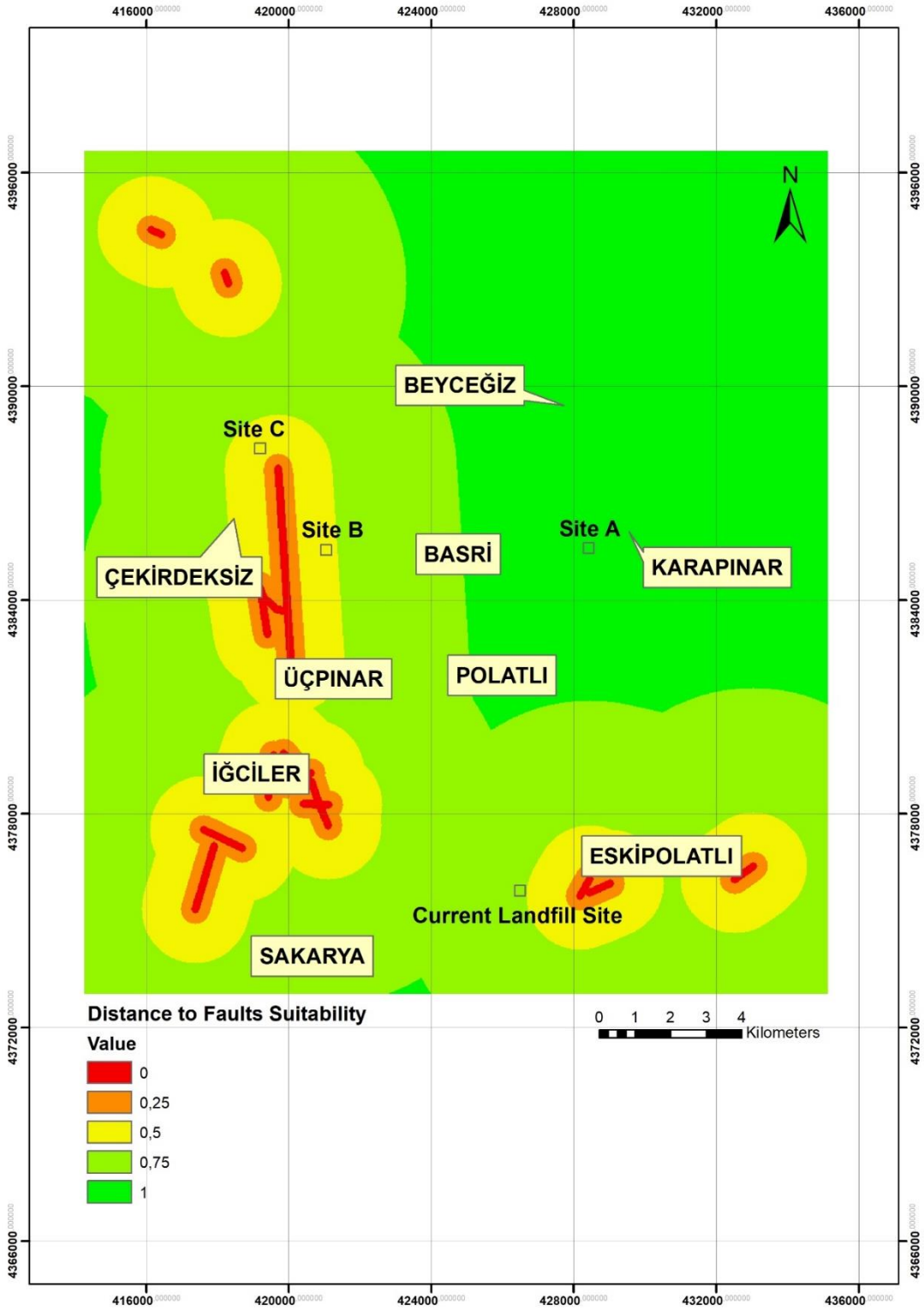


Figure 4.6. Distance to faults suitability map

4.1.7. Hydrogeology (Drainage)

The drainage map was generated by the ArcGIS software based on the digital elevation model (DEM) of the study area. Afterwards, the generated drainage map was reclassified based on the distance to the flow lines and was assigned weights. The distance values suggested by Sharifi et al. (2009), were used prior to the analysis (Table 4.6.). The resultant suitability map is presented by Figure 4.7.

Table 4.6. *Suitability rankings based on the distance to the flow line (modified from Sharifi et al., 2009)*

Distance to Flow Lines (m)	Suitability Rank
0 -100	0
100 – 400	0.25
400 – 1000	0.75
1000+	1

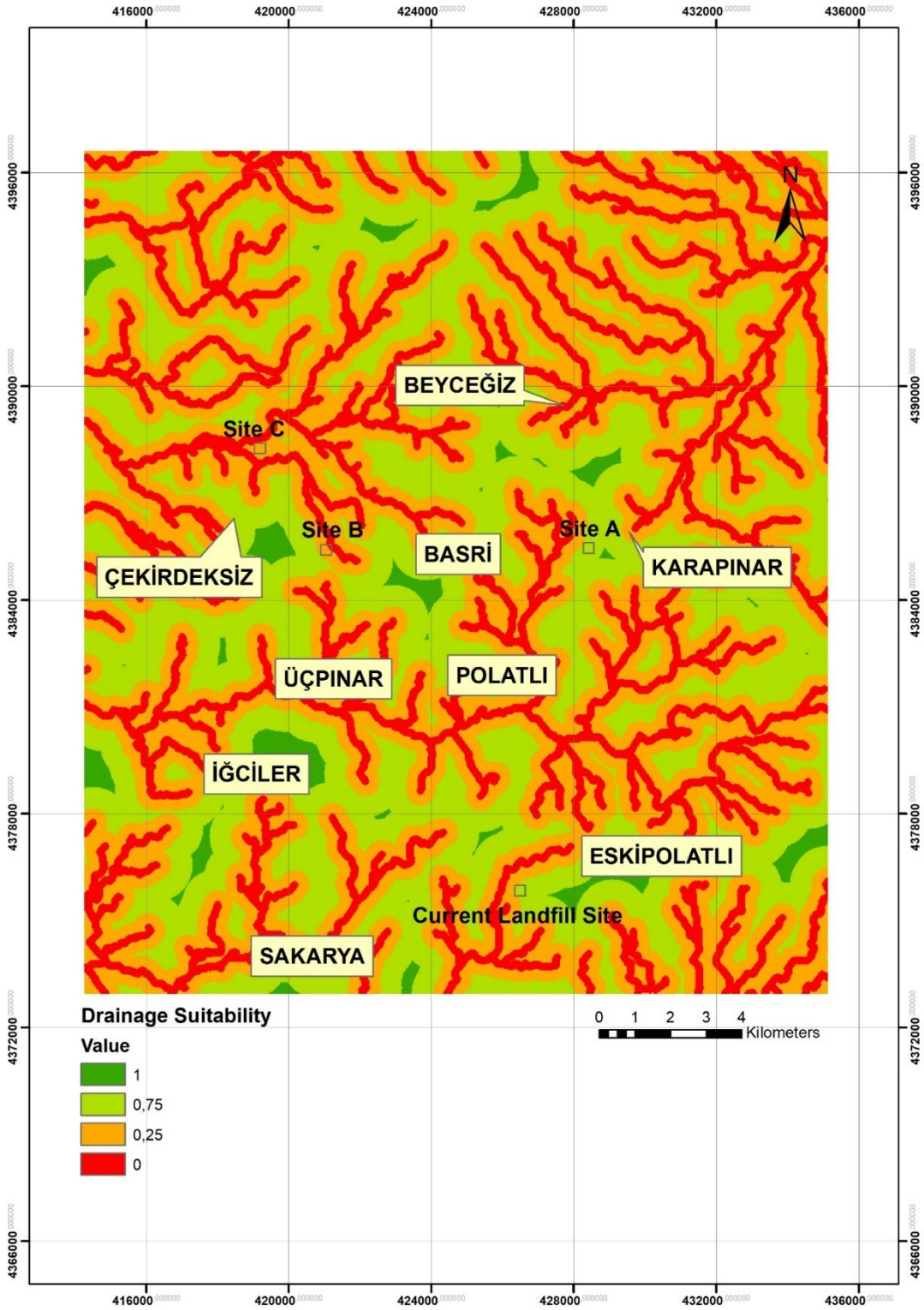


Figure 4.7. Hydrogeology (Drainage) suitability map of the study area

4.1.8. Land Use

The land use map of the study area was acquired from the publicly available Corine Land Cover Map (Figure 4.8.). This map was digitized in an ArcGIS environment and reclassified according to the weights determined before. All of the unused areas, non-irrigated lands were considered to be suitable for a landfill site and a suitability rank of 1 was assigned to these areas. Areas that were utilized in the form of irrigated lands, settlements, factories, on the other hand were considered to be unsuitable and were assigned suitability rank of 0 (Table 4.7.). These suitability rankings were assigned in this thesis since landfills should not be constructed in populated areas, forests, near factories and protected areas etc. in order not to effect negatively the environment, population and natural habitat.

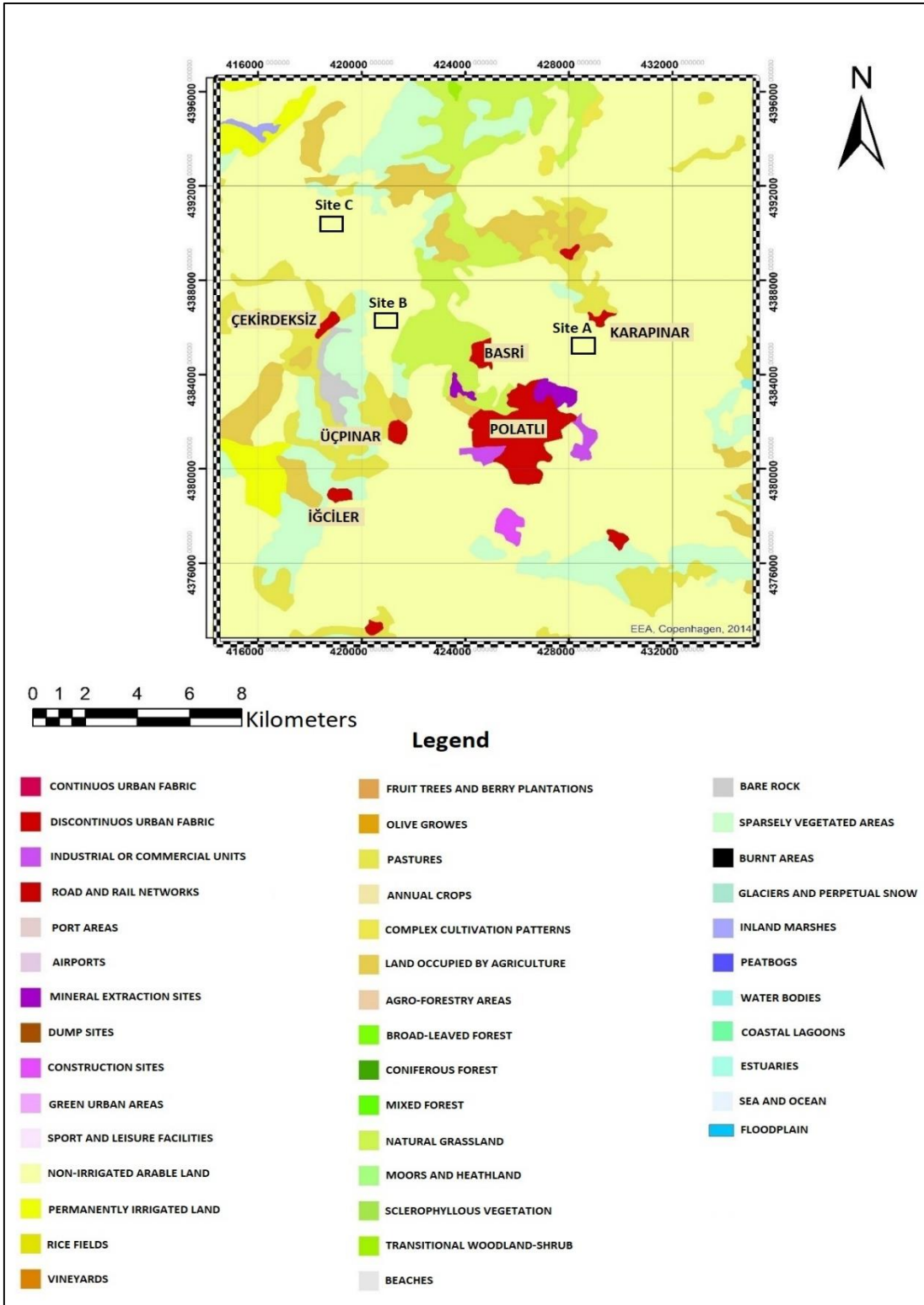


Figure 4.8. Land use map of the study area (EEA, 2018)

Table 4.7. *Land use suitability rankings (Yal and Akgün, 2013)*

Land Use	Suitability Rank
Non-Irrigated Lands, Dry Fields, Unused Areas	1
Irrigated Lands, Forests, Settlements, Occupied Areas	0

Figure 4.9. presents the land use suitability map.

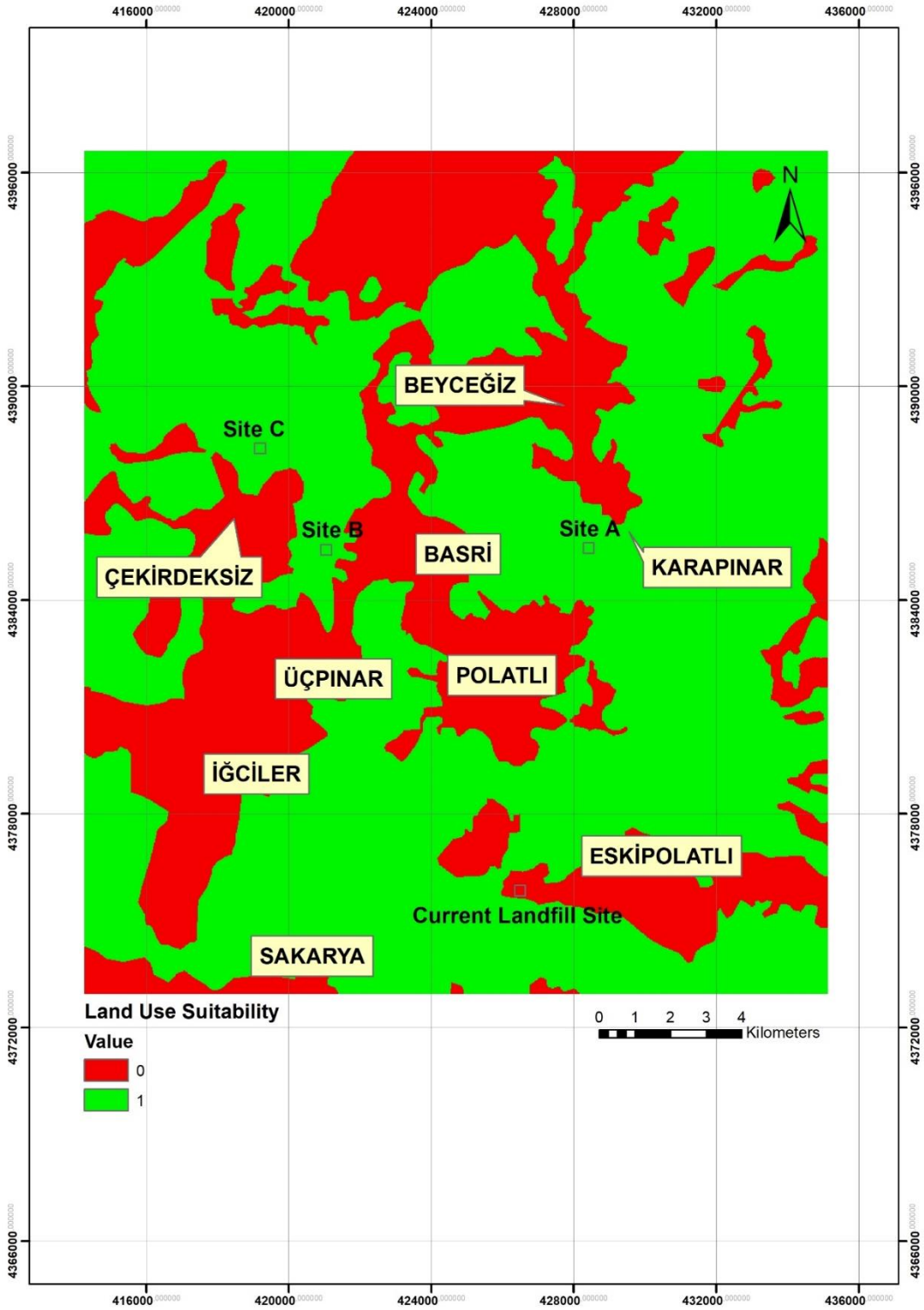


Figure 4.9. Land use suitability map of the study area

4.1.9. Erosion

Areas which are prone to high levels of erosion should be avoided when constructing a landfill site due to the vulnerable geology caused by erosion. Erosion susceptibility is strongly affected by the soil type and lithology (Tehrany et al., 2013). In this thesis, erosion suitability rankings were assigned based on the findings of Bilgin et al. (2009). According to this study, Quaternary sediments are found to be the most prone to erosion and were assigned lowest suitability rankings. Alluvium was considered to have very high erosion potential since it is located at the current river beds and composed of uncemented gravel and sands. Old alluvium was assigned high potential due to its uncemented composition and Pleistocene age. Slope debris was given moderate potential since it is located at the low angle side of the hills and is composed of uncemented gravel and mud deposited as a result of flooding. Rest of the formations were considered as low potential and assigned highest suitability ranking (Table 4.8.). Erosion suitability map is presented in Figure 4. 10.

Table 4.8. *Erosion suitability rankings (modified from Yal and Akgün, 2013)*

Erosion Risk	Suitability Rank
Low Potential	1
Moderate Potential	0,75
High Potential	0,5
Very High Potential	0

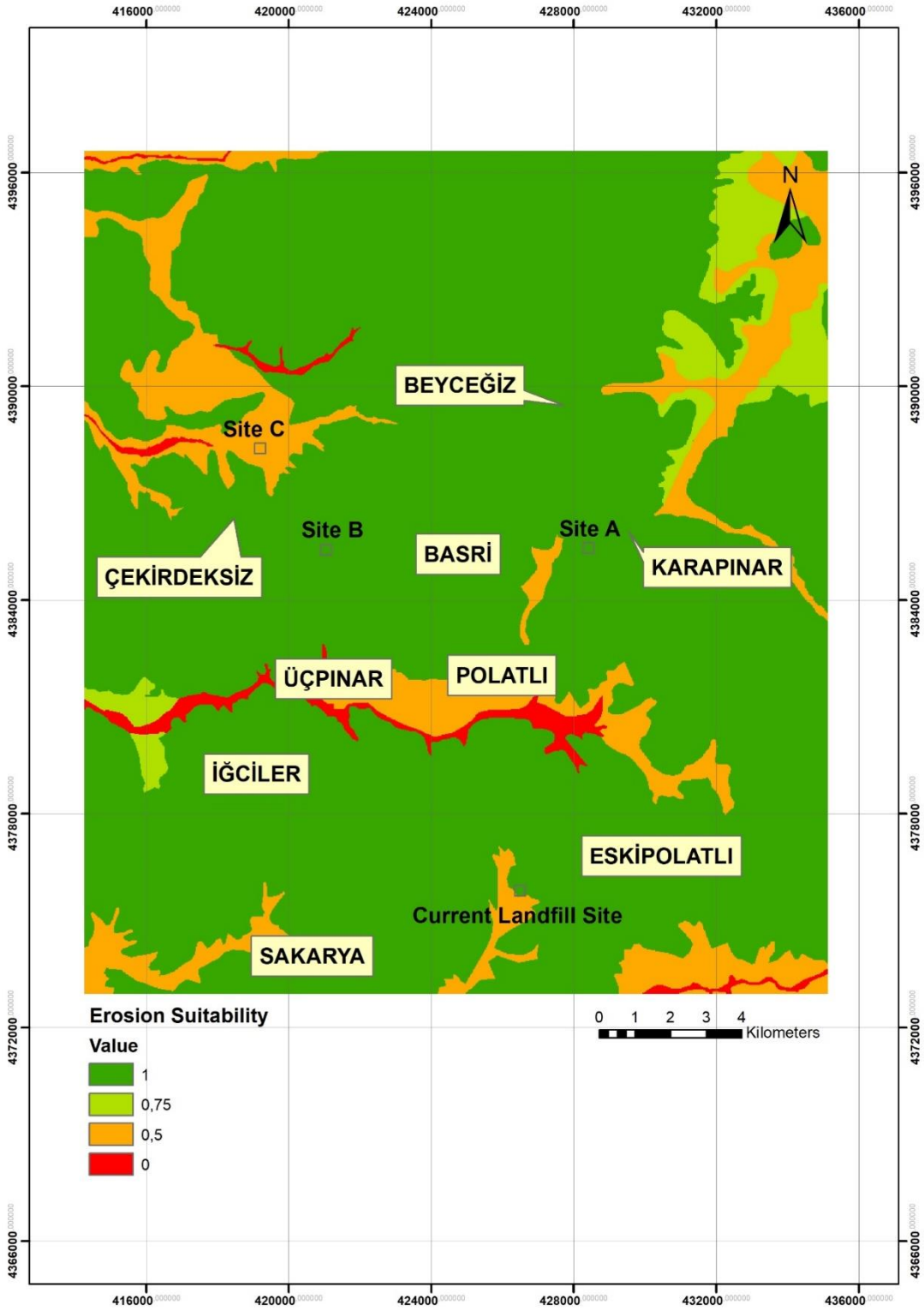


Figure 4.10. Erosion suitability map of the study area

4.1.10. Distance to Earthquake Epicenters

According to the U.S. Environmental Protection Agency (USEPA), new sanitary landfill units should not be located in seismic impact zones and should be designed to resist the maximum horizontal acceleration in lithified earth material. A seismic impact zone implies an area with a ten percent or greater probability that the maximum horizontal acceleration in lithified earth material, expressed as a percentage of the earth's gravitational pull (g), will exceed 0.10g in 250 years.

In this thesis, earthquakes that have occurred in the past 100 years were gathered from the Kandilli Observatory and Earthquake Research Institute (KOERI, 2018), and then imported to a GIS environment. A 60-meter-wide buffer zone was applied and the suitability of the alternative site was increased linearly away from the earthquake epicenters. It is not very common in the literature to use earthquake epicenters as a criterion in landfill site selection. However, based on the definition of a seismic impact zone, epicenters were considered as a restricted criterion in this study. In Table 4.9., the suitability rankings have been assigned relative to the distance from the epicenters.

Table 4.9. *Suitability rankings based on distance to earthquake epicenters*

Distance to Earthquake Epicenters (m)	Suitability Rank
0 – 60	0
60 – 200	0.25
200 – 500	0.5
500 -1000	0.75
>1000	1

The resultant suitability map is presented by Figure 4.11.

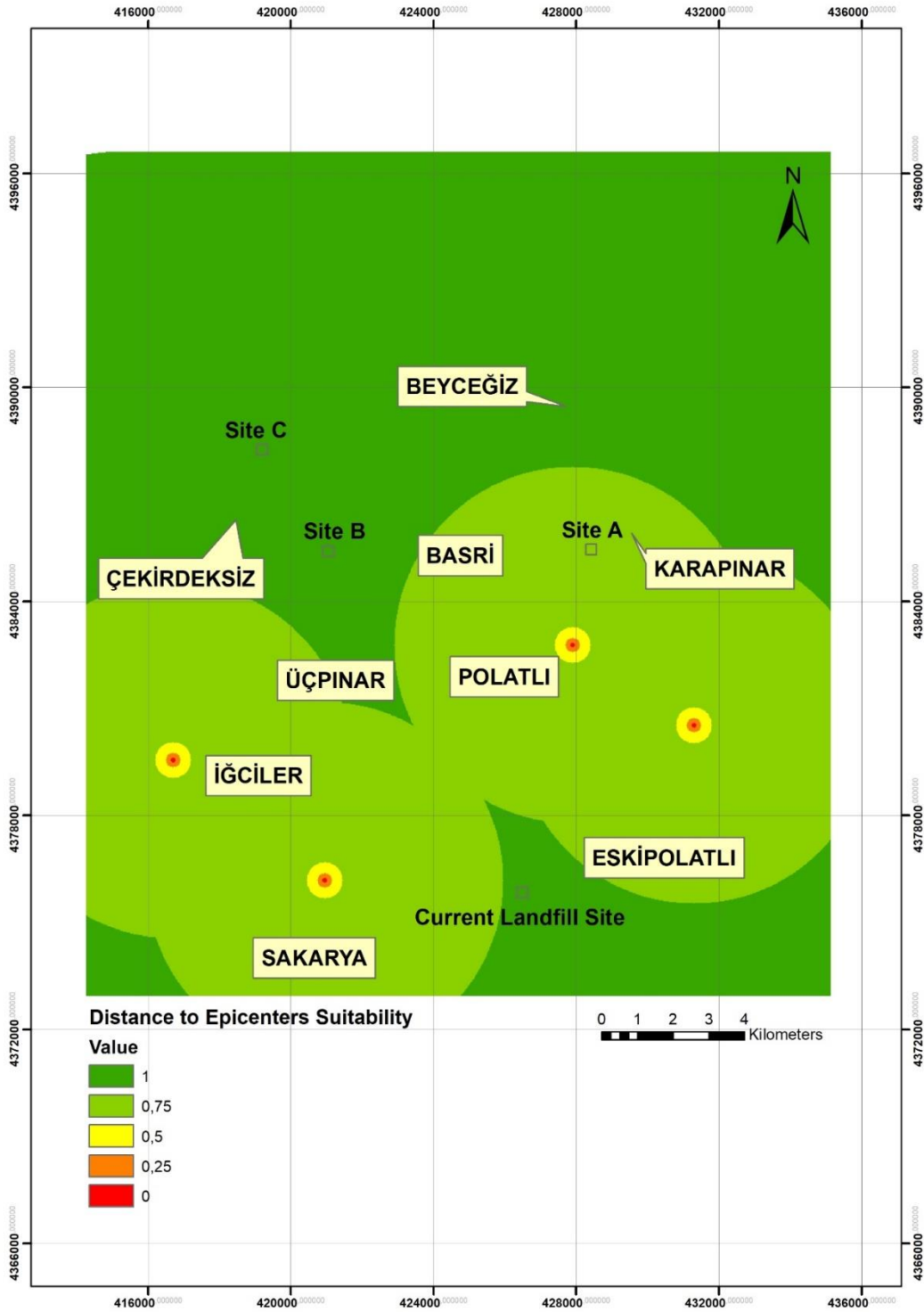


Figure 4.11. Distance to earthquake epicenters suitability map of the study area

4.2. Other Criteria

4.2.1. Air Traffic Safety

According to Baghci (1994), landfills should not be constructed within the 3048 meters of an airport. EPA (2010), also suggests the same distance value. By considering the suggested values, the safe distance for an airport was determined to be 1500 meters in the study of Yesilnacar (2012). Since the closest airport (Temelli Hava Limanı) and its runway are located approximately 25 km from the center of Polatlı Municipality, the effect of airports has not been considered as a restricted criterion (Figure 4.12.).



Figure 4.12. Map showing the closest airport to the alternative sites

4.2.2. Political and Social Criteria

In addition to the selected criteria, landfill site selection studies also require a comprehensive evaluation of the social and political aspects as well (Kharat et al., 2016). All of the selection work has been performed along with authorities from the

Polatlı Municipality. In every stage of the site selection study, municipality personnel were consulted and informed. However, these factors have not been included in this study since it is not possible to incorporate them into the TOPSIS analysis. But it is strongly suggested to take into consideration for further studies.

4.3. TOPSIS Analysis

All of the attribute layers were digitized and prepared prior to TOPSIS analysis. Initially, the layers have been standardized since it was not possible to compare them without standardization. After that, all the layers were reclassified in conjunction with the assigned weight values. Finally, TOPSIS analysis was performed by utilizing the ArcGIS model builder tool (Figure 4. 13.) to obtain the final suitability map presented by Figure 4.14. The final suitability map was also reclassified into 4 different classes, namely, not suitable, fairly suitable, suitable and very suitable. Approximately 15% of the study area was determined to be not suitable, 17.5% fairly suitable, 34.5% suitable and 33% very suitable. According to this map, it should be noted that the current open dump site is situated in an area which is not suitable to construct a landfill. When alternative sites A, B and C are considered, it could be concluded that Site C lies in a fairly suitable area whereas Site A and B are situated in a very suitable part of the study area. These findings show that best locations to construct a landfill are Site A and Site B.

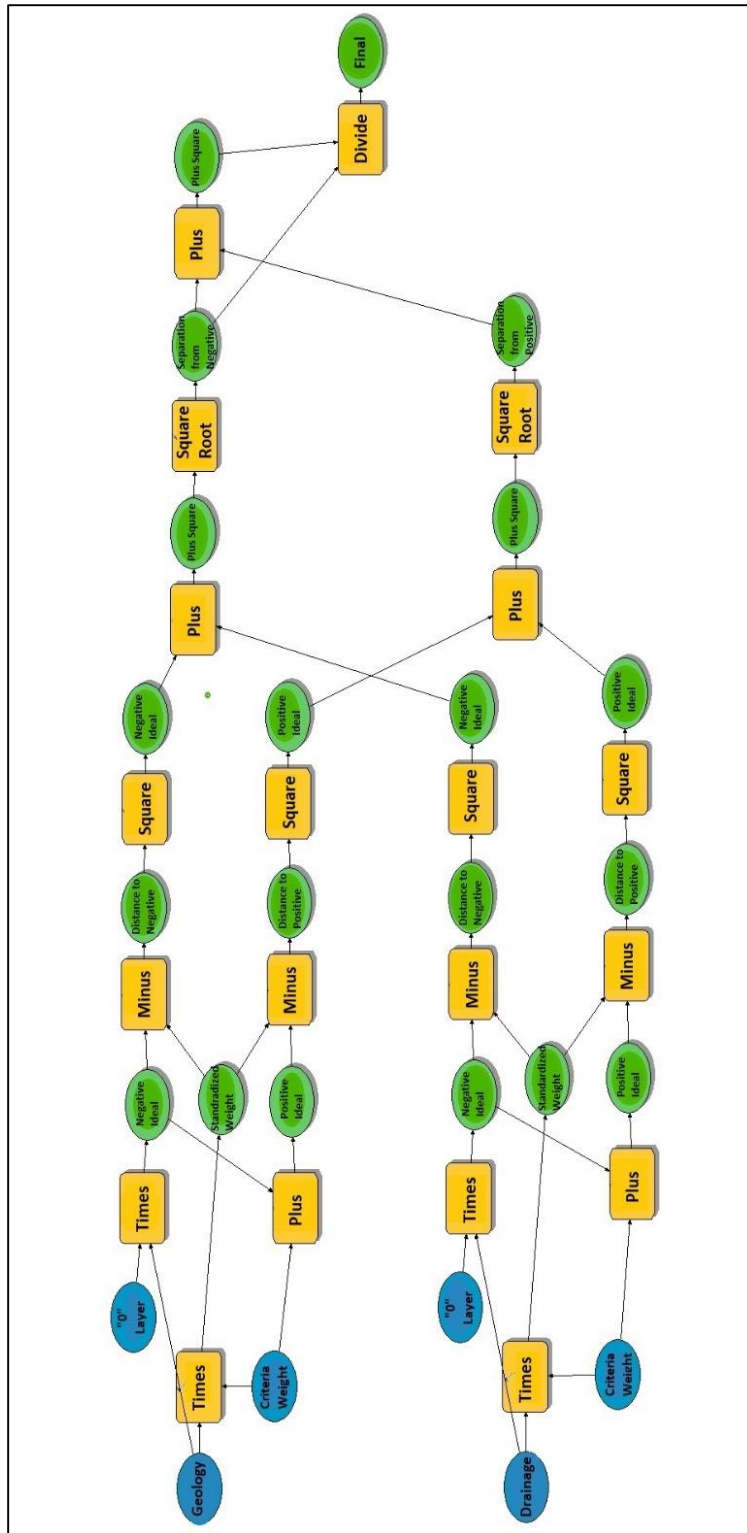


Figure 4.13. Modal builder data tree sample for geology and drainage layers

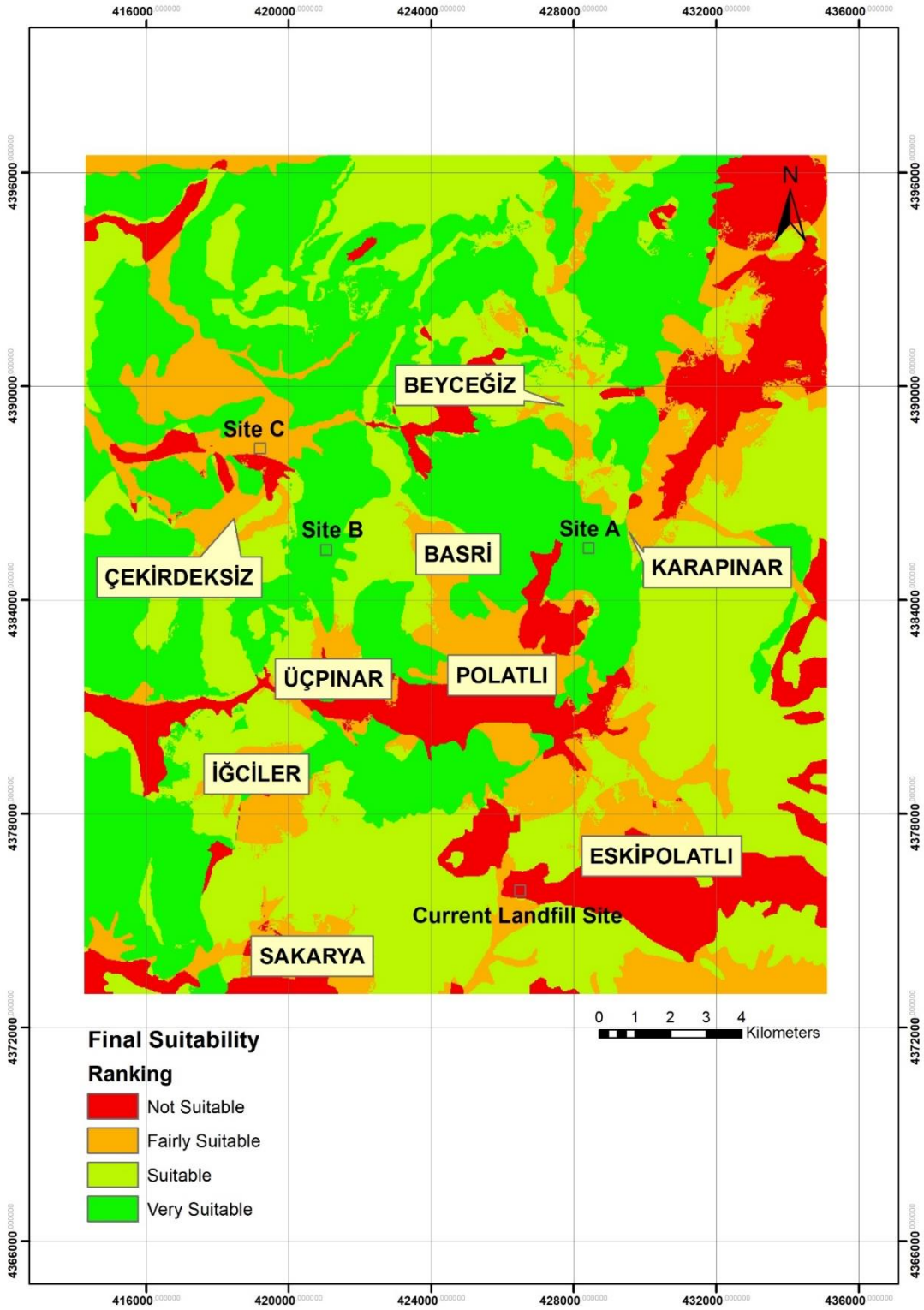


Figure 4.14. Final landfill site suitability map

4.4. Sensitivity Analysis and Discussion

Sensitivity analysis may be performed in various ways like changing the weight values of the criteria layers, changing the buffer zones of the layers and excluding one layer at a time and repeating the analysis to observe its effect on the final resultant map (Yal and Akgün, 2013). A sensitivity analysis was performed in this study to find out the individual effects of each layer to the final suitability map. The analysis was performed and repeated by excluding one layer at a time.

One of the layers was excluded in each analysis and a total of 9 suitability maps were generated. Each layer was reclassified into four classes from 1 to 4 where 1 is the least suitable and 4 is the most suitable. The number of cells corresponding to each suitability class was calculated. Figure 4.15. presents the number of cells corresponding to the suitability class 4. The red bar shows the analysis where every criteria is included. The blue bar, on the other hand, represents the analysis with one layer excluded. The difference between the red and blue bars indicates the effect of that particular layer. The most variation was observed in geology layer. This shows the importance of geology of the area for the analysis. When the geology layer was excluded from the analysis the study area becomes more suitable. Based on this information, it can be concluded that the geology and geotechnical characteristics of the area has to be examined in more detail. The geological information used in this study was gathered from the geological maps and collected soil samples. Comprehensive borehole studies are suggested in order to better understand the geological formations and the geotechnical parameters of the study area. Furthermore, land use and distance to settlement criteria also seem to have a noticeable difference from the analysis where all the layers were included. This can be explained by the importance of this layers.

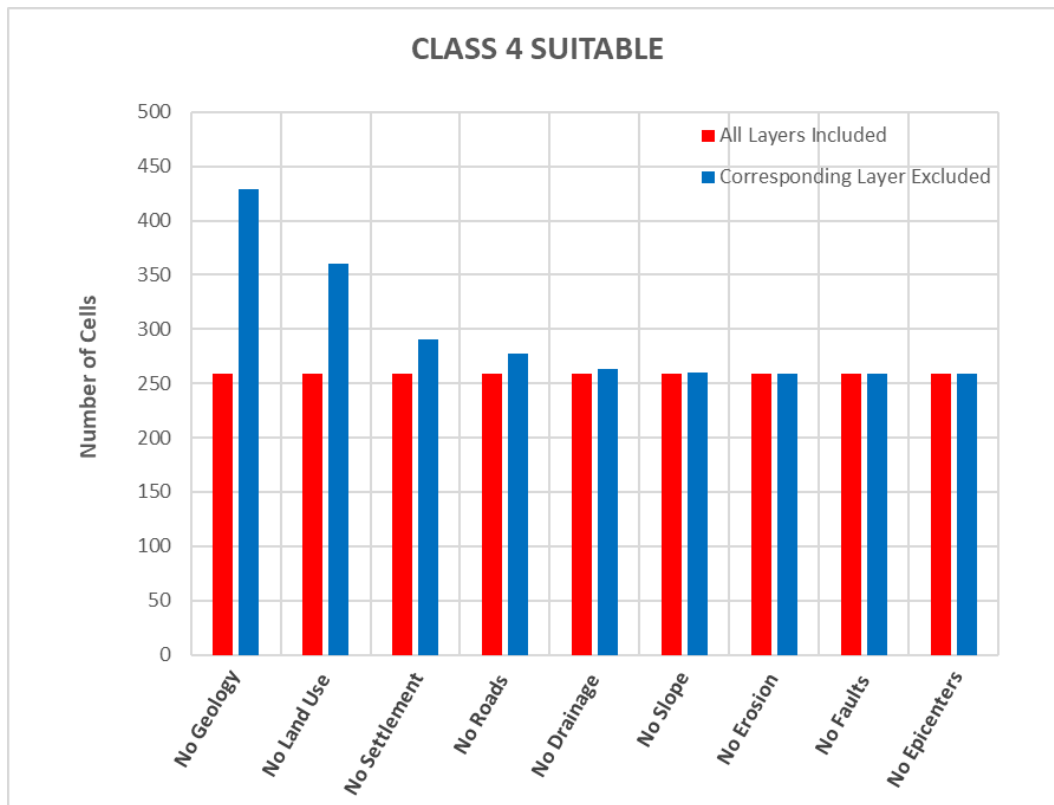


Figure 4.15. The number of cells corresponding to suitability class 4 (most suitable)

The number of cells corresponding to the suitability class 1 (least suitable) is presented in the Figure 4. 16. When the number of cells which correspond to class 1 for the map where a layer is excluded is less than the complete analysis, it indicates a problem. This situation is observed mainly in settlement and road layers. According to many studies and regulations, municipal landfills should be located at least 250 meters away from the settlements. In the study area, all of the alternative landfill sites are located more than 1000 meters away from the nearest settlement. From this point of view, difference can be overseen. When utilizing the road layer for the TOPSIS analysis, distance values suggested by Sharifi et al. (2009), were used. In order to be more precautionous, a more conservative approach may be followed. That means, alternative sites may be placed farther away from the existing roads. Since the study area is relatively small, there is not enough space to site a landfill that too far away from

existing roads. Hence distance values used in this study can be considered as fairly reasonable. Consequently, this sensitivity analysis showed the importance of geological and geotechnical characteristics of the study area. Additionally, more conservative approach may be followed for the distance to roads criteria.

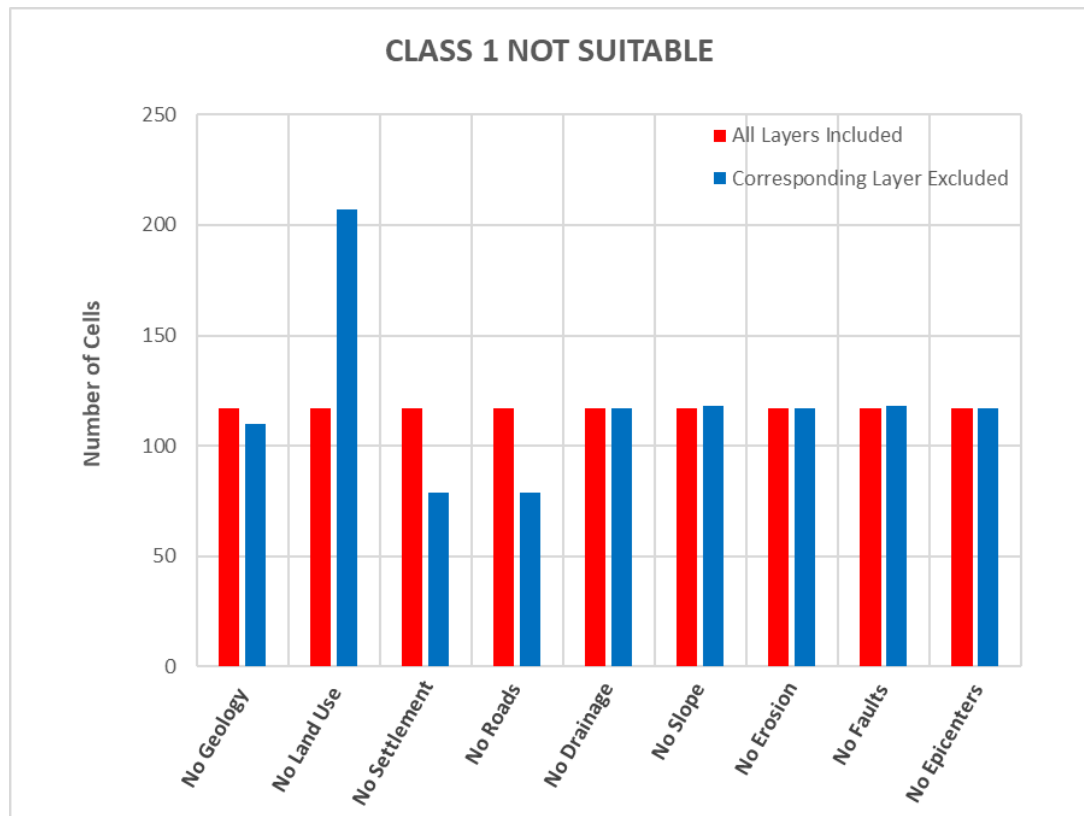


Figure 4.16. The number of cells corresponding to suitability class 1 (least suitable)

CHAPTER 5

LANDFILL LINER DESIGN

5.1. Introduction

The primary objective of landfill liner design is to provide effective control measures to prevent or reduce as far as possible negative effects on the environment, in particular the pollution of surface water, groundwater, soil and air, as well as the resulting risks to human health arising from landfilling of waste. Landfill practice is dynamic in that it will change with both advances in technology and changes in regulations. In this section, different landfill profiles are designed to simulate liquid movement through sanitary landfills by using the Hydrologic Evaluation of Landfill Performance (HELP) model which is a quasi-two dimensional hydrologic model of water movement across, into, through and out of landfills. The model uses three types of data which are weather, soil and design, then uses solution techniques which account for the effects of surface storage, snowmelt, runoff, infiltration, evapotranspiration, vegetative growth, soil moisture storage, lateral subsurface drainage, leachate recirculation, unsaturated vertical drainage, and leakage through soil, geomembrane or composite liners (Schroeder, 1994). Different types of landfill systems can be modeled utilizing the HELP model. In this study, four different landfill profiles were modeled from least to most conservative.

The site selection study was conducted as mentioned in the above sections. After determining the suitable location to construct a landfill site, the next step is to evaluate and ultimately judge geotechnical and mineralogical characteristics of the lining system design at the selected landfill site. The Visual HELP model was utilized in order to simulate the hydrologic processes of the landfill over a period of 20 years.

5.2. Standards and requirements

5.2.1. US Environmental Protection Agency-Criteria for Municipal Solid Waste Landfills

The US Environmental Protection Agency (EPA) requires the use of a composite liner and a leachate collection system that is designed and constructed to maintain less than a 30-cm depth of leachate over the liner when constructing a municipal landfill. For the purposes of this section, a composite liner implies a system consisting of two components; the upper component must consist of a minimum of 30-mil (about 1 mm) thick flexible membrane liner (FML), and the lower component must consist of at least a 0.6 m thick layer of compacted soil with a hydraulic conductivity of no more than 1×10^{-9} m/s. FML components consisting of high density polyethylene (HDPE) shall be at least 60-mil (about 2 mm) thick. The FML component must be installed in direct and uniform contact with the compacted soil component. In addition to these specifications, the following factors have to be taken into consideration (U.S. Environmental Protection Agency, 2010):

- The hydrogeological characteristics of the facility and surrounding land;
- The climatic factors of the area;
- The volume and the physical and chemical characteristics of the leachate;
- The quantity, quality, and direction of flow of groundwater;
- The proximity and withdrawal rate of the groundwater users;
- The availability of alternative drinking water supplies;
- The existing quality of the groundwater, including other sources of contamination and their cumulative impacts on the groundwater, and whether the groundwater is currently used or reasonably expected to be used for drinking water;
- Public health, safety, and welfare effects; and

- Practicable capability of the owner or operator.

5.2.2. Turkish Republic, Ministry of Environment - Criteria for Municipal Solid Waste Landfills

According to the Turkish regulation of solid wastes (TSWCR, 2010), the following standards have to be met:

- The liner of the landfill facility should be constructed in such a way that the landfill generated leachate should not interfere with the groundwater. In order to achieve this, the landfill liners need to be of low permeability. Additionally, the leachate has to be collected with a proper drainage system placed at the bottom of the landfill.
- The bottom of the liner has to be at least 1 meter above the maximum natural groundwater level.
- Clay or the similar low permeability natural or artificial material which has a compacted thickness of 0.60 m should be placed at the bottom of the landfill. The permeability of these materials should not be more than 1×10^{-9} m/s.
- If more than 3 meters thick natural clay or a similar fine grained natural material is to be used at the bottom, the liner of the landfill does not have to be covered with another impermeable material. In this case, it has to be ensured that the permeability is 1×10^{-8} m/s in every part of the landfill.
- The High Density Polyethylene (HDPE) liner to be placed above the low permeability clay or fine-grained low permeability soil layer is required to be at least 2 mm (60-mil) thick. The density of this component should be 941-965 kg/m³. In order to collect the leachate which will originate from the landfill, drainage pipes have to be installed. Permeable materials like sand or gravel are placed to serve as filters. The height of this filter layer should be at least 30 cm from the drainage pipe.
- All of the collected leachate needs to be purified in accordance with discharge limits in control of the water contamination regulations.

5.3. Data Description for Visual HELP

The HELP model requires 3 types of input data for each model profile. These are:

- Weather data,
- Soil properties, and
- Design information.

The meteorological input data required for the HELP model are: monthly temperature and precipitation, evaporative zone depth, maximum leaf area index, annual average wind speed, average quarterly relative humidity and dates starting and ending the growing season. In addition, the software requires soil information to accurately simulate hydrologic processes over the years. This information was acquired by comprehensive geotechnical laboratory tests. Specific gravity, Atterberg limit tests, Standard Proctor and falling head permeability tests were conducted in order to be utilized in the HELP model. Furthermore, mineralogical tests, namely, X-ray diffraction (XRD), methylene blue and Scanning Electron Microscopy (SEM) tests were performed. Even though visual HELP does not use mineralogical properties as input data, they may help better understand the nature of the soil and long term feasibility of this in-situ material. Finally, design information has to be specified prior to modelling. In this study four different landfill profiles were created and evaluated. The thickness, porosity, field capacity, wilting point and saturated hydraulic conductivity of the layers has to be specified. The following sections explain these input data in detail.

5.3.1. Weather data

HELP requires three types of weather data which are evapotranspiration, precipitation and temperature.

Evapotranspiration data is composed of maximum leaf area index, dates starting and ending the growing season, normal average annual wind speed and normal average quarterly relative humidity. The evaporative zone depth is defined as the maximum

depth from which water can be removed by evapotranspiration. The maximum leaf area index (LAI) is the dimensionless ratio of the leaf area of actively transpiring vegetation to the nominal surface area of the land on which the vegetation is growing. The evaporative zone depth and maximum leaf area index (LAI) were entered manually to the software. The rest of the evapotranspiration data were provided by the General Directorate of State Meteorological Works.

5.3.1.1. Evaporative zone depth

This is the maximum depth from which water can be removed by evapotranspiration. The program does not allow the evaporative zone depth to exceed the depth to the uppermost geomembrane liner or to the barrier soil layer. There are three different values of this parameter in the evaporative zone depth box for the specified location. These values are characteristic for grassy vegetation on a thick layer of loamy soil and they correspond, in growing order, to bare soil, fair and excellent stand of grass, respectively. The evaporative zone depth can be 2-3 times shallower for sandy soil and 2-5 times deeper for clayey or fine-grained soil. In this study, the evaporative zone depth was taken as 66 cm considering a fair stand of grass.

5.3.1.2. Maximum leaf area index (LAI)

The leaf area index is the ratio of the leaf area of actively transpiring vegetation to the surface area on which the vegetation is growing. The maximum value for bare soil is 0. For a poor stand of grass, the typical value is 1. For a fair, good and excellent stand of grass, typical values are 2, 3.5 and 5, respectively. LAI was taken to be 2 due to the fair stand of grass in the area.

5.3.1.3. Growing season start and end days

The start and end of the growing season are determined, generally, by air temperature. For example, in North America the growing season starts when the mean daily temperature rises above 10-12 °C (50 - 55 °F). The input data for the growing season

starting and ending days were obtained from the meteorological database of HELP (Table 5. 1.).

The other evapotranspiration data were gathered from the Turkish State of Meteorological Works as presented in Table 5.1. Since the landfill is planned for a lifespan of 20 years, it is assumed that the precipitation and temperature distribution data between the years 1998-2018 is representative of the next 20 years (Figures 5. 1. and 5. 2.).

Table 5.1. *Weather input data for the HELP model*

Precipitation/Temperature				Evapotranspiration	
Mean Monthly Temperature (C)		Mean Monthly Precipitation (mm)		Evaporative Zone Depth (cm)	66
January	-0,07	January	30,31	Maximum Leaf Area Index (LAI)	2
February	1,55	February	33,36	Growing Season Start Day	243
March	5,56	March	31,44	Growing Season End Day	145
April	10,82	April	52,48	Average Wind Speed (km/h)	8,31
May	15,29	May	48,03	1. Quarter Relative Humidity (%)	73,3
June	20,02	June	26,60		
July	23,01	July	13,50	2. Quarter Relative Humidity (%)	57,02
August	22,72	August	18,88		
September	18,68	September	19,58	3. Quarter Relative Humidity (%)	45,3
October	12,67	October	27,76		
November	6,55	November	23,70	4. Quarter Relative Humidity (%)	70,96
December	2,26	December	52,70		

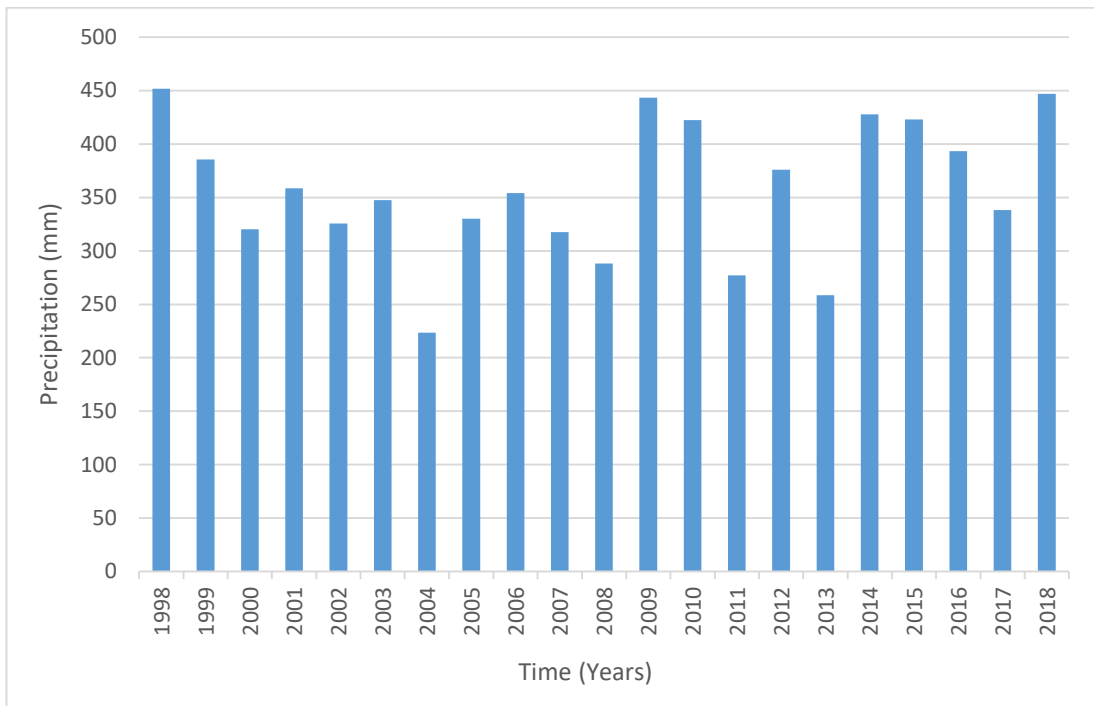


Figure 5.1. Annual precipitation totals for Ankara between 1998 and 2018

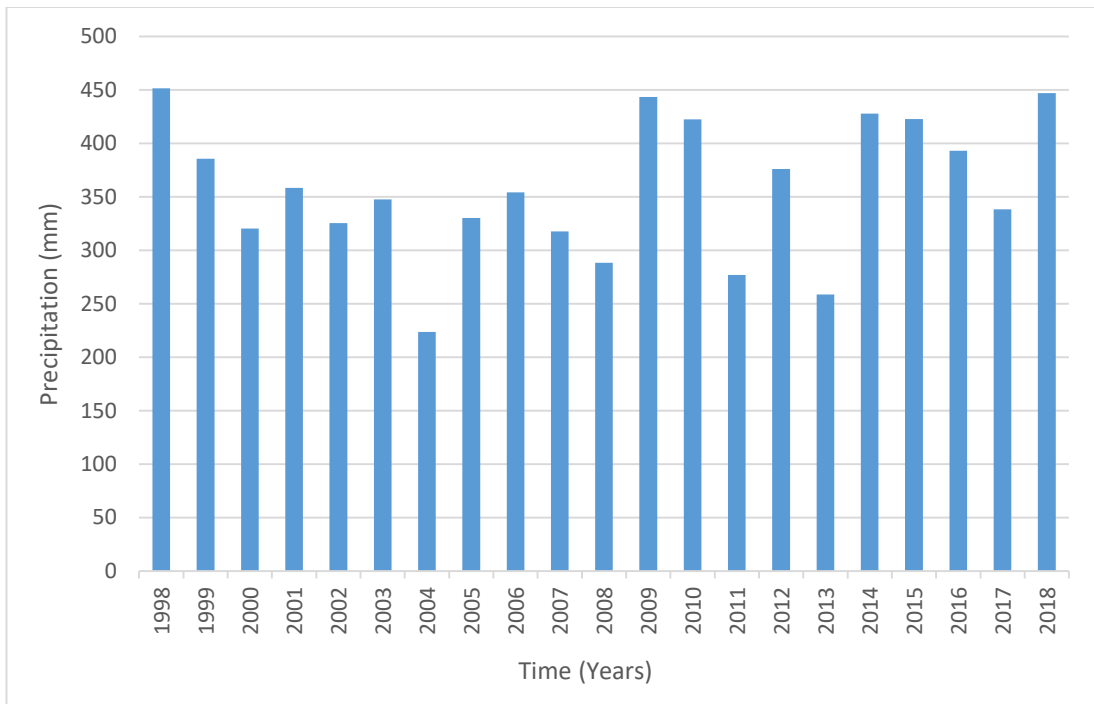


Figure 5.2. Mean monthly temperatures for Ankara between 1998 and 2018

5.3.2. Soil and design data

In addition to the meteorological data, visual HELP requires certain soil parameters for simulation. Comprehensive geotechnical and mineralogical tests were performed in order to be used as an input data for the visual HELP model. The soil sampling locations (Figure 5. 3.) and detailed information about the tests are given in the sections below. The soil samples were taken from the Hançili formation at all three alternative sites A, B and C.

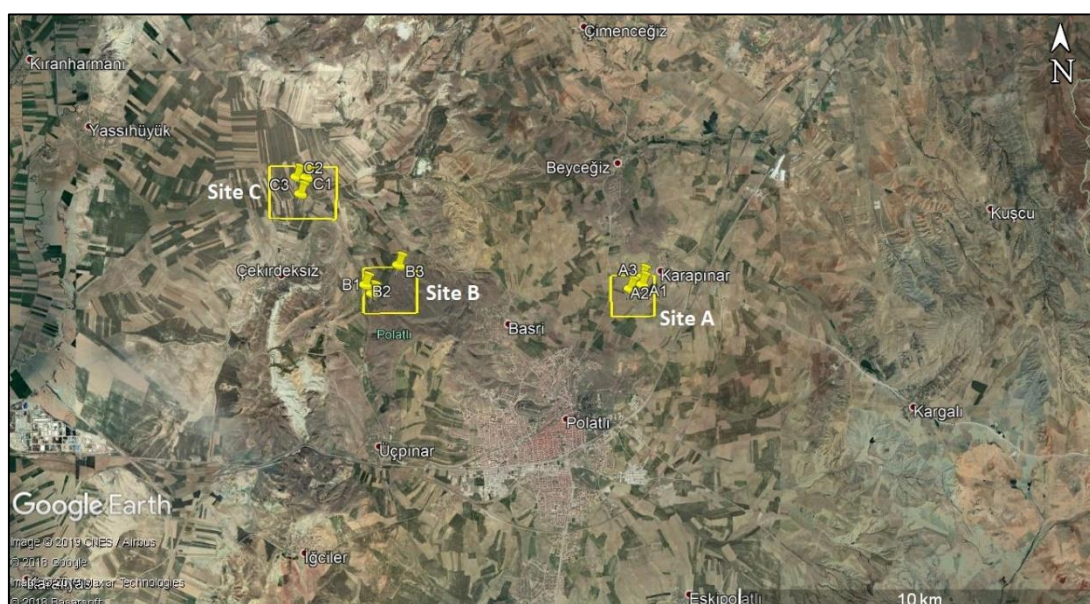


Figure 5.3. Soil sampling locations

Several borehole studies up to 15 meters depth were conducted by private companies in Polatlı city center for construction purposes. Location map of these boreholes are presented in the Figure 5. 4. As can be seen from the map, boreholes were situated approximately three kilometers away from the nearest alternative site. In addition, index tests were performed in these studies. Based on the data gathered from borehole and index tests, all of the samples were classified as CL (clay of low plasticity) and

CH (clay of high plasticity) according to unified soil classification system with fine grain percentages ranging from 52% to 86%. Plasticity indices (PI) on the other hand, were found to in the order of 13 to 29. These findings were consistent with the information collected from the laboratory experiments conducted in this thesis. In addition, no groundwater was encountered in these boreholes. Consequently, it can be inferred that the fine soil content has a continuity and assumptions were reasonable.

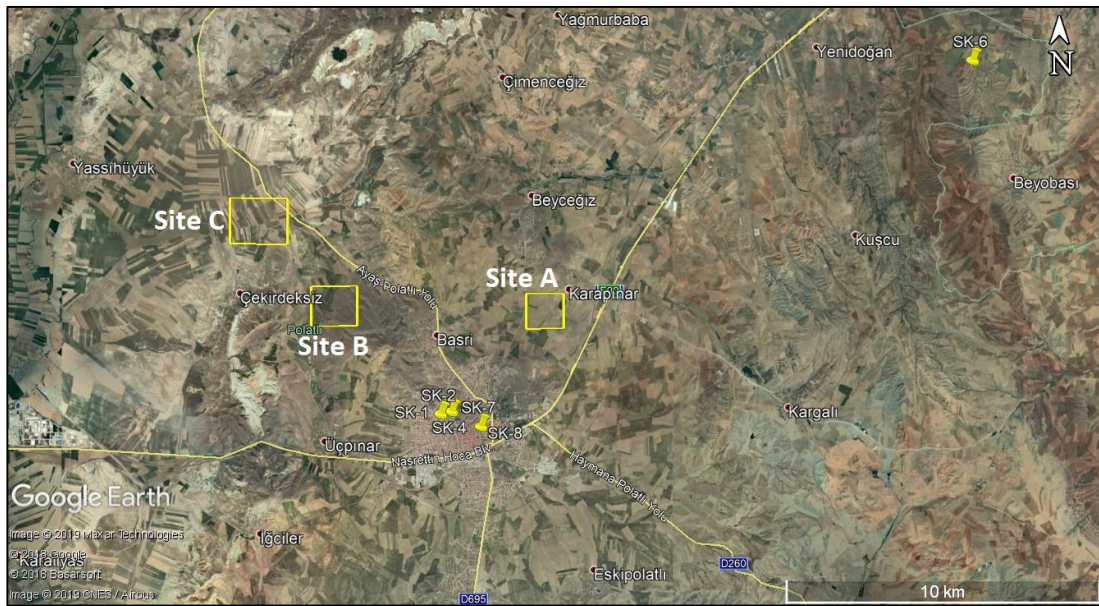


Figure 5.4. Borehole locations around the study area

5.3.2.1. Geotechnical Tests

Specific Gravity, Particle Size Distribution and Plasticity Index

In order to obtain the geotechnical characteristics of the samples, a series of laboratory tests have been conducted including specific gravity, sieve analysis, hydrometer and Atterberg limit tests. The specific gravity tests were performed according to ASTM D854-02. The particle size distribution of the soil samples was obtained by sieve analysis (ASTM D422-63, 2002). Hydrometer tests were performed to separate the

fine grained particles of the samples (ASTM D422). The results of these tests are presented in Tables 5.2.-5. 4., where a total of nine samples have been tested (i.e., three samples from each of the alternative sites, namely, Sites A, B and C, respectively, have been tested). Particle size distribution plots of the samples are presented in Figures 01 to 09 in appendix. Plasticity index of the samples were calculated by using the following equation:

$$PI = LL - PL \quad (5.1.)$$

Table 5.2. *Specific gravity of the samples*

Alternative Site	Sample ID	Specific Gravity, G_s
Site A	A1	2.68
	A2	2.68
	A3	2.67
Site B	B1	2.71
	B2	2.72
	B3	2.7
Site C	C1	2.67
	C2	2.66
	C3	2.68

Table 5.3. *Atterberg limits of the samples*

Alternative Site	Sample ID	Liquid Limit (%)	Plastic Limit (%)	Plasticity Index (%)	Soil Type
Site A	A1	Non-Plastic			SM
	A2	31.71	18.60	13.12	CL
	A3	39.16	21.86	17.30	CL
Site B	B1	53.36	29.75	23.61	MH
	B2	52.03	31.26	20.78	MH
	B3	34.69	21.65	13.03	CL
Site C	C1	24.43	20.79	3.64	SM
	C2	30.12	21.34	8.77	CL
	C3	33.09	20.45	12.63	CL

Table 5.4. Particle size distribution of the samples

Alternative Site	Sample ID	Percent (%)			
		Coarse Grained		Fine Grained	
		Gravel	Sand	Silt	Clay
Site A	A1	5.2	71.8	21.99	1.01
	A2	1.6	35.4	60.66	2.34
	A3	1.8	26.4	69.87	1.93
Site B	B1	16.8	12.2	68.43	2.57
	B2	5.2	13.8	78.64	2.36
	B3	17	23.2	58.47	1.33
Site C	C1	15.2	39.2	44.89	0.71
	C2	4.2	21.2	73.48	1.12
	C3	6.4	30.4	61.36	1.84

The results presented by Tables 5.3. and 5.4. indicate that the soil samples have plasticity indices (PI) in the range of non-plastic (N.P.) to 23.61% and that the majority of the soil samples (i.e., eight out of nine) are rich in silt-sized particles with very low clay fraction in the order of 0.71% to 2.57%.

Standard Proctor Compaction Test

Soil samples with varying water contents were compacted by using the Standard Proctor compaction apparatus according to laboratory compaction characteristics of soil using standard effort (ASTM D698). The bulk density and water content of the compacted soil samples were determined in order to calculate the corresponding dry unit weights. Samples were compacted at least five times to obtain more accurate results. The dry unit weight increases with increasing water content until it reaches a peak point. After that point, dry unit weight decreases with increasing water content. The dry unit weight versus water content graphs are presented as Figures 010-018 in Appendix A.

The Standard Proctor tests were performed on each of the nine soil samples that were collected from the alternative landfill sites. Table 5.5. gives the results of the Standard

Proctor tests which led to maximum dry densities (γ_{dmax}) ranging from 14.70 kN/m³ (Sample B3) to 17.65 kN/m³ (Sample C1) and optimum water contents (w_{opt}) ranging from 14.90% (Sample C1) to 24.40% (Sample B1).

Table 5.5. Summary of the maximum dry unit weight (kN/m³) and optimum water content (w_{opt}) values for the soil samples.

Alternative Site	Standard Compaction Test		
	Sample ID	γ_d max (kN/m ³)	w_{opt} (%)
Site A	A1	17.01	15.50
	A2	17.09	15.89
	A3	16.42	18.04
Site B	B1	14.74	24.40
	B2	14.82	23.78
	B3	14.70	19.00
Site C	C1	17.65	14.90
	C2	16.67	17.02
	C3	17.07	18.98

Falling head permeability tests

Hydraulic conductivity tests were conducted in accordance with ASTM D5856. Figure 5. 5. presents the falling head permeability test setup. The tests apparatus consists of four compaction permeameters, deairing tank, four burettes, distilled water tank and a vacuum pump.

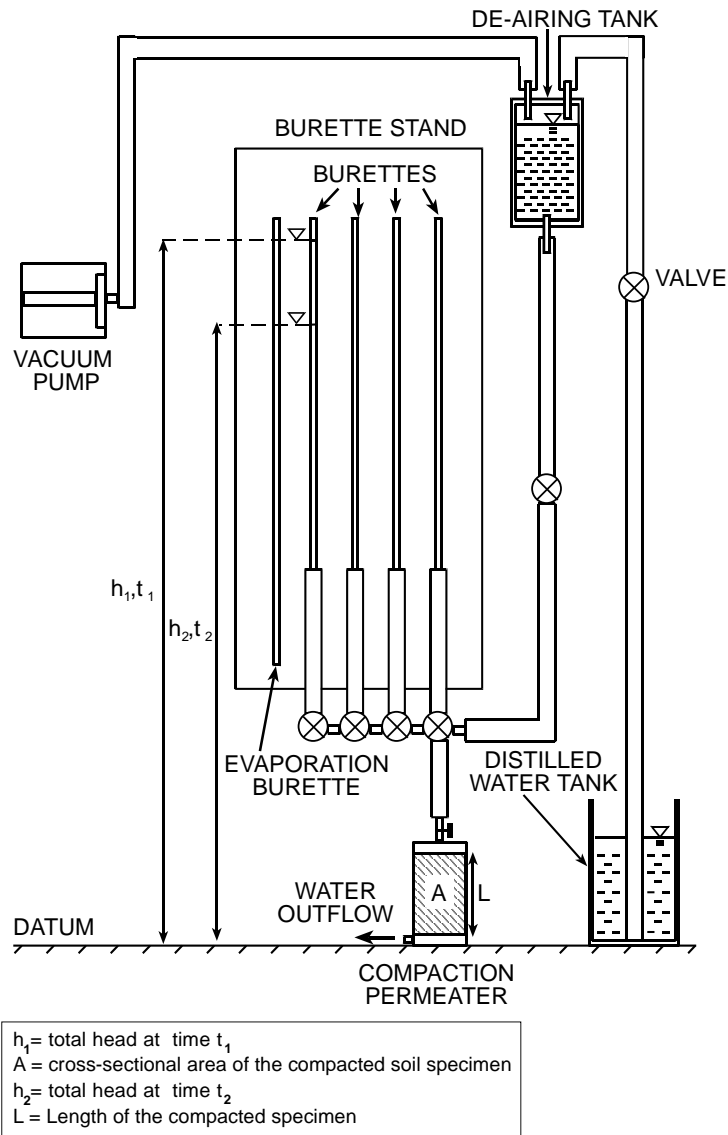


Figure 5.5. Schematic sketch of falling head permeability test apparatus (from Met, 1999; not to scale)

Equation (5.2.) was used to calculate the hydraulic conductivity (k) of the samples:

$$k = \frac{aL}{A(t_2 - t_1)} \ln \frac{h_1}{h_2} \quad (5.2.)$$

where a is the inside cross-sectional area of the burette, L is the length of the compacted specimen, A is the cross-sectional area of the compacted soil specimen, h_1 is the total head at time t_1 and h_2 is the total head at time t_2 (Figure 5.5.).

Table 5.6. gives the results of the permeability tests that were selected from one sample from each site, namely, Samples B1, C3 and A3 from alternative sites A, B and C, respectively, that possess the highest plasticity index (PI) values. It should be noted that prior to permeability testing, specimens were compacted 2-4% on the wet sides of their optimum water contents since fine-grained soils compacted on the wet sides of the optimums permits greater remolding of clods, elimination of large interclod voids and preferential re-orientation of soil particles, all of which result in lower hydraulic conductivity (Benson et al., 1994). The tests were performed on fully saturated samples where distilled water was used as the permeant. Full saturation was distinguished from the flow coming through the nozzles of the permeameters. It took 5 to 12 days for each specimen to be fully saturated.

Table 5.6. *Hydraulic conductivity values determined from falling head permeability testing*

Falling Head Permeability Test	
Sample ID	Hydraulic Conductivity (m/s)
A3	1,24E-07
B1	3,65E-07
C3	8,43E-07

As a result of the falling head permeability tests it was determined that all of the samples (A3, B1 and C3) were yielded in the order of 10^{-7} m/s hydraulic conductivity values. Since the maximum allowable limit for a compacted soil liner 1×10^{-9} m/s according to Turkish and US regulations, hydraulic conductivity of the samples has to be decreased to the acceptable levels. In order to do that samples were mixed with 5% bentonite. Falling head permeability and standard proctor tests were later performed on samples obtained from the same locations that were compacted after they were thoroughly mixed with 5% bentonite. Bentonite has been widely used in the literature to decrease permeability values of sandy and silty materials. Akgün et al., (2017), used sand-bentonite mixture to be utilized in underground nuclear waste repositories. In

their study, they used 5% to 15% bentonite. Ören et al., (2014) investigated long term compaction and hydraulic conductivity behaviors of zeolite-bentonite mixtures. In their study, hydraulic conductivities of ZBMs compared with those of sand-bentonite mixtures. Based on this information, it can be concluded that the bentonite mixtures are very common. At the first stages of the study, 5% and 10% bentonite content was planned, but 10% mixture has not been performed since 5% bentonite yielded satisfied results.

Table 5.7. gives the results of the Standard Proctor tests of the samples mixed with 5% bentonite which led to maximum dry densities ($\gamma_d \text{ max}$) ranging from 15.30 kN/m³ (Sample B1) to 18.00 kN/m³ (Sample C3) and optimum water contents (w_{opt}) ranging from 15.50% (Sample A3) to 21.50% (Sample B1). As can be observed in Table 5.7., the maximum dry unit weight of the samples increased with increasing bentonite content. The optimum water content, on the other hand decreased with increasing bentonite content. These findings are consistent with the findings of similar studies in the literature (i.e., Gokalp et. al., 2011, Komine, 2004). The dry unit weight versus water content graphs are presented as Figures 019-021 in Appendix A.

Table 5.7. *Standard proctor compaction test results for soil samples mixed with 5% bentonite.*

Alternative Site	Sample ID	$\gamma_d \text{ max}$ (kN/m³)	w_{opt} (%)
Site A	A3	17.9	15
Site B	B1	15.3	21.5
Site C	C3	18.2	14.1

The powdered Na-bentonite obtained from the Karakaya Bentonit Co., Ankara, was used in this study. The bentonite contains %77 Na-smectite, %10 cristobalite, %6 plagioclase, %4.5 quartz and %2.5 illite. The mineralogical and geotechnical characteristics of the karakaya bentonite are presented in the Table 5. 8.

Table 5.8. *Mineralogical and index properties of the karakaya bentonite used in this study (From Karakaya, 2019 as quoted by Ören et al., 2014)*

Properties	Bentonite
Mineralogy	Smectite (77%)
	Cristobalite (10%)
	Plagioclase (6)
	Quartz (4,5%)
	Illite (2,5%)
Particle size distribution (ASTM D422)	
Gravel (>2 mm)	-
Sand (2-0,075 mm)	4%
Silt (0,075-0,002 mm)	21%
Clay (<0,002 mm)	75%
Atterberg Limits	
Liquid limit (BS 1377)	%405
Plastic limit (ASTM D4318)	%57
Plasticity index (ASTM D4318)	%348
Specific gravity (D854)	2,71

Table 5.9. gives the results of the permeability tests for Samples B1, C3 and A3 that were mixed with 5% bentonite. The tests were performed on fully saturated samples where distilled water was used as the permeant. Full saturation took 10 to 18 days for each specimen which was distinguished from the flow coming through the nozzles of the permeameters.

The results show that using 5% bentonite decreased the hydraulic conductivity values several orders of magnitude. Variation of hydraulic conductivity values with the increasing bentonite content is plotted in Figure 5.6. Based on this Figure, it can be inferred that the hydraulic conductivity of the silty soil samples decreased approximately three orders of magnitude by using 5% bentonite and that bentonite contents less than 5% would not be sufficient to reduce the hydraulic conductivity of the mixtures below the regulatory allowed maximum limits. The US and Turkish regulations require that the permeability of the liner material to be at least 1×10^{-9} m/s. Since the soil samples collected from the alternative sites did not meet these conditions

in their natural state, consequently, the samples were mixed with 5% bentonite to decrease their permeability. All of the three samples yielded satisfied results after they were mixed with 5% bentonite. Sample B1 from alternative Site B gave the lowest hydraulic conductivity value.

The termination criteria for falling head hydraulic conductivity tests are subject to opinion. According to the Pierce and Witter (1987), permeability tests should continue until at least one pore volume of flow is passed through the specimen and the slope of hydraulic conductivity versus the number of cumulative pore volumes doesn't change significantly from zero. Appendix A, Figures 022-024 present PVF vs. hydraulic conductivity for all three samples. Appendix A, Figures 025-027 present hydraulic conductivity vs. time.

Considering this information, permeability tests were terminated after at least one pore volume of flow passed through the specimen. Additionally, it was taken into consideration that the permeability of the specimens was not changed significantly. After these conditions were met, the tests were finalized.

Table 5.9. *Hydraulic conductivity of soil samples mixed with 5% bentonite*

Falling Head Permeability Test	
Sample ID	Hydraulic Conductivity (m/s)
A3	2.70E-10
B1	2.28E-10
C3	5.72E-10

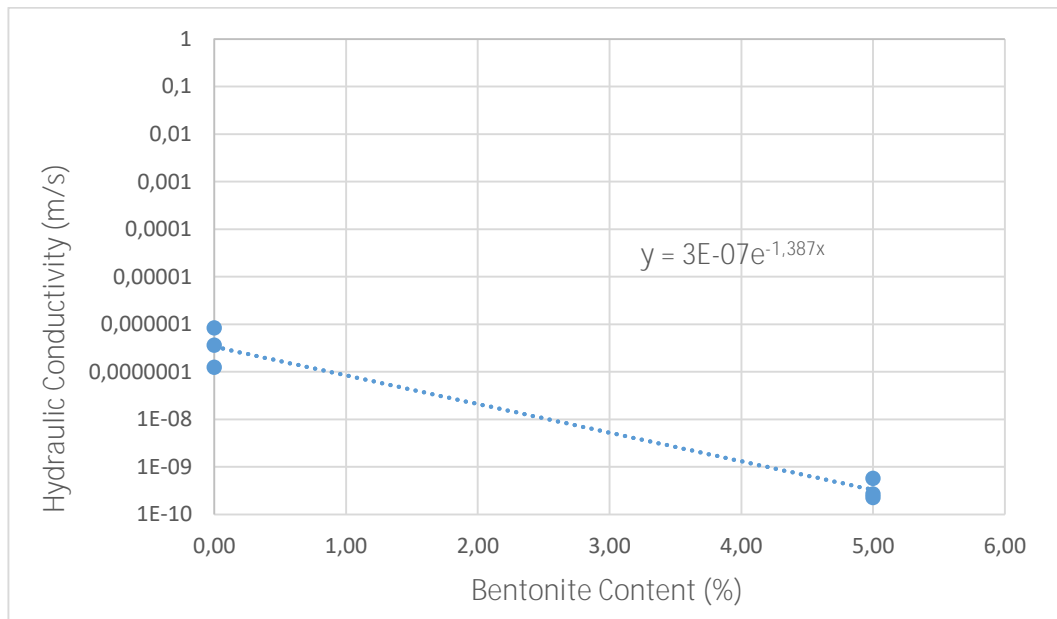


Figure 5.6. Hydraulic conductivity (m/s) vs bentonite content (%)

5.3.2.2. Mineralogical Tests

Mineralogical characteristics of the samples is very important since one of the main aim of this study is to find a suitable landfill liner material. Understanding the mineralogical composition could give valuable information. Even though samples are mostly silt-sized with very little clay fractions, dominant clay mineral could affect the behaviour significantly. Smectite type clay mineral is preferred due to their swelling and absorption capacity. This is due to restrain the spreading of leakage beneath the compacted soil liner and mixing with the groundwater. Sezer et al. (2003), investigated mineralogical and sorption capacity characteristics of Ankara clay which has a wide distribution around the Ankara region. In their study, suitability of Ankara clay as a landfill liner was studied by examining its mineralogical characteristics. After determining the geotechnical properties of the samples, comprehensive mineralogical tests such as XRD, methylene blue and Scanning Electron Microscopy (SEM) tests were conducted to understand the mineralogy of the clay fraction of the Hançili formation and also to justify that the clay fraction was negligible as presented in the

particle size distribution of the samples (Table 5. 4.). By performing these tests, one may comment on the dominant clay mineral, specific surface area (SSA) and cation exchange capacity (CEC) of the mineral. Detailed information about the mineralogical tests are given in the following sections:

X-Ray Diffraction (XRD)

X-ray powder diffraction is considered to be one of the best approaches for the qualitative and quantitative examination of the clay fraction of geological samples and a variety of researchers has worked with this method over the years (Liu et al., 2018, Moore and Reynolds, 1997, Chipera and Bish, 2013). X-rays are directed towards the sample while slowly rotating, which produce a diffraction pattern which show the intensity of the X-rays collected at different angles. These patterns or basal reflections give the d spacing of the basal layer which represents the thickness of the silicate layers and the unit cell often contains multiple layers. Clay minerals usually can be distinguished from the peaks. Well-defined crystalline minerals have sharp peaks while clays, which range from crystalline to non-crystalline, produce broad peaks with a noticeable width on both sides. These broad peaks make it easy to pick out which peaks are contributed by clays. These peaks can be compared to known diffraction patterns for better identification but if some peaks are broader than others, it is likely that multiple clays are present (Reynolds et al. 1997).

Within the context of X-ray diffraction study, a total of 3 powdered (B1, C3, A3) bulk samples were used. Samples were obtained by sieving the soil with #200 sieve in order to get $< 2\mu$ fraction. Each sample has been stirred with distilled water and after that the clay fraction has been collected by settling according to Stoke's law and by centrifugation. Then, the centrifuged samples were coated onto petrographic slides to be used in the analysis. The analysis was conducted in random, natural (air-dried), ethylene glycolated and thermal treated (300 °C and 550 °C) conditions. METU central laboratory's Rigaku Ultima-IV X-ray diffractometer with Cu targeted X-ray tube and water cooler was utilized for the test. It uses a high resolution graphite

monochromator which has the ability to obtain monochromatized X-rays. The resultant graphs are given in Figures 5. 7. through 5. 9.

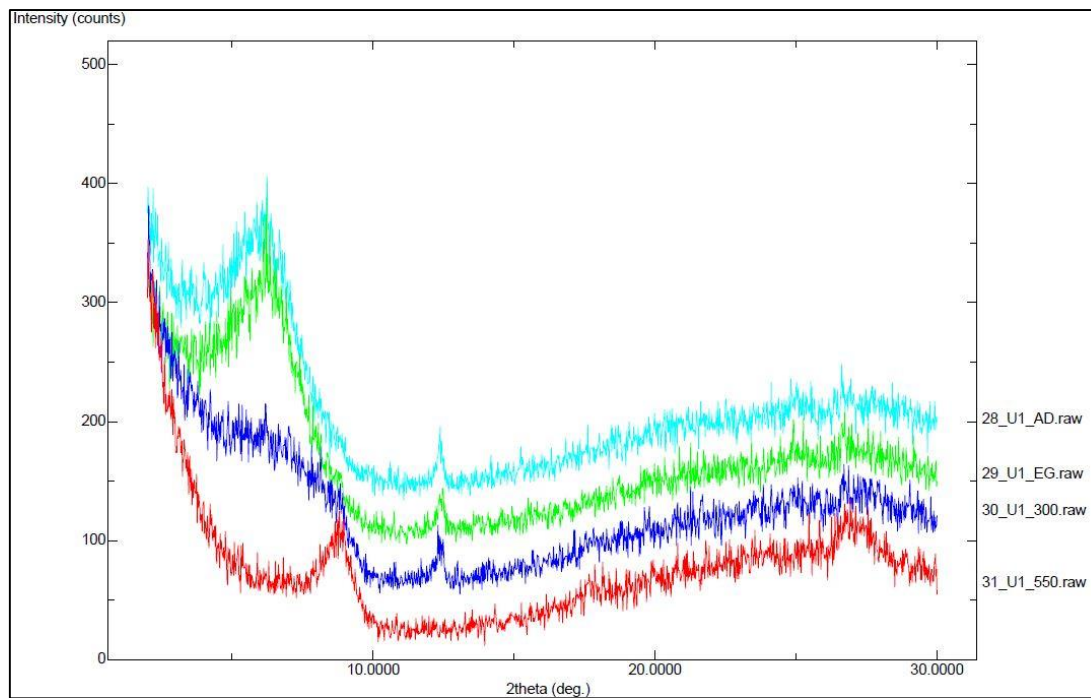


Figure 5.7. XRD graph of B1

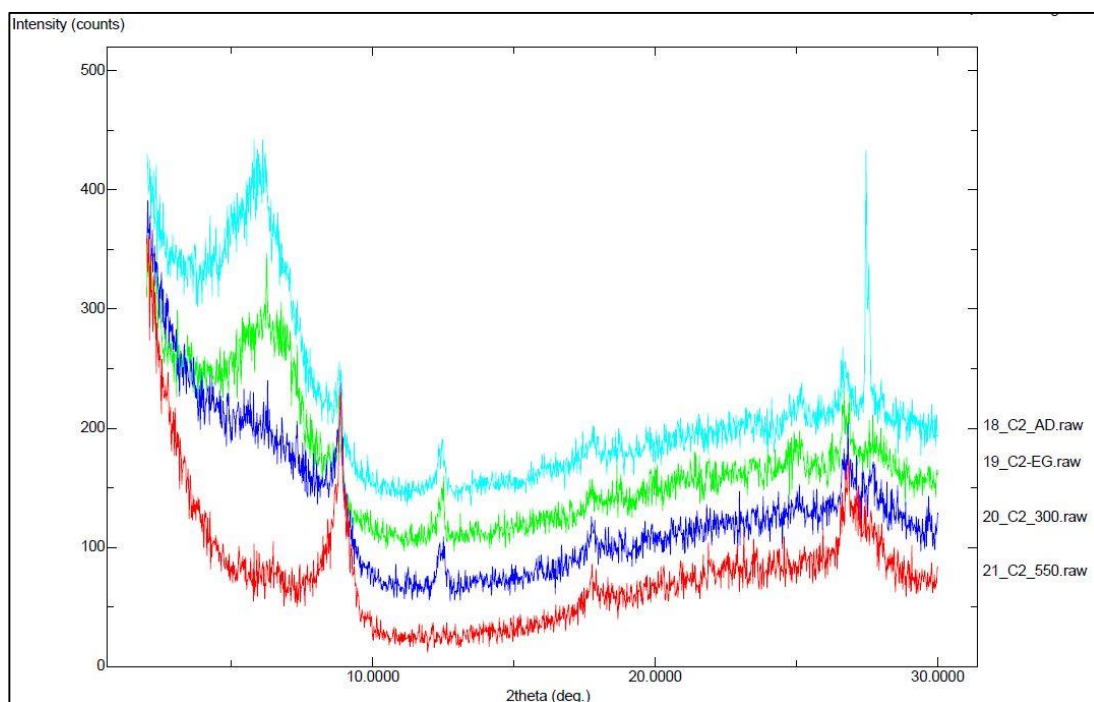


Figure 5.8. XRD graph of C3

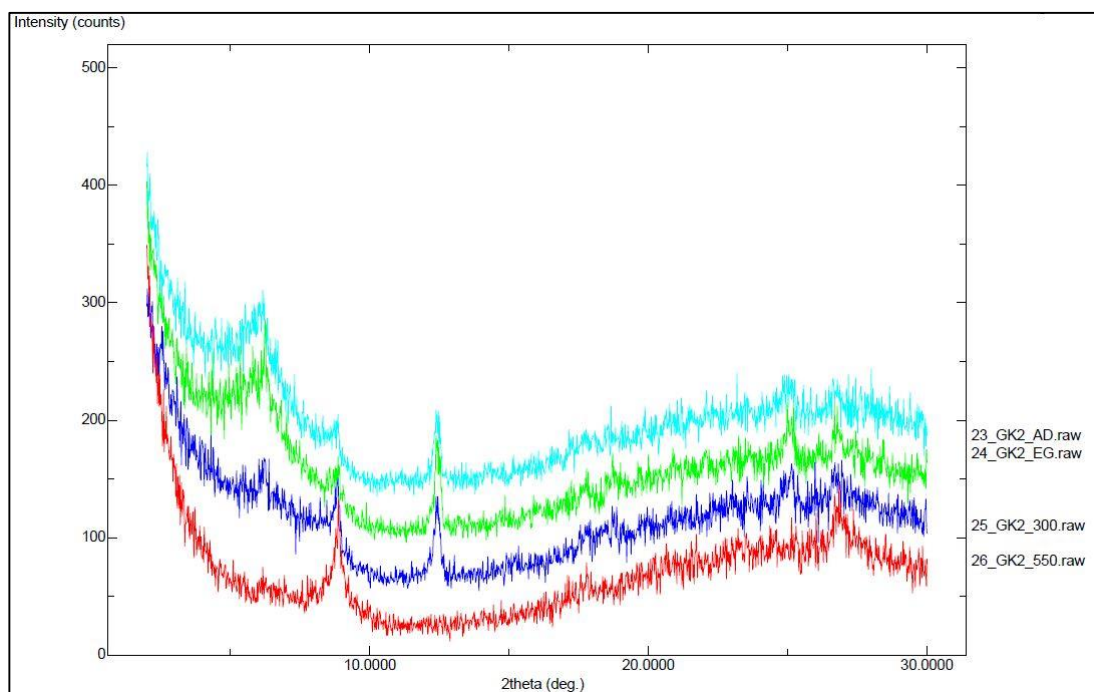


Figure 5.9. XRD graph of A3

The peaks of these graphs were compared to the reference values given in Chen (1977). These results indicate that the main clay minerals in B1, C3 and A3 are smectite, kaolinite and illite, respectively. Additionally, in every sample Ca, Mg, Fe and K elements were observed in different amounts.

Methylene Blue Test

Methylene blue test is considered as one of the fastest and reliable method when determining the clay minerals in soils and used by many researchers in the literature (Cokca, 2002, Akgün et al., 2017, Yukselen and Kaya, 2008). In this study, methylene blue tests were conducted according to the ASTM C837-09 method on all 3 samples which are representative of the candidate sites. Significance of this test is to obtain important parameters like cation exchange capacity (CEC) and specific surface area (SSA) of the clay minerals. By using these parameters, it is possible have an opinion about the dominant type of clay mineral and its swelling behavior.

The methylene blue powder behaves like a cationic dye when mixed with water and it is identified with the chemical formula of $(C^{16}H^{18}N^3S)^+Cl^-$. When it is mixed with soil solution, the chloride ions in the methylene blue solution replace the cations that are adsorbed on the surface of the clay minerals. By using the amount of methylene blue solution, the CEC and SSA of the clay minerals can be calculated by using the following equations:

$$\text{Specific surface area of clay (SSA)} = 20.93 \times V_{cc} (1/f) \quad (5. 3.)$$

$$\text{Cation Exchange Capacity (CEC) of clay} = (100 \times V_{cc} \times N_{MB}) / f \quad (5. 4.)$$

where $20.93 \text{ m}^2/\text{cm}^3$ = Specific surface area corresponding to 1 cm^3 methylene blue solution; V_{cc} = methylene blue solution used (cc), f = the weight of the sample in grams and $N_{MB} = 0.028$.

When conducting the test, initially, 7.5 grams of a sample (passing #200 sieve) was obtained and mixed with 50 ml of distilled water. After that, methylene blue dye was gradually added to the mixture which at the same time, was continually mixed with a

magnetic stirrer. Immediately after adding the solution, saturation of the mixture was checked by applying it to a filter paper. The test was continued until the mixture was saturated. Saturation was checked by the light blue halo surrounding the blue stain in the center (Figure 5.10.). The test was terminated after the solution became saturated.

In the following Figure, the difference between negative(Figure 5.10.a.) and positive outcome(Figure 5.10.b.) of the test is presented. Positive outcome of the test can be differentiated from the blue stain surrounded by a light blue halo.

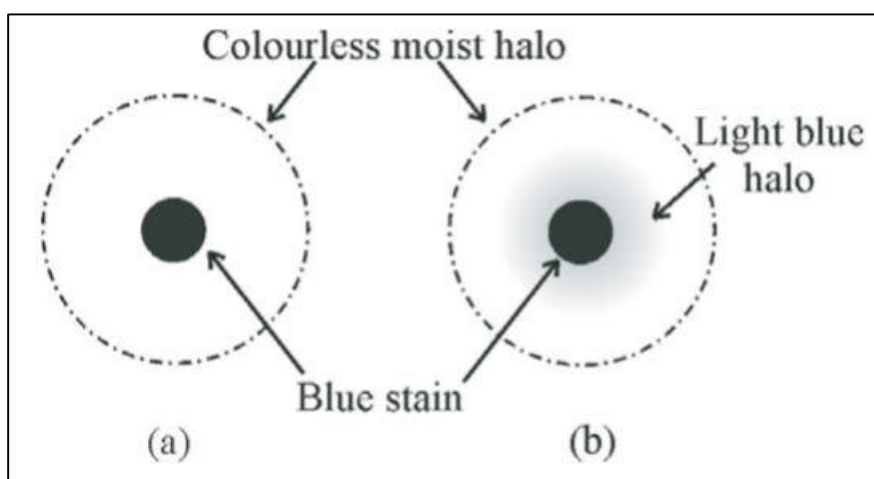


Figure 5.10. Methylene blue stain test (from Chiappone, 1999)

The different types of clay minerals can be briefly classified as follows: (i) inert — chlorite, illite, and kaolinite with cation exchange capacity (CEC) of 3–25 meq. /100 g, specific surface area of 10–100 m²/100 g, liquid limit (LL) of 50–120, and plasticity index (IP) of 20–60; and (ii) active — smectite and vermiculite with CEC of 80– 150 meq. /100 g, specific surface area of 100– 700 m²/100 g, LL of 100–700, and IP of 80–600 (Chiappone, 1999). Some mineralogical specifications of clay minerals are given in Table 5. 10. The samples exhibited CEC values between 10.45 and 28.75 meq/100 g and SSA values between 78.14 and 214.88 m²/g. The results of the methylene blue tests can be seen in Table 5.11.

Table 5.10. Mineralogical characteristics of main clay minerals (Velasco, 2013)

Mineral	Kaolinite	Illite	Montmorillonite
Classification	Nondispersive	Moderately Dispersive	Dispersive
Type	1:1	2:1	2:1
Interlayer Bond	Hydrogen Bonds	Potassium ions	Van der Waals forces
Cation Exchange Capacity	Lowest	Intermediate	Highest
Specific Surface Area	Lowest	Intermediate	Highest

Table 5.11. Methylene blue test results

Sample ID	V _{cc}	f (gr)	N _{MB}	Cation Exchange Capacity (CEC)	Specific Surface Area (SSA)
A3	56	7.5	0.028	20.91	156.28
B1	77	7.5	0.028	28.75	214.88
C3	28	7.5	0.028	10.45	78.14

According to the cation exchange capacity and specific surface area values, all samples possess low CEC values in the range of 10 to 29 where Samples C3 and A3 are considered to possess kaolinitic clay minerals. Sample B1 is determined to possess smectite type of clay minerals since it possesses higher values.

Scanning Electron Microscopy (SEM) Analysis

Scanning electron microscope (SEM) is used to generate surface images of a specimen on a microscopic level. It scans the specimen with a beam of high energy electrons in an optical column. The electrons emitted by the beam then interact with the atomic structure of the specimen and generate topographic images. SEM analysis is found to be very suitable for examining the configuration, texture and fabric of the clay samples (Bohor and Hughes, 1971). With the help of this analysis above mentioned

characteristics of the clay minerals were studied. Furthermore, elemental composition of the samples was determined by EDAX analysis.

Within the context of the study, Quanta 400F scanning electron microscope (SEM) of the Central Laboratory of METU was used with an operating voltage of 10-30 kV and working distance of 10.5-11.2 mm. Samples B1, C3 and A3 which were collected from the 3 alternative landfill sites were analyzed. Samples were prepared by spreading the dry powder on double sided adhesive tape.

SEM images and EDAX graphs of samples are presented by Figures 5. 11. through 5. 16:

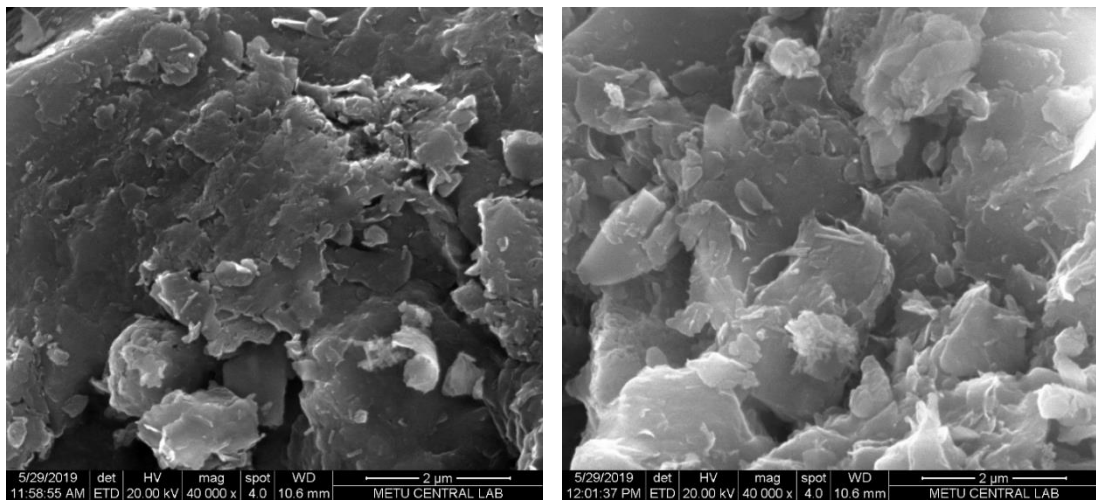


Figure 5.11. SEM images of sample C3

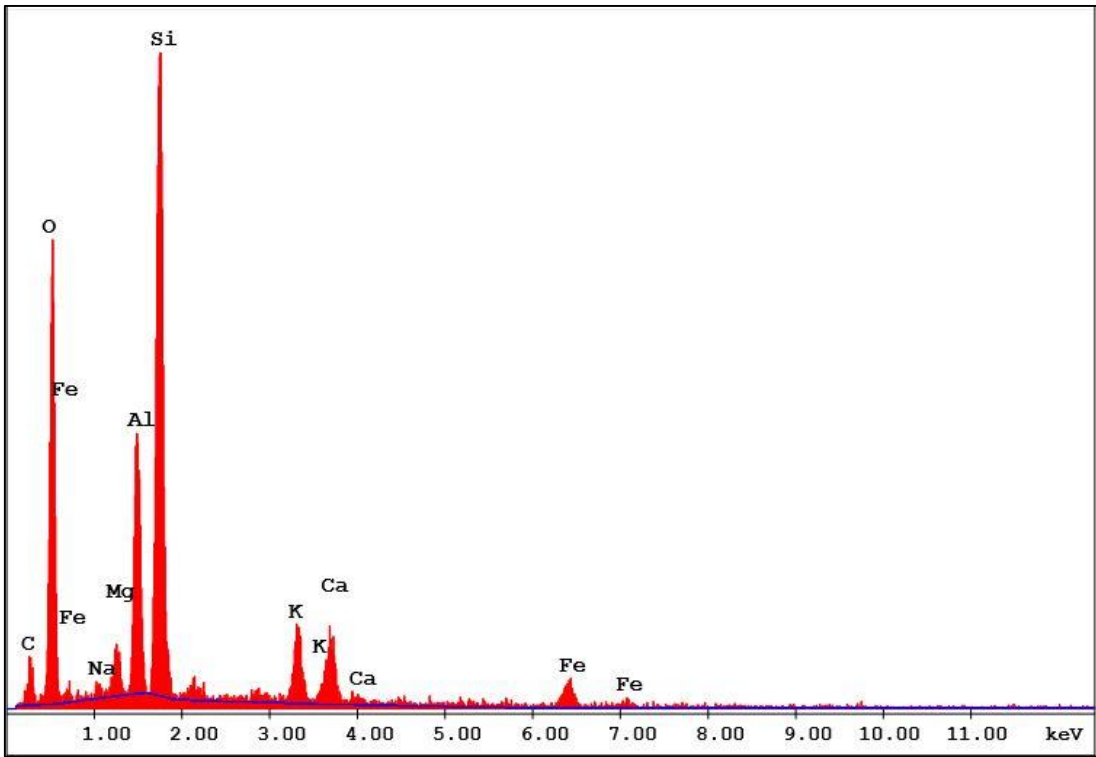


Figure 5.12. EDAX analysis of the sample C3

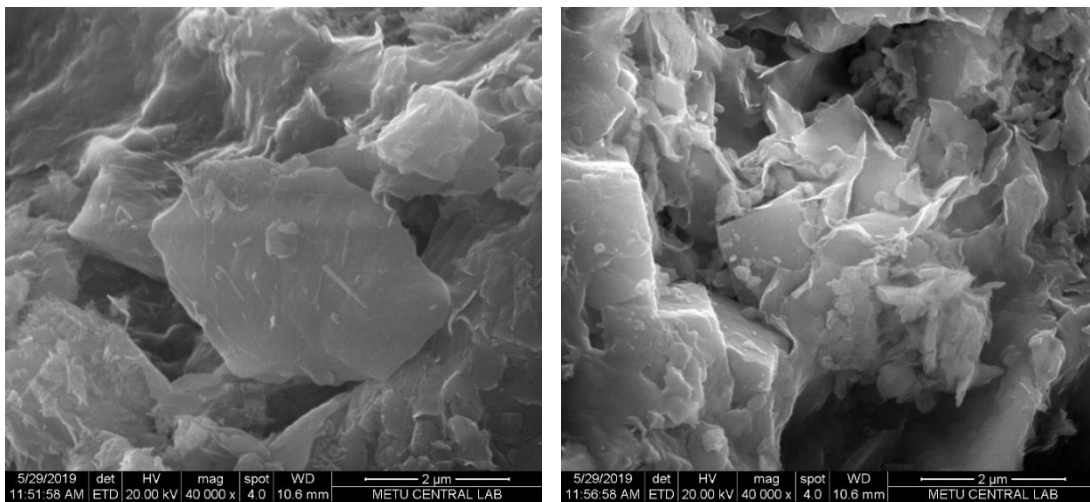


Figure 5.13. SEM images of sample A3

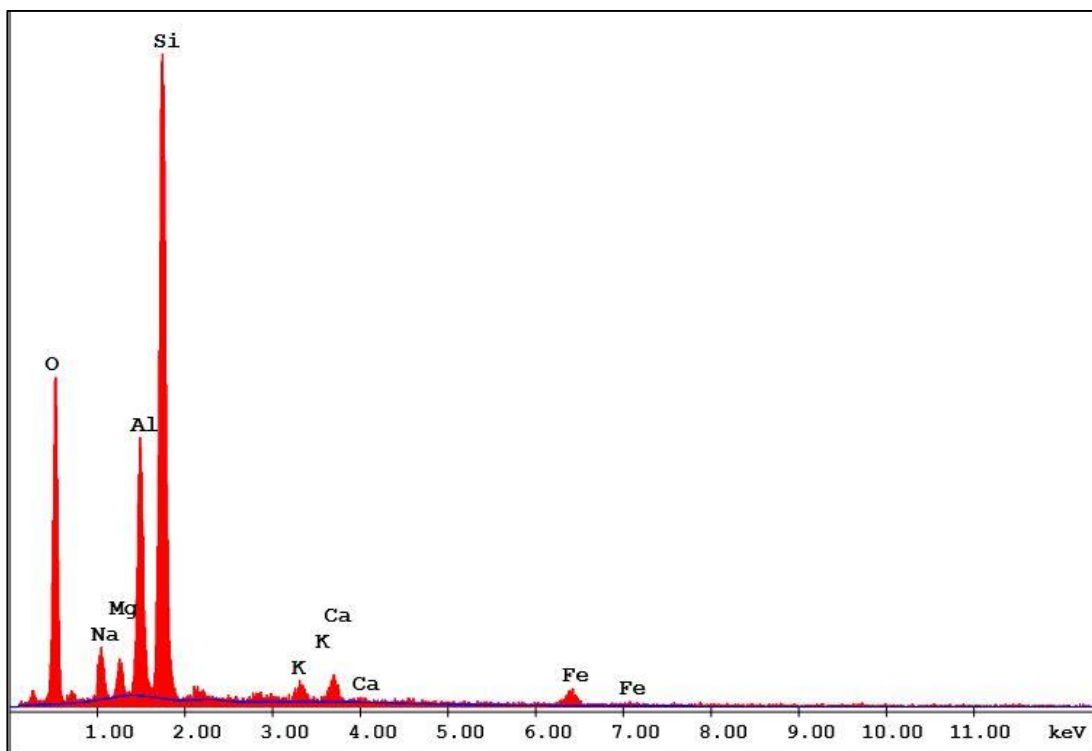


Figure 5.14. EDAX analysis of the sample A3

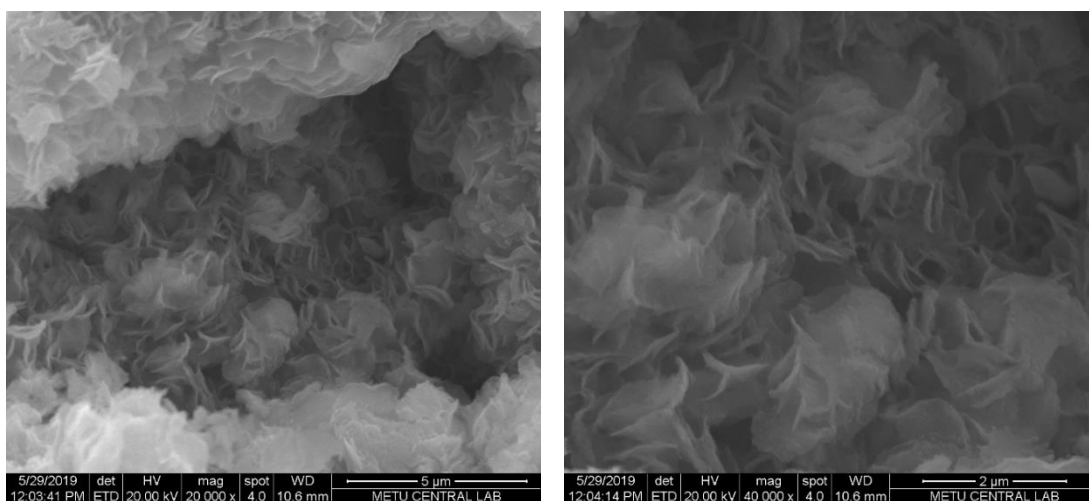


Figure 5.15. SEM images of sample B1

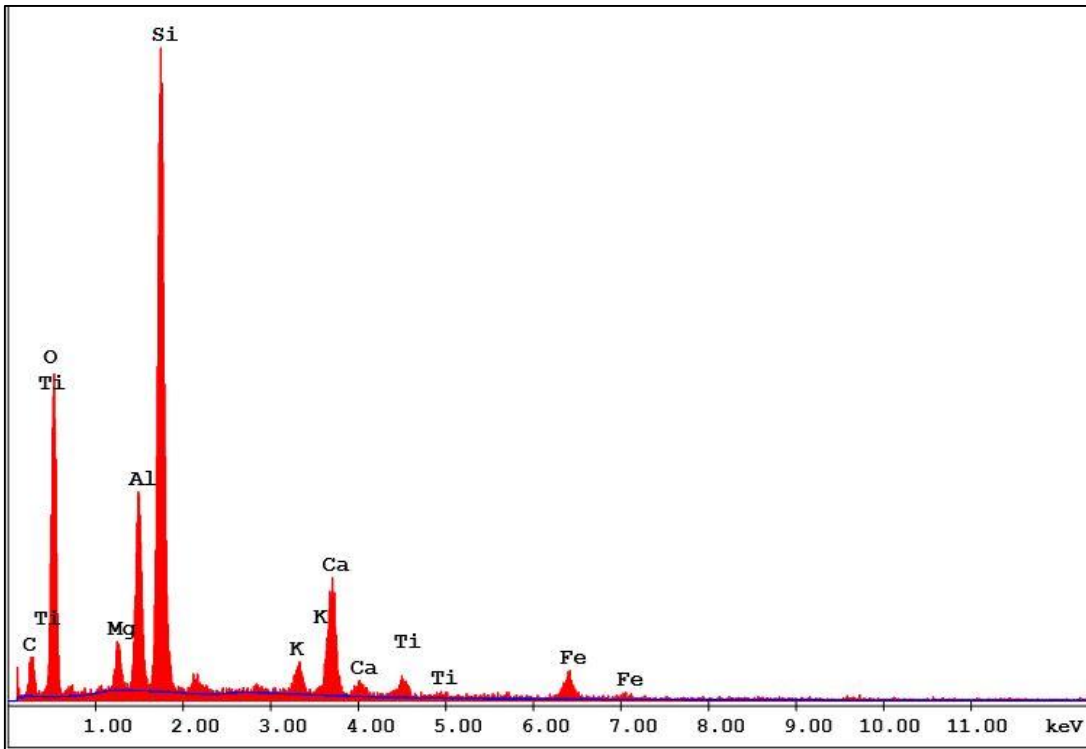


Figure 5.16. EDAX analysis of the sample B1

The SEM micro-images and EDAX analysis revealed that Samples C3 and A3 are rich in kaolinite whereas Sample B1 has dominant clay mineral as smectite.

5.4. Analysis of the Results

Visual HELP uses numerical solution techniques that account for the effects of surface storage, snowmelt, runoff, infiltration, evapotranspiration, vegetative growth, soil moisture storage, lateral subsurface drainage, leachate recirculation, unsaturated vertical drainage, and leakage through soil, geomembranes, or composite liners. In the context of this study four different profiles were modeled from least conservative to most conservative (Figures 5. 17. to 5. 20.). The geotechnical parameters required for the program were gathered from the laboratory tests as mentioned above. The hydraulic conductivity value of sample B1 with 5% bentonite content was used in every profile of the model since it achieves the lowest value and landfill site B was

selected as one of the two optimum sites (Site A and Site B) to situate a landfill. The thickness of the municipal waste layer was taken as 7.5 meters. The rest of the input data were entered in accordance with the US (EPA, 2010) and Turkish (TSCWR, 2010) regulations. The input parameters are given in Table 5.12.

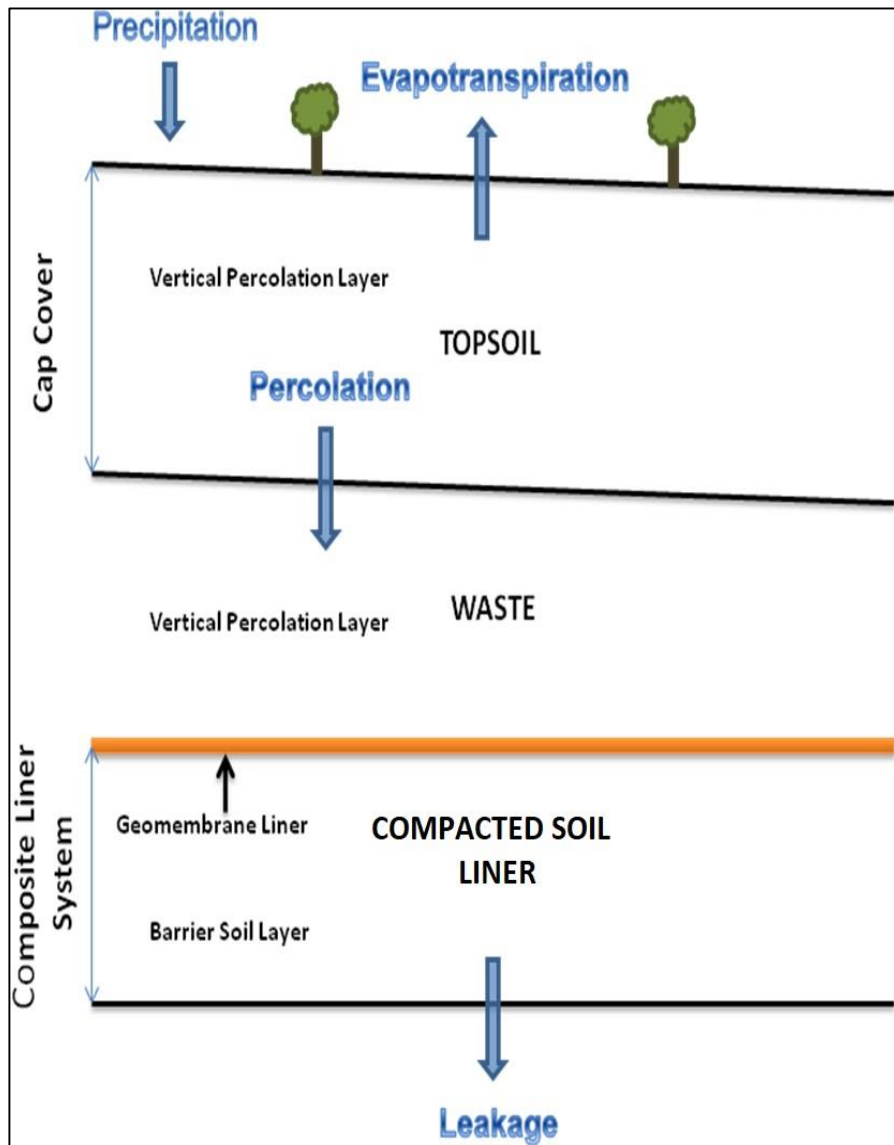


Figure 5.17. Visual HELP profile 1 (modified from Schroeder, 1994)

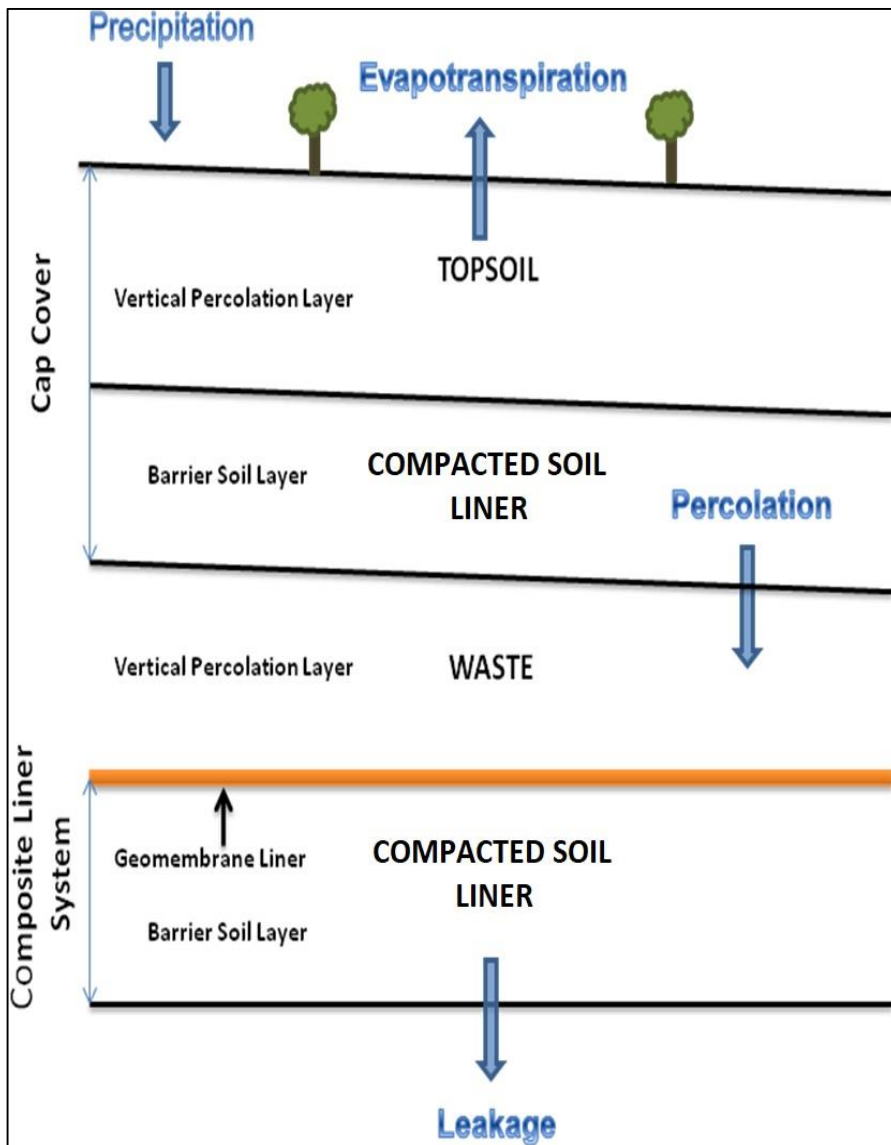


Figure 5.18. Visual HELP profile 2 (modified from Schroeder, 1994)

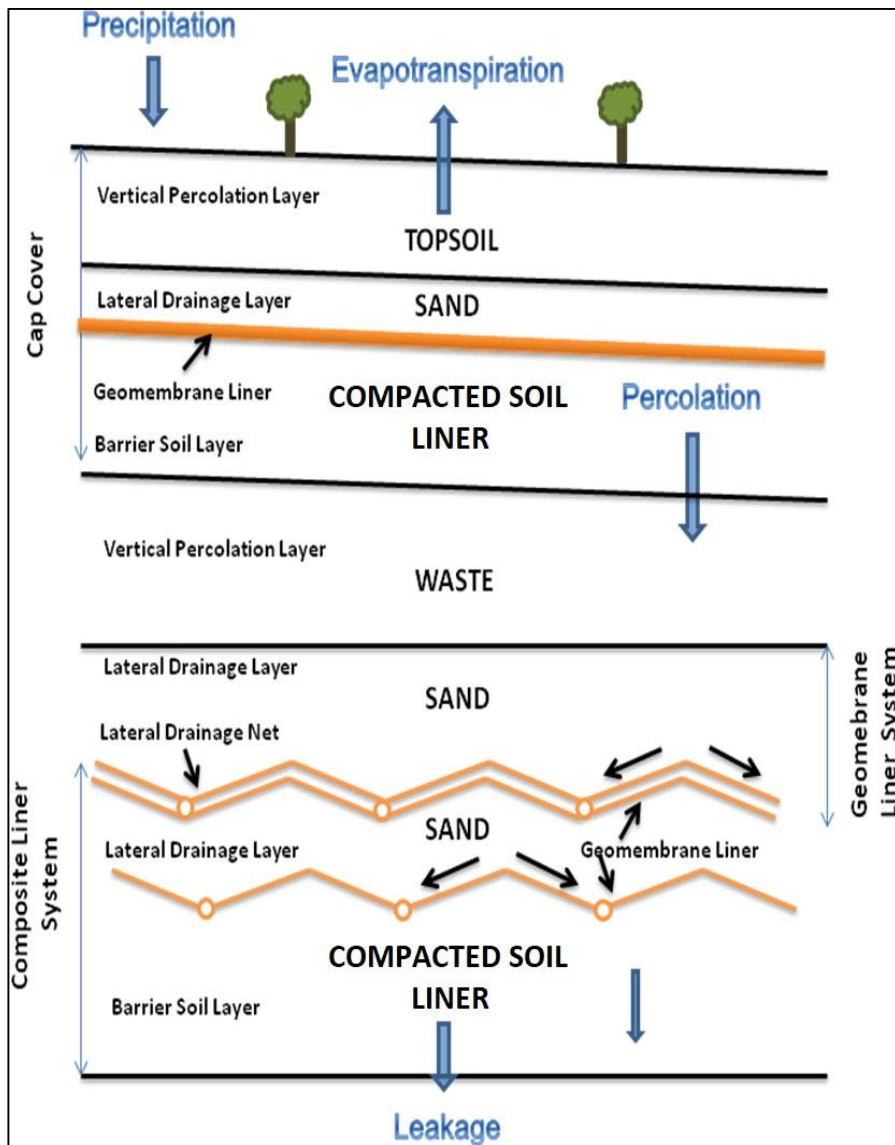


Figure 5.19. Visual HELP profile 3 (modified from Schroeder, 1994)

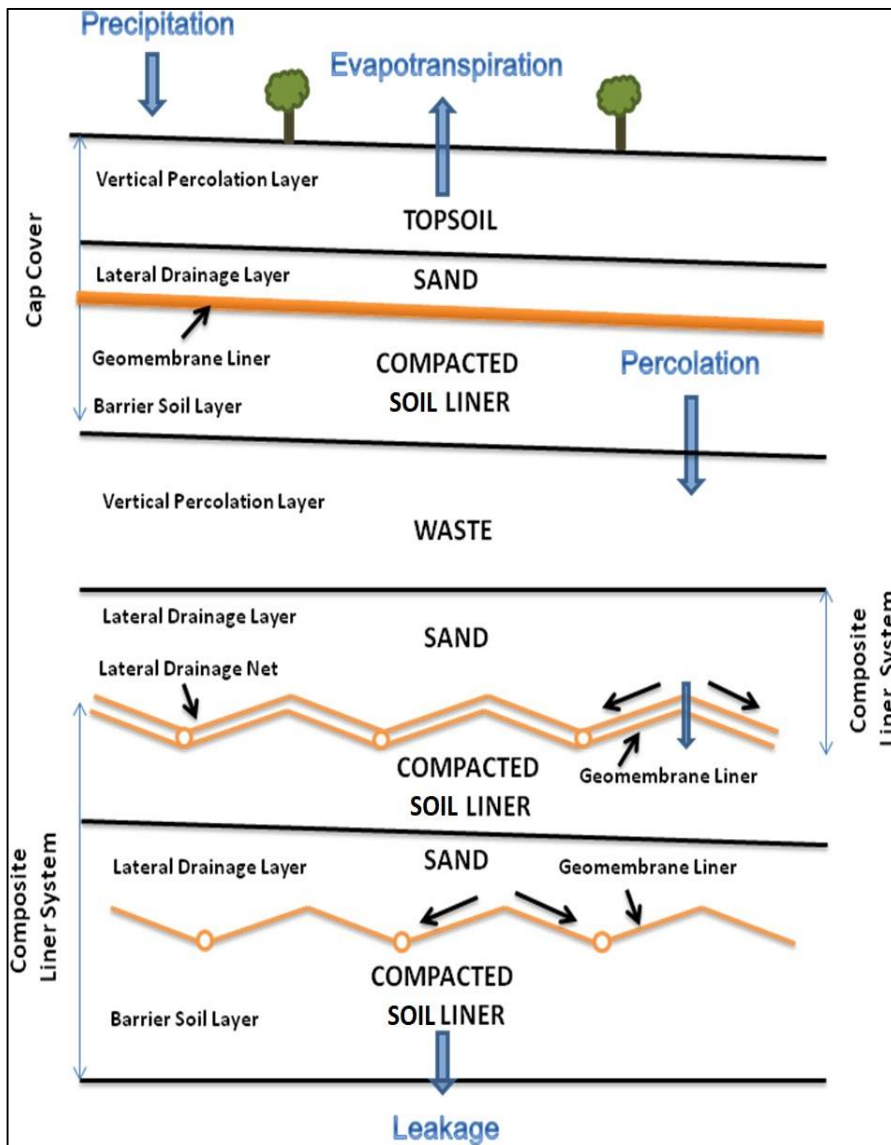


Figure 5.20. Visual HELP profile 4 (modified from Schroeder, 1994)

Table 5.12. *Some of the input parameters utilized in the analysis (from Schroeder, 1994)*

Layer	Thickness (m)	Total porosity	Saturated Hydraulic Conductivity (cm/s)
Fine Sandy Loam	1	0,475	0,17E-04
Municipal Waste	7,5	0,671	0,1E-02
High Density Polyethylene (HDPE)	0,002	-	0,2E-12
Compacted Soil Liner	0,6	0,462	2,47E-08
Drainage Net	0,005	0,85	10

The first profile, from top to bottom consisted of a topsoil layer, a waste layer, and a geomembrane/compacted soil composite liner. A compacted soil liner was added to the cap below the topsoil for the second profile. The second profile, from top to bottom consisted of a topsoil layer, a compacted soil liner, a waste layer and a geomembrane/compacted soil composite liner. A lateral drainage layer in order to collect leachate was added below the waste layer for the third profile. The third profile, from top to bottom consisted of a topsoil layer, a lateral drainage layer, a compacted soil liner, a waste layer, a lateral drainage layer, a lateral drainage net, a geomembrane top liner, a lateral drainage layer and a geomembrane/compacted soil composite bottom liner. The last and the most conservative landfill profile of the model from top to bottom consisted of a topsoil layer, a lateral drainage layer, a compacted soil liner, a waste layer, a lateral drainage layer, a lateral drainage net, a geomembrane/compacted soil composite top liner, a lateral drainage layer and a geomembrane/compacted soil composite bottom liner. This profile was expected to have the least damage to the environment.

The HELP model was performed for the four profiles selected for 20 years of simulation. The cumulative unitized expected leachate rate and cumulative leachate heads are plotted in the Figures 5. 21. and 5. 22., respectively. The expected leakage rates ($\text{m}^3/\text{year}/10,000 \text{ m}^2$) were determined to be 6.69, 1.08, 4.04×10^{-4} and 2.04×10^{-6} for Profiles 1, 2, 3, and 4 respectively (Figure 5. 20.). At the end of the 20 years of simulation, the average heads were found to be 1,89, 0,218, $1,98 \times 10^{-5}$ and $2,46 \times 10^{-7}$ m respectively (Figure 5. 21.). As a conclusion, it is strongly suggested to use profile four for a future landfill in the study area. Maximum allowable leachate head required for the US and Turkish regulations are 30 centimeters. By considering these limits, profile 2, 3, and 4 yielded satisfactory values.

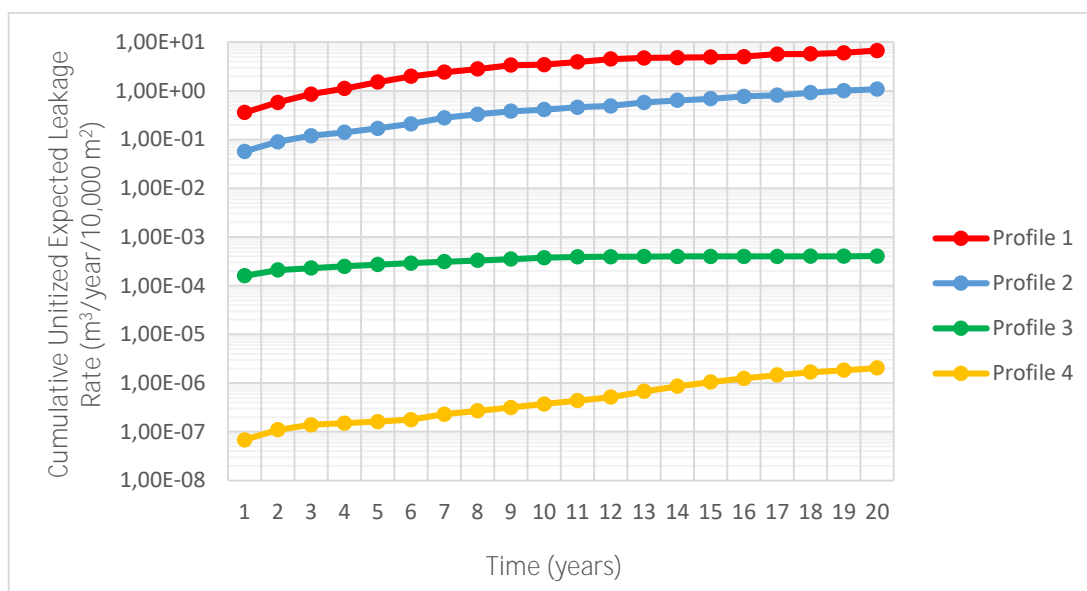


Figure 5.21. Cumulative unitized expected leakage rate ($\text{m}^3/\text{year}/10,000 \text{ m}^2$) for 20 years of simulation

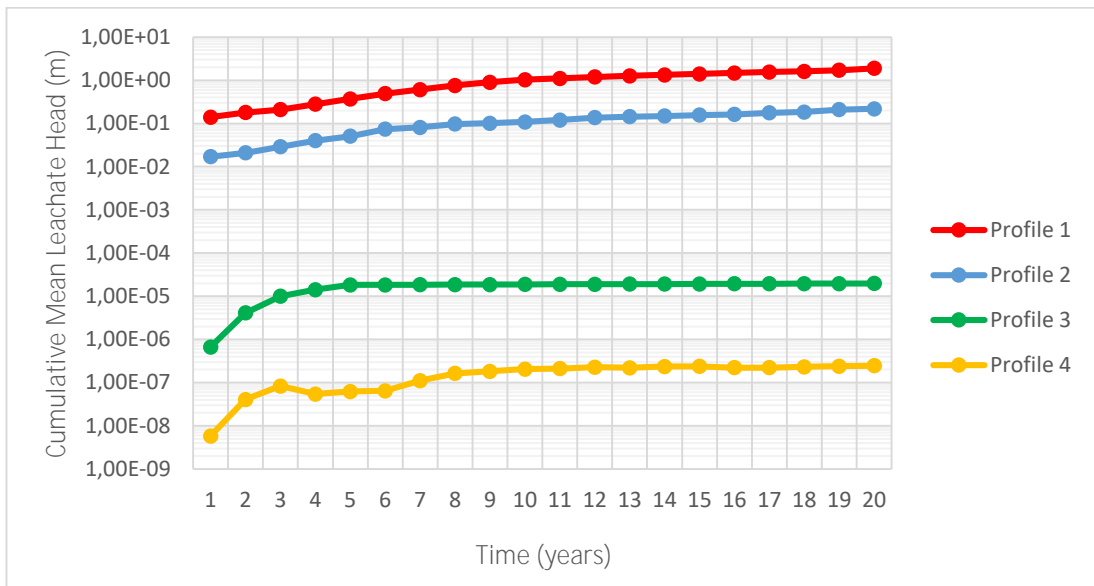


Figure 5.22. Cumulative average leakage head (m) for 20 Years of simulation

CHAPTER 6

SUMMARY AND CONCLUSIONS

The aim of this study is to find a suitable landfill location and design a suitable landfill liner for the Polatlı Municipality. In order to find the best location possible, criteria such as distance to roads, distance to settlements, geology, hydrogeology, distance to faults were used and then gathered in a GIS environment. The TOPSIS methodology was utilized as a multi-criteria decision making analysis since it is widely used to select the best alternative out of many possibilities. By combining the GIS and TOPSIS, a final suitability map of the study area was generated. After that, geotechnical and mineralogical characteristics of the samples which were collected from the 3 alternative landfill sites were examined by comprehensive laboratory tests to assess their suitability as a component of a landfill lining material. Geotechnical index tests (i.e., sieve analysis, Atterberg limit tests, hydrometer tests, compaction tests) showed that these units vary from ML to CL. In addition, falling head permeability testing was conducted in order to assess the hydraulic conductivity of the samples. Consequently, since none of the samples met the regulatory permeability limit of 1×10^{-9} m/s, the samples were mixed with 5% bentonite to reduce the permeability to the regulatory limits. Mineralogical tests namely, X-ray diffraction (XRD), scanning electron microscopy (SEM) and methylene blue, were mainly conducted in order to find out the dominant clay minerals and their mineralogical properties. As a result of the mineralogical tests, dominant clay mineral in sample B1 was found to be smectite.

After comprehensive laboratory experiments and site selection study long term hydrologic evaluation of the alternative sites were examined. By using permeability values obtained from permeability tests four landfill profiles from least to most conservative was modeled utilizing the visual HELP model. 20 years of simulation

were conducted via HELP model. The result of this model proved that using a composite lining system would improve the long term hydrologic performance of the landfill. The most conservative profile yielded leachate rate and leakage rate of $2,04 \times 10^{-6} \text{ m}^3/\text{year}/10,000 \text{ m}^2$ and $2,46 \times 10^{-7} \text{ m}$. After careful consideration of the site selection study and laboratory tests Site B was chosen as the most suitable place to locate landfill since it is situated in the most suitable part of the study area and its dominant clay mineral is smectite.

REFERENCES

Akbari, V., Rajabi, M.A., Chavoshi, S.H., Shams, R., 2008. Landfill site selection by combining GIS and fuzzy multi criteria decision analysis, case study: Bandar Abbas, Iran. *World Applied Sciences Journal* 3, 39–47.

Akgün, H., 2010. Geotechnical Characterization and Performance Assessment of Bentonite/sand Mixtures for Underground Waste Repository Sealing. *Applied Clay Science*, 49(4), 394–99.

Akgün, H., Koçkar, M. K., 2018. Evaluation of a Sand Bentonite Mixture as a Shaft/borehole Sealing Material. *Applied Clay Science* (December):0–1, retrieved (<http://dx.doi.org/10.1016/j.clay.2017.12.043>).

Akgün, H., Türkmenoğlu, A. G., Kelam, A. A., Yousefi-Bavil, K., Öner, G., Koçkar, M., 2017. Assessment of the effect of mineralogy on the geotechnical parameters of clayey soils: A case study for the Orta County, Çankırı, Turkey. *Applied Clay Science* 64 (November) 44-53. retrieved (<http://dx.doi.org/10.1016/j.clay.2017.08.029>).

Akgün, H., Türkmenoğlu, A. G., Met, I., Yal, G. P., Koçkar, M., 2017. The use of Ankara Clay as a compacted clay liner for landfill sites. *Clay Minerals*, 52, 391–412.

Akyurek, B., Bilginer, E., Catal, E., Dager, Z., Soysal, Y. Ve Sunu, O., 1980. Eldivan-Şabanözü(Çankırı) Hasayaz-Çandır (Kalecik-Ankara) dolayının jeolojisi. General Directorate of Mineral Research and Exploration, Report No: 6741.

ASTM D854–02, Standard Test Methods for Specific Gravity of Soils. Annual Book of ASTM Standards, Section 4, Vol.04, No.1, Soil and Rock; Building Stones, ASTM, Philadelphia.

ASTM D422–63, 2002. Standard Test Methods for Particle-Size Analysis of Soils. Annual Book of ASTM Standards, Section 4, Vol.04, No.1, Soil and Rock; Building Stones, ASTM, Philadelphia.

ASTM D4318–00, Standard Test Methods for Liquid Limit, Plasticity Limit, And Plasticity Index of Soils. Annual Book of ASTM Standards, Section 4, Vol.04, No.1, Soil and Rock; Building Stones, ASTM, Philadelphia.

ASTM D698–00, Standard test Methods for Laboratory Compaction Characteristics of Soil Using Standard Effort (12,400 ft-lbf/ft³(600kN-m/m³)). Annual Book of ASTM Standards, Section 4, Vol.04, No.1, Soil and Rock; Building Stones, ASTM, Philadelphia.

ASTM D5856–95, 2002. Standard Test Methods for Measurement of Hydraulic Conductivity of Porous Material Using a Rigid-Wall, Compaction-Mold Permeameter. Annual Book of ASTM Standards, Section 4, Vol.04, No.1, Soil and Rock; Building Stones, ASTM, Philadelphia.

ASTM D837–09, Standard Test Method for Methylene Blue Index of Clay. Annual Book of ASTM Standards, Section 4, Vol.04, No.1, Soil and Rock; Building Stones, ASTM, Philadelphia.

Baban, S. J., & Flannagan, J., 1998, Developing and implementing GIS-assisted constraints criteria for planning landfill sites in the UK. *Planning Practice and Research*, 13(2), 139–151. doi:10.1080/ 02697459816157.

Bagchi, A., 1994. *Design, Construction and Monitoring of Landfills*. 2nd Edition, John Wiley & Sons, Inc., New York.

Benson, C.H., Zhai, H., and Xiaodong, W., 1994. Estimating hydraulic conductivity of compacted clay liners. *Journal of Geotechnical and Geoenvironmental Engineering*, 120(2), 366–387

Beskese, A.; Demir, H.H.; Ozcan, H.K.; Okten, H.E., 2015. Landfill site selection using fuzzy AHP and fuzzy TOPSIS: A case study for Istanbul. *Environmental Earth Science*, 73, 3513–3521.

Bilgin, A.Z., Uğuz, M.F., Sevin, M., Parlak, O., Pekgöz, M., Elibol, H., Erdem, Y., Özden, U.A., 2009. Ayaş-Temelli-Polatlı (Ankara) dolayının jeolojisi (Ankara-İ28

Paftası). General Directorate of Mineral Research and Exploration Report No:11215, Ankara.

Bohor, B.F., Hughes, R.E., 1971. Scanning electron microscopy of clays and clay minerals. *Clay Mineralogy*, 19, 49–54.

Cambazoğlu, S., Yal, G.P., Eker, A.M., Şen, O., Akgün, H., 2019. Geothermal resource assessment of the Gediz Graben utilizing TOPSIS methodology. *Geothermics* 80, 92–102. <https://doi.org/10.1016/j.geothermics.2019.01.005>.

Chang, N.B., Parvathinathan, G., Breeden, J.B., 2008. Combining GIS with fuzzy multicriteria decision-making for landfill siting in a fast-growing urban region. *Journal of Environmental Management* 87 (1), 139–153.

Chen, P., 1977. Table of key lines in X-ray powder diffraction patterns of minerals in clays and associated rocks. Indiana, Department of Natural Resources Geological Survey Occasional Paper 21.

Chiappone, A., 1999. Gli scivolamenti planari delle Langhe: uno studio di tipo meccanico e mineralogico per la definizione del modello geotecnico. Dottorato di Ricerca in Ingegneria Geotecnica, XII Ciclo, Dipartimento di Ingegneria Strutturale, Politecnico di Torino, Torino, Italy.

Chipera, S.J., Bish, D.L., 2013. Fitting full x-ray diffraction patterns for quantitative analysis: a method for readily quantifying crystalline and disordered phases. *Adv. Mater. Phys. Chem.* 03, 47-53.

Cokca, E., 2002. Relationship between Methylene Blue Value, Initial Soil Suction and Swell Percent of Expansive Soils. *Turkish J. Eng. Env. Sci.* 26, 521 – 529.

Daniel, D. E., Trautwein, S. J., 1994. Hydraulic conductivity and waste contaminant transport in soil. Retrieved from <https://books.google.com.tr>.

EEA, 2018. The European Environment Agency – Data and Maps. CORINE Land Cover classes. Retrieved on 2018-11-01 from <https://land.copernicus.eu/pan-european/corine-land-cover/clc2018>

Hosgor, I., 2012. Paleocology, paleogeography and taxonomic of paleocene Molluscs from the Haymana-Polatlı basin and correlation with benthic Foraminiferas biostratigraphy (Doctoral dissertation). Ankara University, Ankara, Turkey.

Hwang CL, Yoon K., 1981. Multiple attribute decision making methods and applications. Springer, New York.

Gokalp Z., Başaran M. ve Uzun, O., 2011. Compaction and swelling characteristics of sand-bentonite and pumice-bentonite mixtures, Clay Minerals, 46, 49-459.

Guiqin, W., Li, Q., Guoxue, L., Lijun, C., 2009. Landfill site selection using spatial information technologies and AHP: a case study in Beijing, China. Journal of Environmental Management 90, 2414–2421.

Karadenizli, L., Sarac, G., Şen, S., Seyitoglu, G., Antoine, P.O., Kazancı, N., Vaol, B., Alciçek, M.C., Gül, A., Erten, H., Esat, K., Ozcan, F., Savascı, D., Antoine, A., Filoreau, X., Hervet, S., Bauvrain, G., Bonis, L.D., Hakyemez, Y., 2004. Oligo-Miocene Mammalian biostratigraphy and depositional evolution of the western and southern parts of Çankırı-Çorum Basin, Central Anatolia. TÜBİTAK Project No:101Y108. General Directorate of Mineral Research and Exploration Report No:10706, Ankara.

Karakaya Bentonit Co., Ankara. Retrieved on 2019-11-6 from <https://www.karakaya.com.tr/urunler/>

Kharat, M. G., Kamble, S. J., Raut, R. D., Kamble, S. S., & Dhume, S. M., 2016. Modeling landfill site selection using an integrated fuzzy MCDM approach. Modeling Earth Systems and Environment, 2(2), 53.

Komine, H., 2014. Simplified evaluation on hydraulic conductivities of sand-bentonite mixture backfill. Applied Clay Science, 26, 13-19.

Kumar S., Yong, W.L., 2002. Effect of Bentonite on Compacted Clay Landfill Barriers. *Soil and Sediment Contamination: An International Journal*, volume 11, issue 1, 71-89.

Liu, D., Zhou, X., Bu, H., Deng, L., Liu, H., Yuan, P., Du P., Song H., 2018. XRD-based quantitative analysis of clay minerals using reference intensity ratios, mineral intensity factors, Rietveld, and full pattern summation methods: A critical review. *Solid Earth Sciences*, Volume 3, Issue 1, 16-29.

Malczewski, J., 1997. Propagation of errors in multicriteria location analysis: A case study. In G. Fandel & T. Gal (Eds.). *Multiple criteria decision making* 154– 155, Springer, Berlin.

Malczewski, J., 1999. *GIS and Multicriteria Decision Analysis*. New York: John Wiley and Sons, Canada, 392 p.

Mitchell, J.K., Soga, K., 2005. *Fundamentals of Soil Behavior*, 3rd edn. John Wiley & Sons Inc., New Jersey, 652 p.

Met.I., 1999. Engineering geological assessment of clayey soils in Ankara for being utilized as compacted clay liners. MSc thesis, Middle East Technical University, Department of Geological Engineering, Ankara, Turkey, 151 p.

Met, I, Akgün, H., 2015. Geotechnical evaluation of Ankara clay as a compacted clay liner. *Environmental Earth Science*, 74, 2991–3006. DOI 10.1007/s12665-015-4330-x.

Moore, D.M., Reynolds, R.C., 1997. *X-ray Diffraction and the Identification and Analysis of Clay Minerals*. second ed. Oxford University Press, Oxford.

Nas, B., Cay, T., Iscan, F., Berktaş, A., 2008. Selection of MSW landfill site for Konya, Turkey using GIS and multi-criteria evaluation. *Environmental Monitoring Assessment* 160 (1–4), 491–500.

Nyimbili, P.H.; Erden, T.; Karaman, H., 2018. Integration of GIS, AHP and TOPSIS for earthquake hazard analysis. *Nat. Hazards*, 92, 1523–1546.

Ören, A. H., Durukan, S., Kayalar, A. Ş., 2014. Influence of compaction water content on the hydraulic conductivity of sand-bentonite and zeolite-bentonite mixtures. *Clay Minerals*, 49, 109-121.

Pasvanoglu, S., Gocmez, G., Sen, O., 1998. The Hydrogeological study on thermal and mineral water of Ilıcapınar (Polatlı). *Journal of Engineering Sciences*, 4 (1-2), 557-562.

Reynolds, Duane M. Moore; Robert C., 1997. X-ray diffraction and the identification and analysis of clay minerals (2. ed.). Oxford [u.a.]: Oxford Univ. Press. ISBN 9780195087130.

Rigo de Righi, M. ve Cortesini, A., 1959. Regional studies central Anatolian basin, progress report 1. Turkish Gulf Oil Com, Ankara.

Saaty, T. L., 1991. Multicriteria decision making - the Analytical Hierarchy Process. Pittsburgh: RWS Publications.

Schroeder, P.R., Lloyd, C.M., Zappi, P.A., and Aziz, N.M., 1994. The Hydrologic Evaluation of Landfill Performance (HELP) Model: User's Guide for Version 3. Risk Reduction Engineering Laboratory, Office of Research and Development, EPA/600/R-94/168a, US Environmental Protection Agency, Cincinnati, Ohio.

Sener, B., 2004. Landfill Site Selection by using geographic information systems (Msc. thesis). Middle East Technical University, Ankara, Turkey.

Sezer G.A., Türkmenoğlu A.G., Göktürk E.H., 2003. Mineralogical and sorption characteristics of Ankara Clay as a landfill liner. *Applied Geochemistry*, 18, 711-717.

Sharifi M., Hadidi M., Vessa E., Mosstafakhani P., Taheri K., Shahoie S., 2009. Integrating multi-criteria decision analysis for a GIS based hazardous waste landfill siting in Kurdistan Province, Western Iran. *Waste Management* 29, 2740–2758.

Sirel, E., ve Gunduz, H., 1976. Stratigraphical distribution and definitions of Mummulites, Assilina and Alveolina species in Haymana region (S of Ankara). *Bulletin of the Geological Society of Turkey*, 19, 1, 31-44.

Tehrany, M.S., Pradhan, B., Jebur, M.N., 2013. Spatial prediction of flood susceptible areas using rule based decision tree (DT) and a novel ensemble bivariate and multivariate statistical models in GIS. *J. Hydrol.*, 504, 69–79.

TSWCR 2010. Solid waste control regulation. Ministry of Environment and Forestry of Turkey, Official Gazette No.27533, Ankara, Turkey.

Turkecan, A. Dincel, A., Hepsen, N., Papak, I., Akbas, B., Sevin, M., Ozgur, I.B., Bedi, Y., Mutlu, G., Sevin, D., Unay, E., Sarac, G. ve Karatas, S., 1991. Bolu-Çankırı (Köroğlu Dağları) arasındaki Neojen yaşlı volkanitlerin stratigrafisi ve petrolojisi. *Bulletin of the Geological Society of Turkey* 6, 85-103.

TURKSTAT 2016. Turkish statistical institute, population statistics. <http://www.turkstat.gov.tr>. Access date: September 2018.

Unalan, G., Yuksel, V., Tekeli, T., Gonenc, O., Seyirt, Z., Huseyin, S., 1976. The stratigraphy and paleogeographical evolution of the Upper Cretaceous-Lower Tertiary sediments in the Haymana-Polatli region (SW of Ankara). *Bulletin of the Geological Society of Turkey*, v. 19, 159-176.

U.S. Environmental Protection Agency, 2010. Code of Federal Regulations, Title 40, Part 258 Subtitle D, Criteria for Municipal Solid Waste Landfills.

Velasco E. S., 2013. Scanning Electron Microscope (SEM) images as a means to determine dispersibility (Unpublished master's thesis). Iowa State University, IA, USA.

Yal, G.P., Akgün, H., 2014. Landfill site selection utilizing TOPSIS methodology and clay liner geotechnical characterization: a case study for Ankara, Turkey. *Bull. Eng. Geol. Environ.*, 73(2), 369-388.

Yal, G., Akgün, H., 2013. Landfill site selection and landfill liner design for Ankara, Turkey. *Environmental Earth Sciences*, 70:2729–2752.

Yesilnacar, M.I., Suzen, M.L., Kaya, S. B., and Doyuran V., 2012. Municipal solid waste landfill site selection for the city of Sanliurfa-Turkey: an example using MCDA integrated with GIS”, *International Journal of Digital Earth*. 5, 147-164.

Yoon K. P., Hwang C. L., 1995. *Multiple attribute decision making: an introduction*. Sage University Paper series on quantitative applications in the social sciences, Thousand Oaks, CA

Yukselen, Y., and Kaya, A., 2008. Suitability of the methylene blue test for surface area, cation exchange capacity and swell potential determination of clayey soils. *Engineering Geology*, 102, 38-45.

APPENDICES

A. Test Results

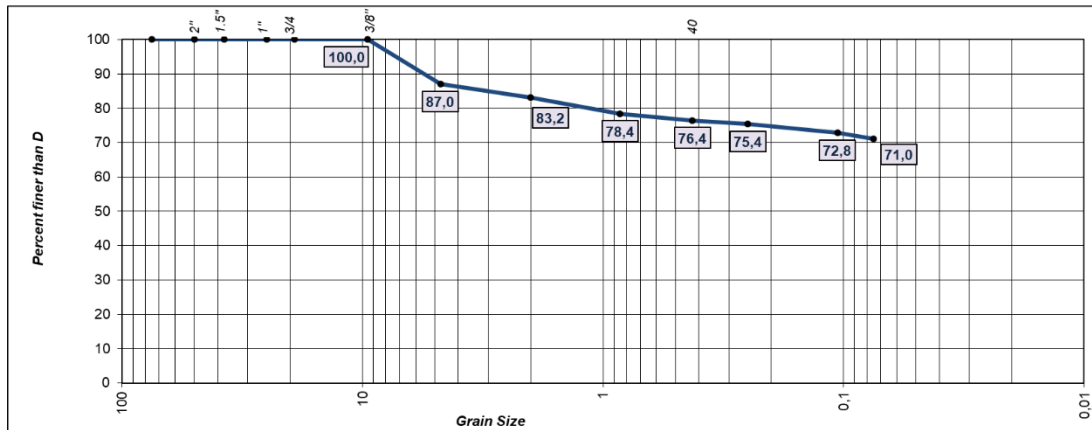


Figure 0.1. Particle size distribution plot of sample B1

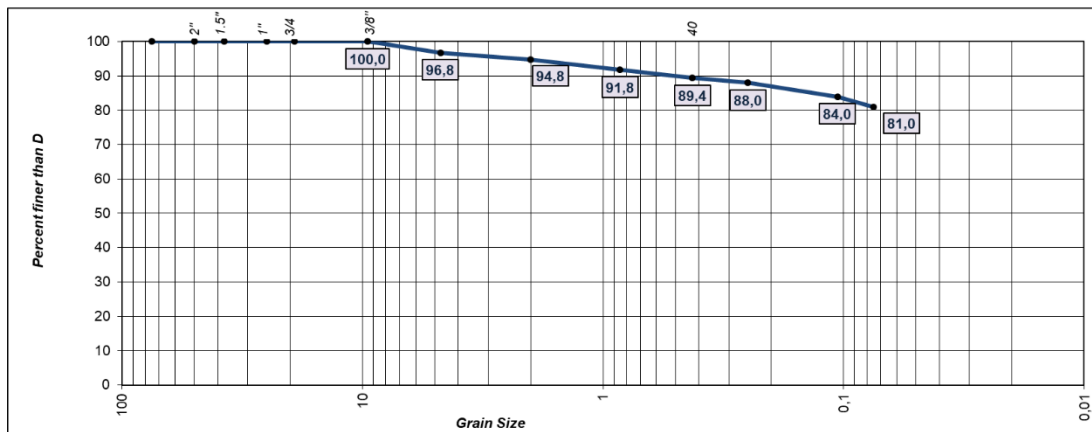


Figure 0.2. Particle size distribution plot of sample B2

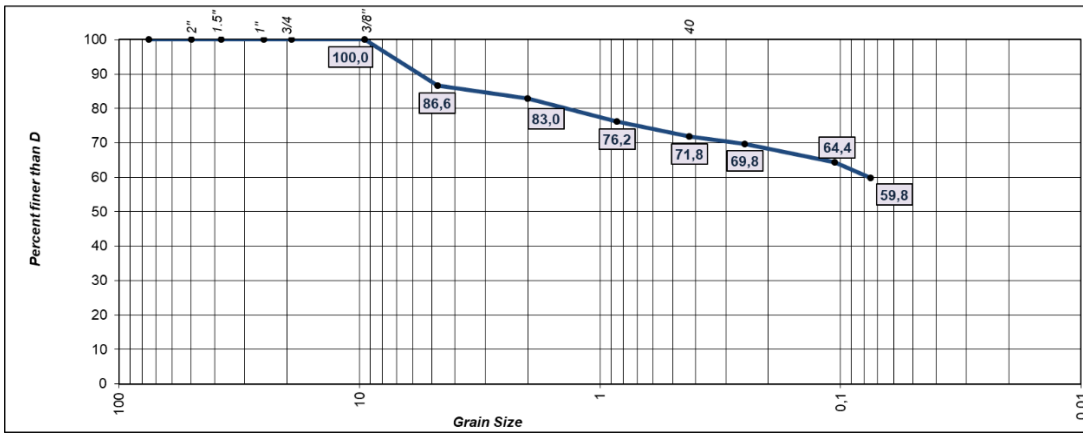


Figure 0.3. Particle size distribution plot of sample B3



Figure 0.4. Particle size distribution plot of sample C1

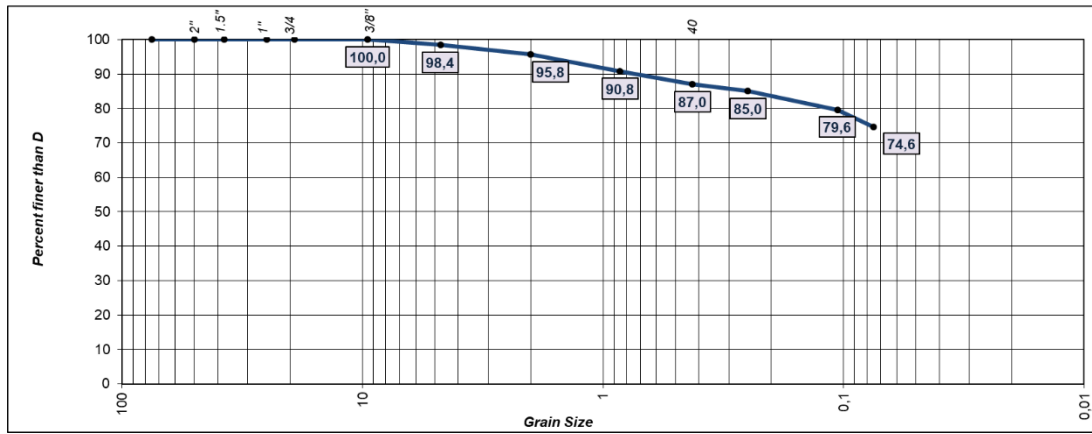


Figure 0.5. Particle size distribution plot of sample C2

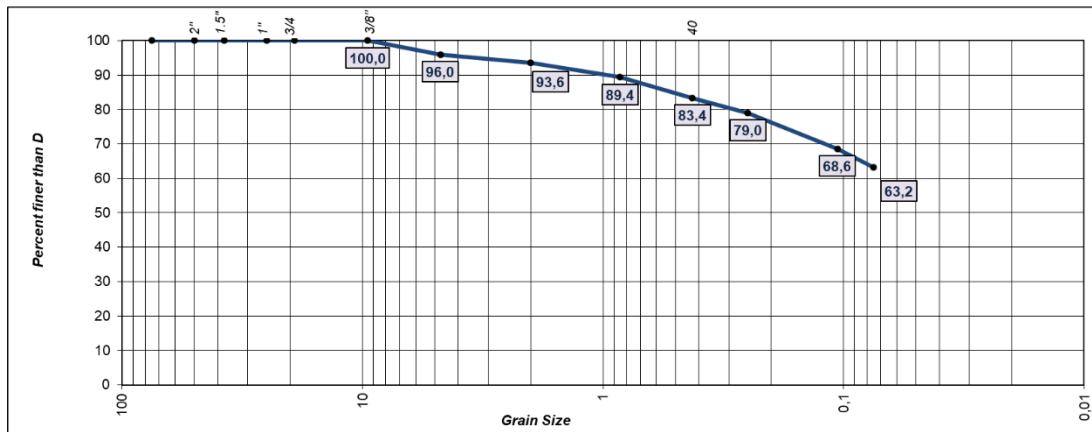


Figure 0.6. Particle size distribution plot of sample C3

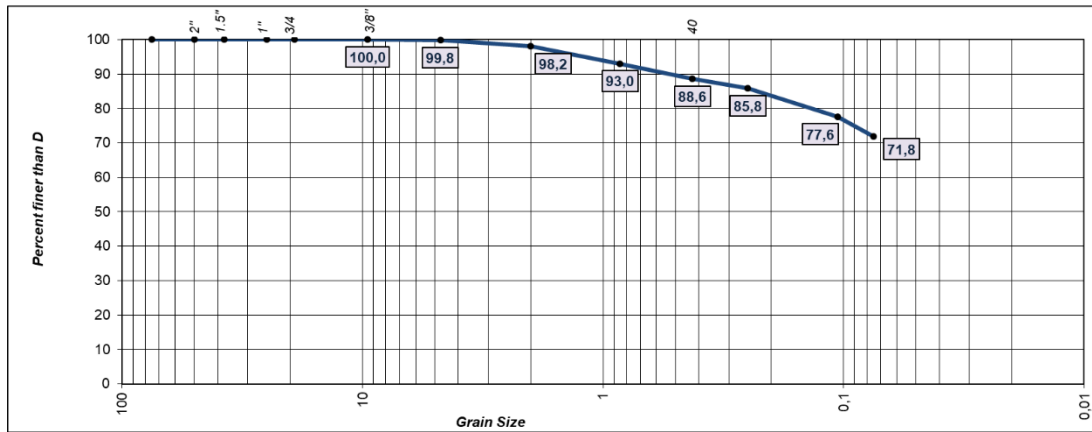


Figure 0.9. Particle size distribution plot of sample A3

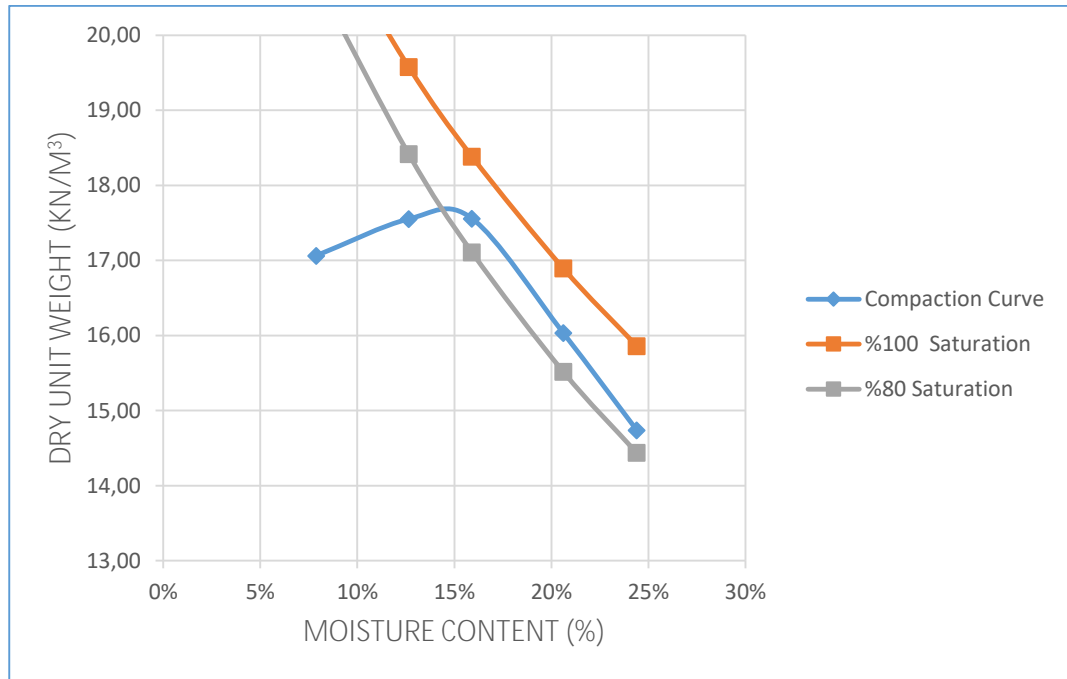


Figure 0.10. Dry unit weight vs moisture content graph of C1

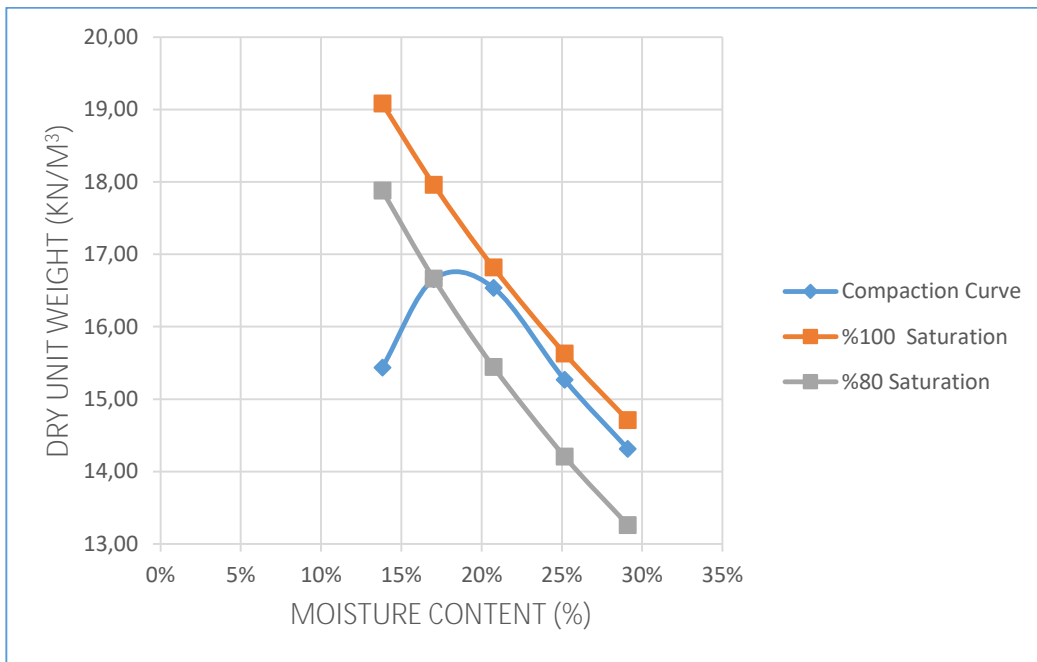


Figure 0.11. Dry unit weight vs moisture content graph of C2

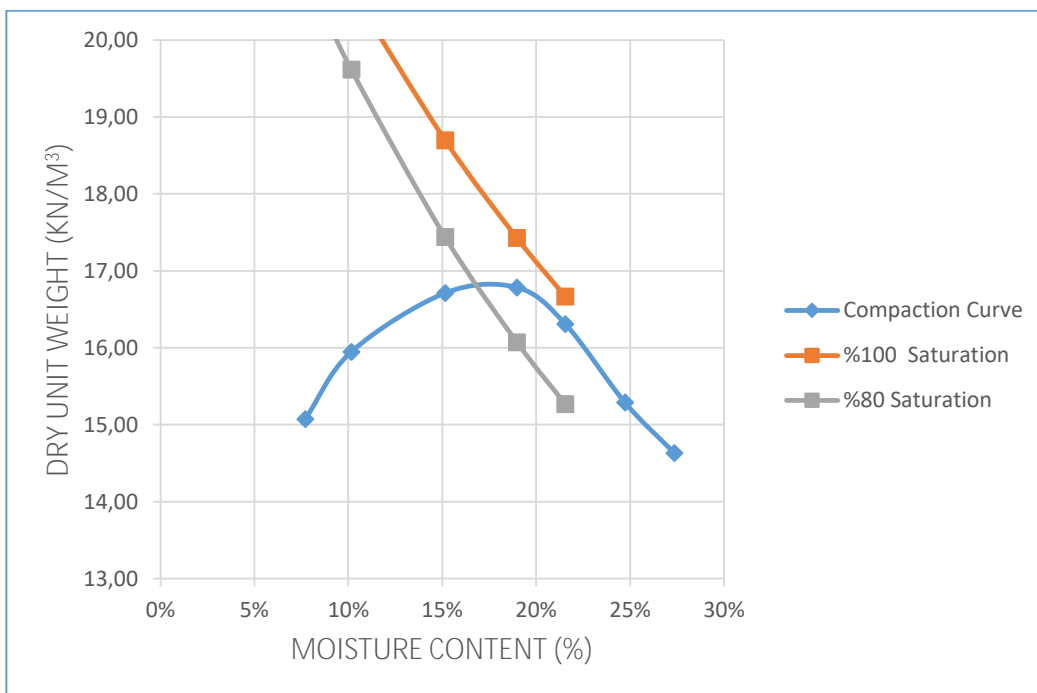


Figure 0.12. Dry unit weight vs moisture content graph of C3

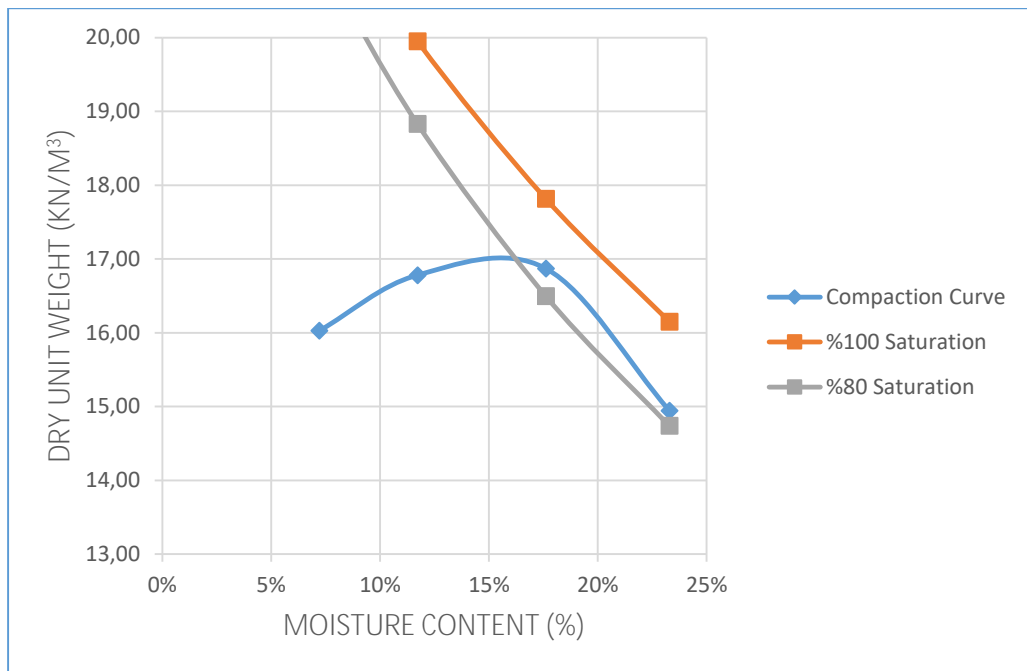


Figure 0.13. Dry unit weight vs moisture content graph of A1

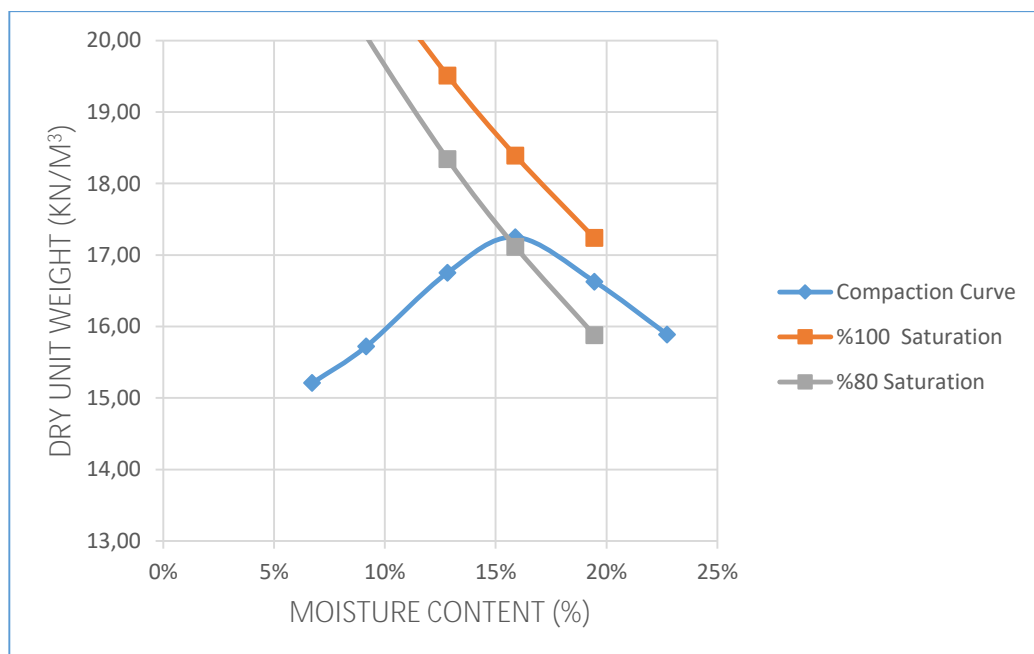


Figure 0.14. Dry unit weight vs moisture content graph of A2

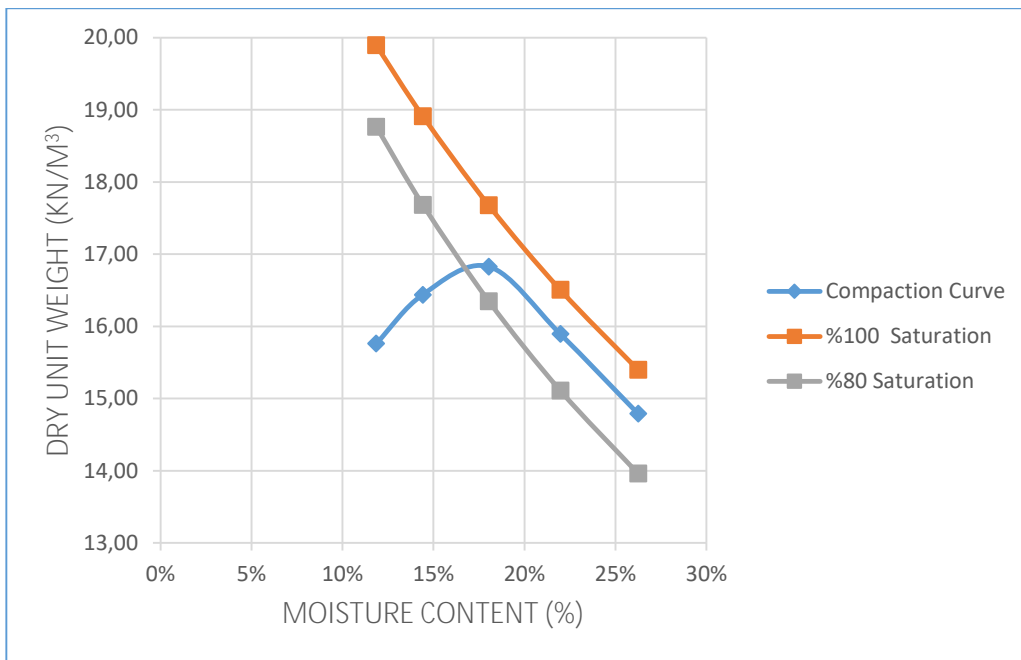


Figure 0.15. Dry unit weight vs moisture content graph of A3

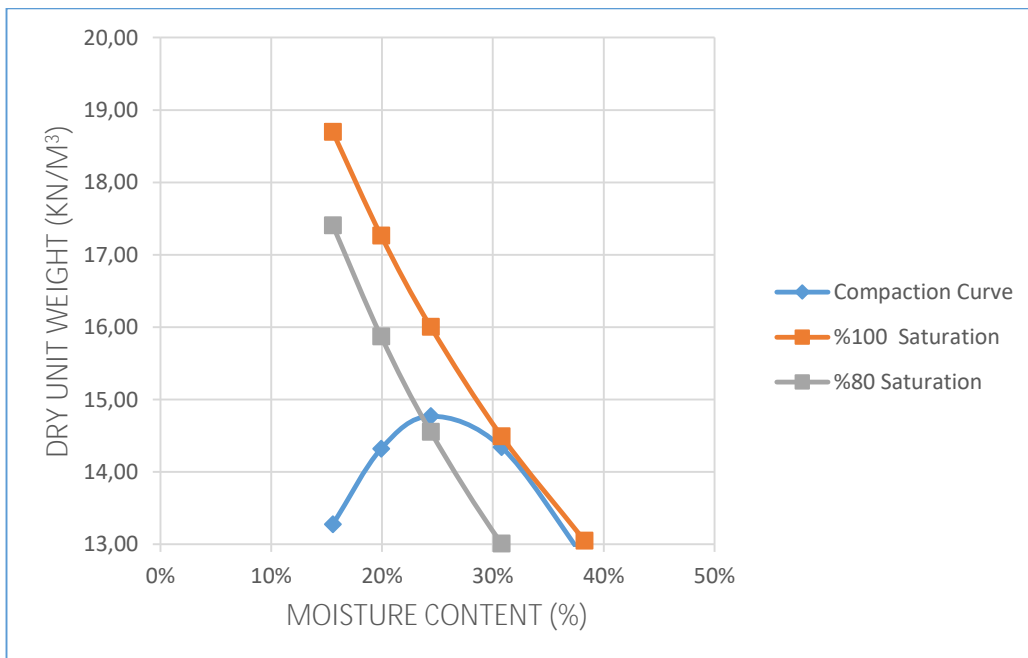


Figure 0.16. Dry unit weight vs moisture content graph of B1

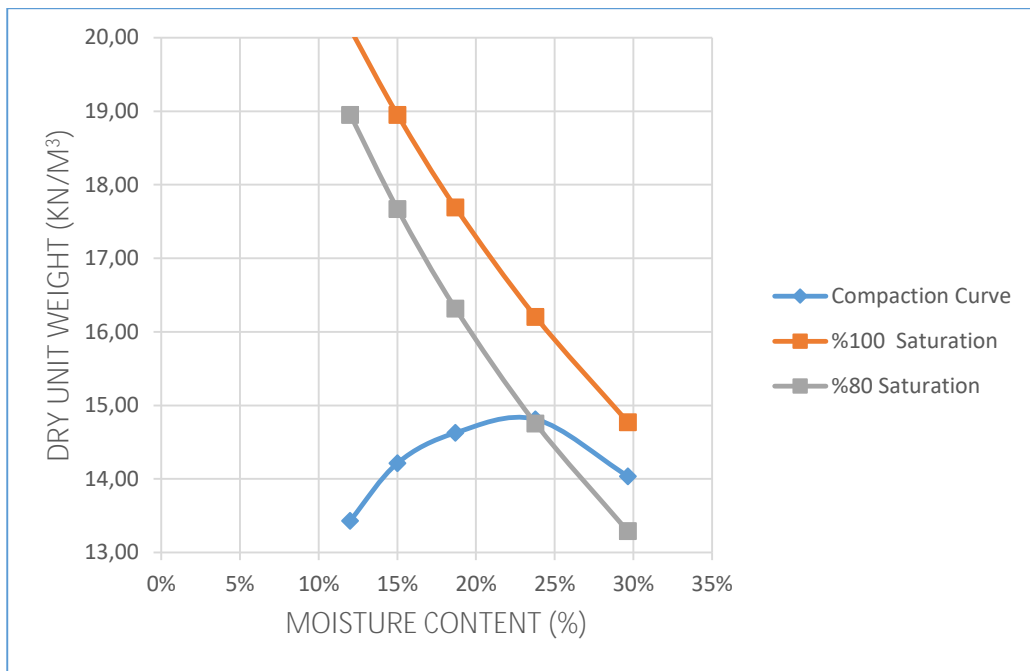


Figure 0.17. Dry unit weight vs moisture content graph of B2

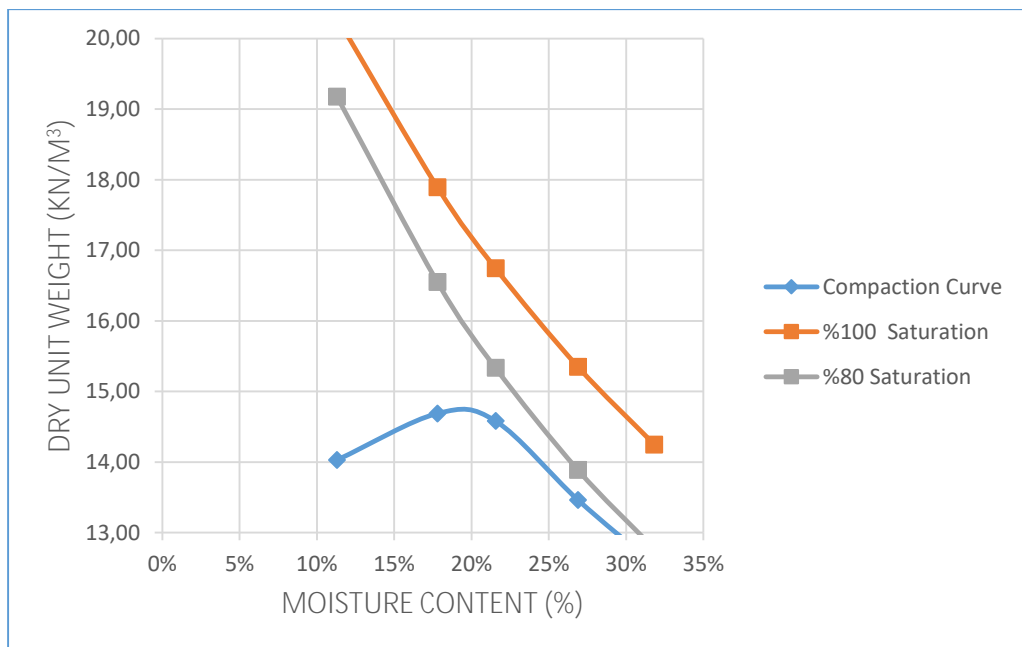


Figure 0.18. Dry unit weight vs moisture content graph of B3

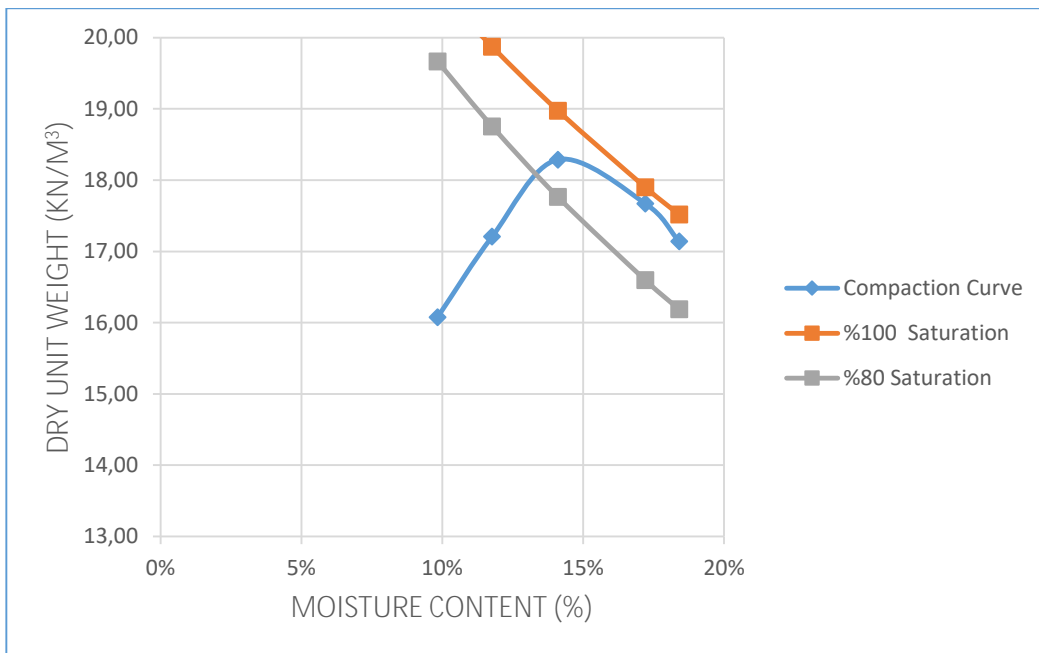


Figure 0.19. Dry unit weight vs moisture content graph of C3 (%5 Bentonite)

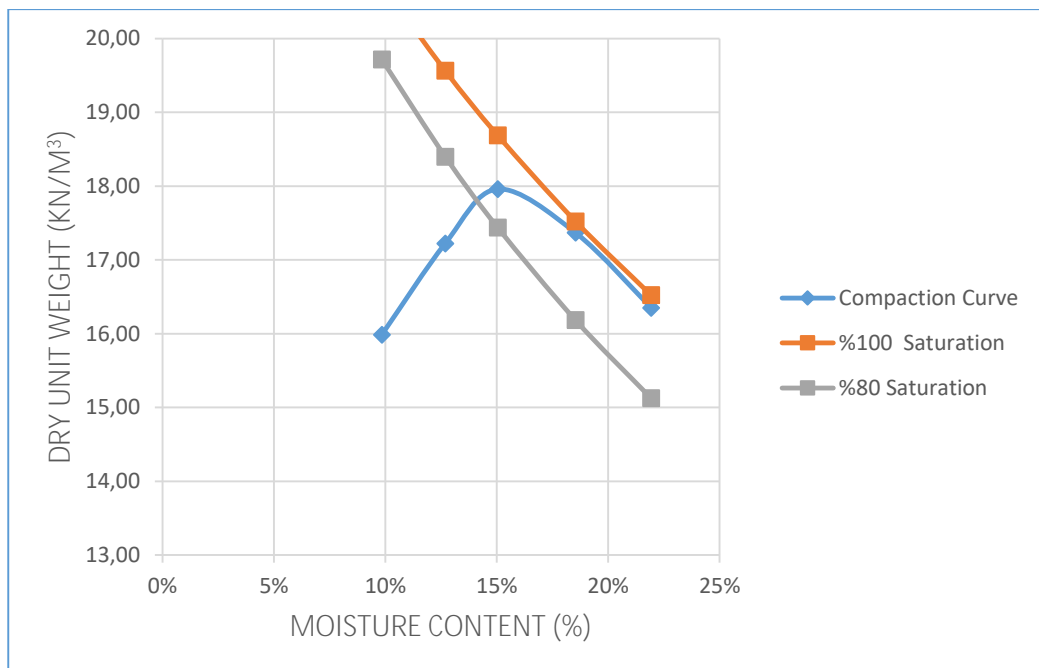


Figure 0.20. Dry unit weight vs moisture content graph of A3 (%5 Bentonite)

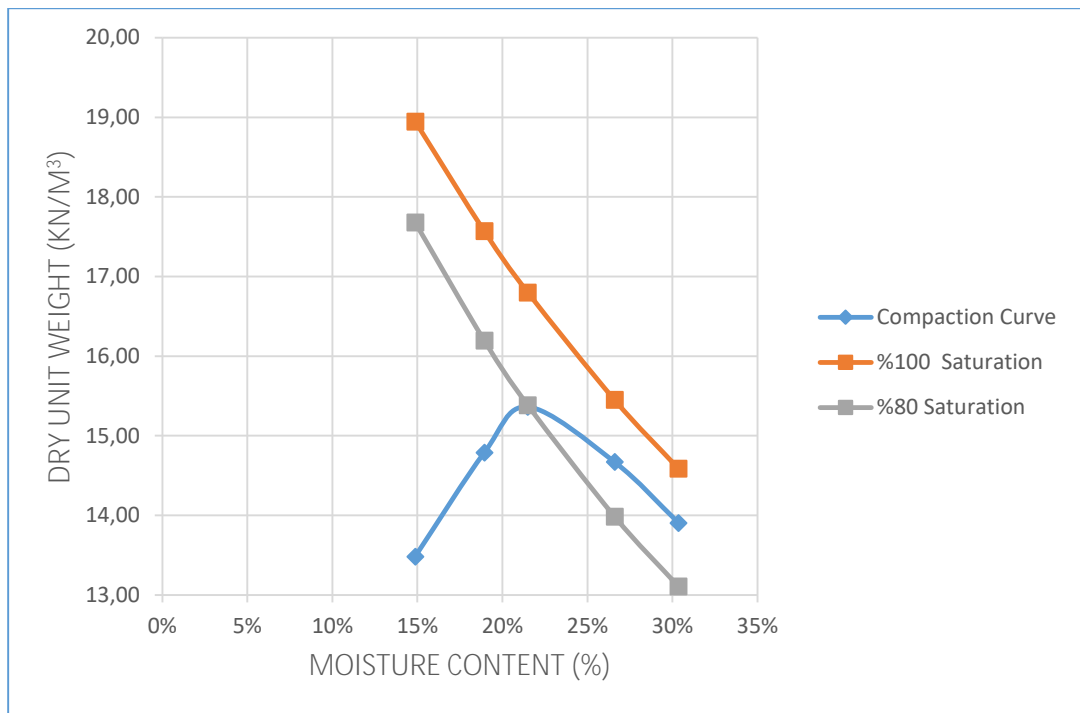


Figure 0.21. Dry unit weight vs moisture content graph of B1 (%5 Bentonite)

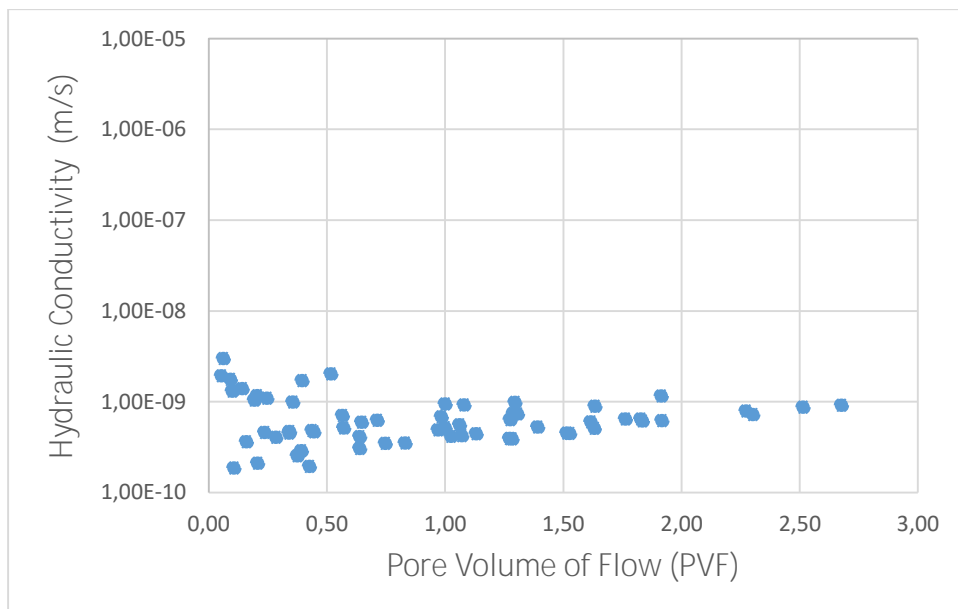


Figure 0.22. Hydraulic conductivity vs pore volume of flow graph of C3 (%5 Bentonite)

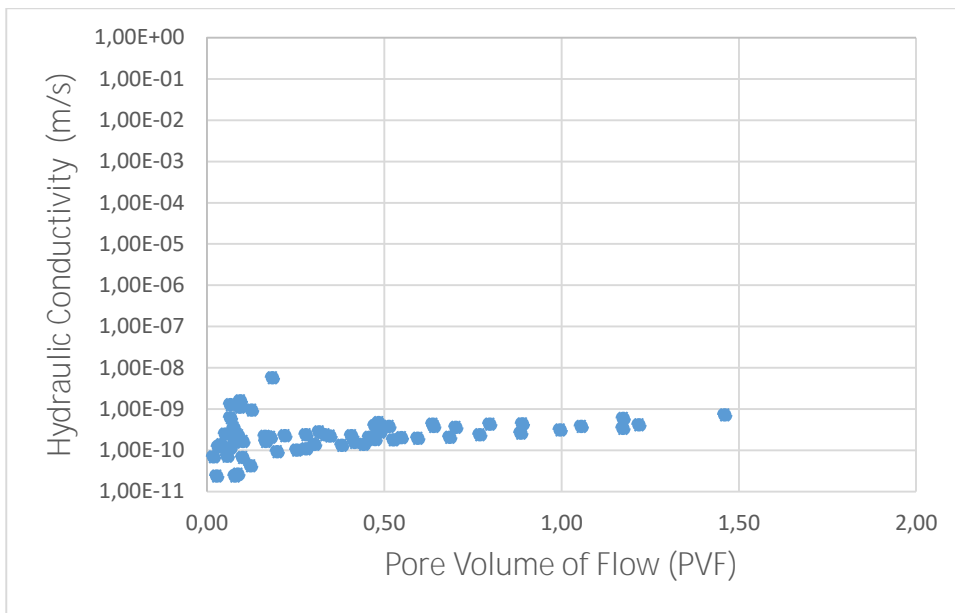


Figure 0.23. Hydraulic conductivity vs pore volume of flow graph of A3 (%5 Bentonite)

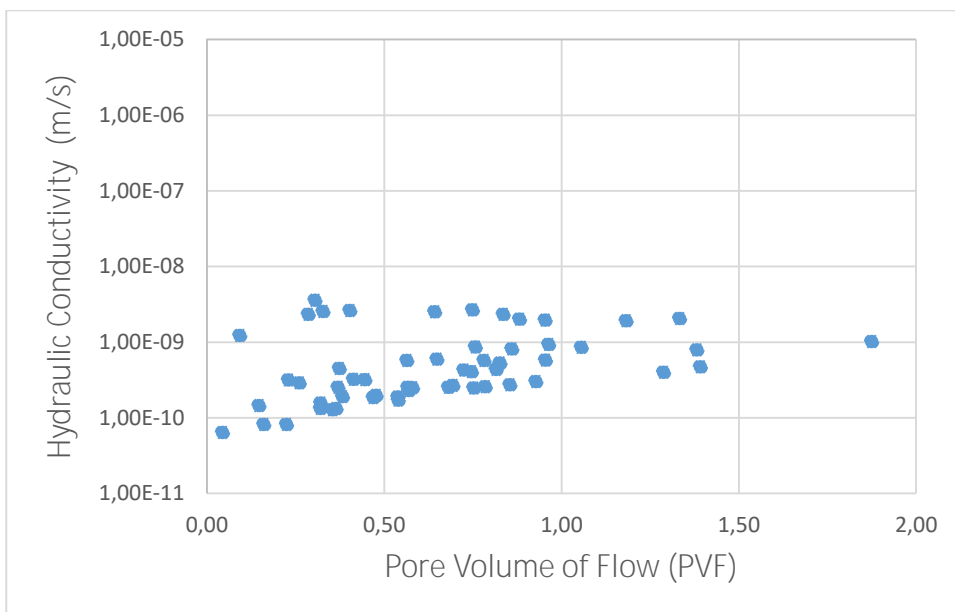


Figure 0.24. Hydraulic conductivity vs pore volume of flow graph of B1 (%5 Bentonite)

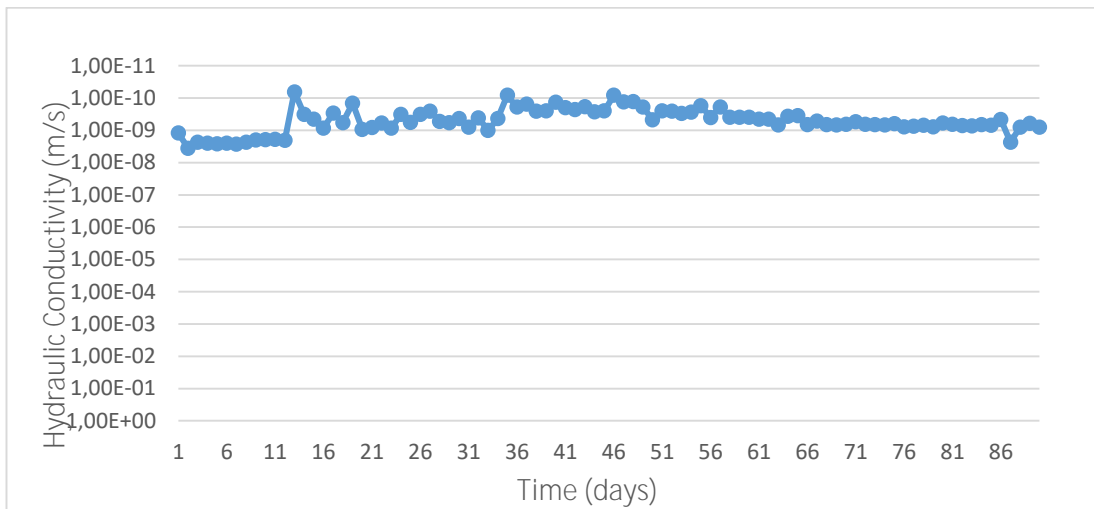


Figure 0.25. Hydraulic Conductivity vs time graph of sample B1

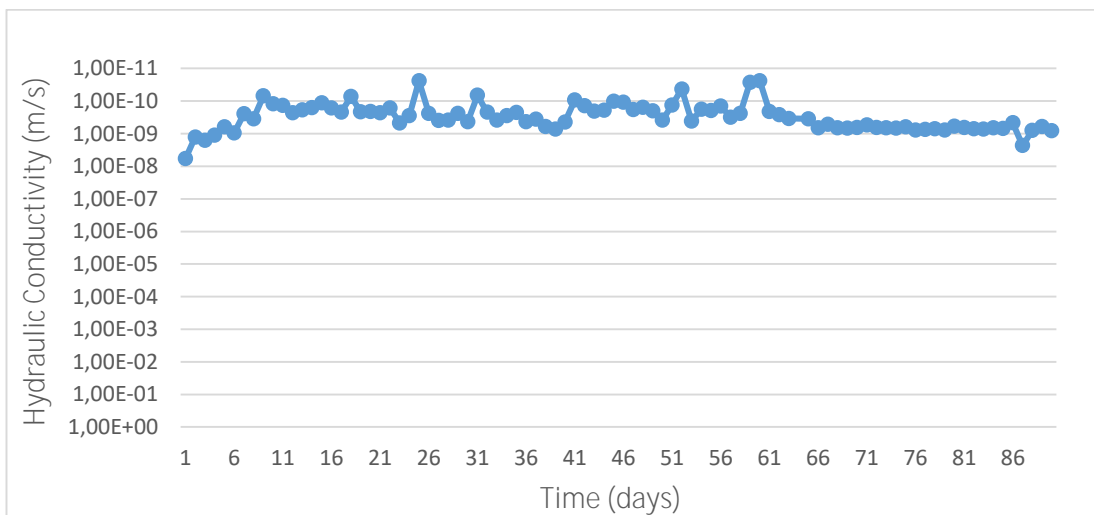


Figure 0.26. Hydraulic Conductivity vs time graph of sample A3

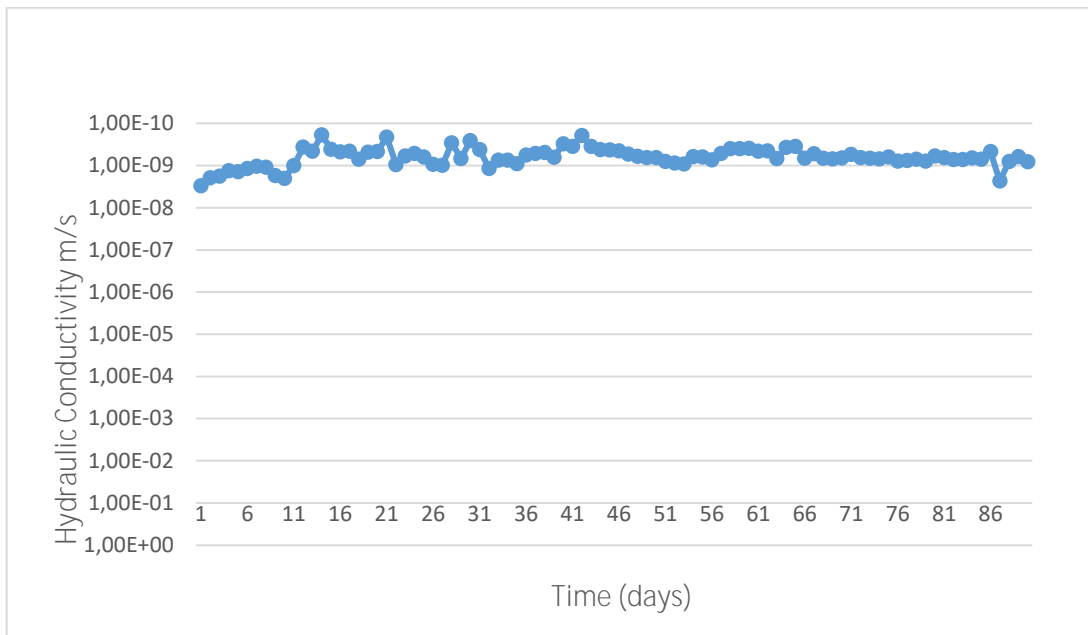


Figure 0.27. Hydraulic Conductivity vs time graph of sample C3